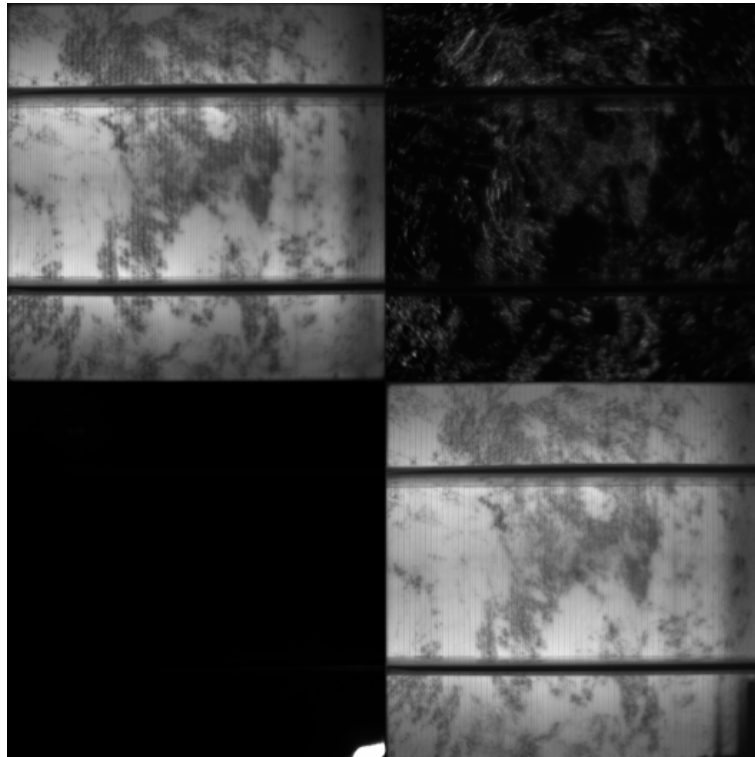


# CHALMERS



## **Usage of Highly Accelerated Stress Test (HAST) in Solar Module Ageing Procedures**

*Master of Science Thesis*

**TOMAS HULKOFF**

Department of Electrical Engineering  
*Division of Energy and Environment*  
CHALMERS UNIVERSITY OF TECHNOLOGY  
Göteborg, Sweden, 2009



# Usage of Highly Accelerated Stress Test (HAST) in Solar Module Ageing Procedures

Tomas Hulkoff



## **Abstract**

In this thesis the correlation between two accelerated ageing methods are established. The concept is to carry out the Damp Heat test and the Highly Accelerated Stress Test in order to accelerate the time of testing for solar module production. The choice of materials fell on four types of mini modules to be tested, three with standard embedding materials and one with naked cells. All of the samples had the same type of cells, glass and back sheet foil. The tests were carried out and measurements were made at specific times in order to compare the results. Measurements of transmittance, IV-characteristics, electroluminescence and a visual control were performed.

Keywords: Damp Heat, HAST, solar cell, artificial ageing, environmental chamber.



## **Acknowledgements**

I would like to thank Henry Höhne, Sebastian Pingel and all colleagues at SOLON SE in Berlin, Torbjörn Thiringer at Chalmers University of Technology, friends and family and of course Sophie.



## List of Figures

Figure 1. A standard module composition .....	19
Figure 2. Projected Long Term Performance of Module Based on Damp Heat Testing .....	21
Figure 3. Phase diagram over water states according to pressure and temperature. ....	23
Figure 4. The HAST relative THB water absorption over time.....	23
Figure 5. The 2-diode model describes the inner characteristics of a solar cell.....	25
Figure 6. The series resistance decided from measurements at 1000 W/m <sup>2</sup> and 500 W/m <sup>2</sup> ...	26
Figure 7. An exaggerated relation between the FF, R <sub>sh</sub> and R <sub>ser</sub> to I <sub>sc</sub> and U <sub>oc</sub> .....	27
Figure 8. Efficiency degradation of Cz boron cells.....	29
Figure 9. The spectral region concerned for the EL pictures. ....	30
Figure 11. The typical module design for all samples. ....	34
Figure 12. The sample A show a white haze after 500 hours, appearing after being all transparent at the beginning. ....	35
Figure 13. At 1000 hours the white haze has a brown tone. ....	36
Figure 14. The front of the DH-A3 lead after 500 hours DH and the clearly corroded back side of the same lead.....	36
Figure 15. DH-A2 show beginning corrosion on the front side leads as well. ....	36
Figure 16. At 1500 hours DH-A show corrosion on the bus bars on the back of the cell. ....	36
Figure 17. DH-A5 at 2000h front side corrosion and at the back side bus bar also green copper corrosion is to be seen. ....	36
Figure 18. The sample A show a proceeding de-lamination at the corners at 1000h, it is seen that the back sheet foil no longer grips the glass.....	37
Figure 19. At 1500 hours it is slowly getting worse, now covering the entire edge of the cell. ....	37
Figure 20. At the 2000 hours stage the sample A de-lamination at the edges is clear.....	37
Figure 21. Transmittance average for DH over test time.....	38
Figure 22. The DH-A samples at 0, 500, 1000, 1500, and 2000 hours.....	38
Figure 23. IV-characteristics at 0, 1500 and 2000 hours of DH for DH-A4.....	39
Figure 24. P <sub>mpp</sub> degradation over DH test time .....	39
Figure 25. Pale area on the front side of the H3-A cells at 48 hours. ....	40
Figure 26. The H1-A samples also show a clear discolouring above the cell after 72 hours. .	40
Figure 27. No corrosion after 12 hours. ....	40
Figure 28. Corrosion inside the A sample at 48 hours of HAST on the back of the lead.....	40
Figure 29. Here H2-A2 showing front side corroded leads after 72 hours. ....	40
Figure 30. H3-A3 front side corrosion after 96 hours.....	40
Figure 31. Corroded back side bus bar in the H3-A samples at 72 hours, this occurred at 96 hours for the H2 samples.....	41
Figure 32. HAST 24 hours: A samples show some de-lamination at the edges similar to DH. ....	41
Figure 33. The same view of the A module at 48 hours. Now the embedding have a light browning but the bubbles does not seem to expand. The de-lamination at the edge is also seen. ....	41
Figure 34. The A modules are still transparent (left part) in difference to in DH and some bubbles between cell and glass at 24 and 48 hours. ....	42
Figure 35. Transmittance average for HAST (H1: 110°C, H2: 120°C, H3: 130°C) over test time.....	43
Figure 36. HAST 120°C A sample transmittance degradation with trend line. ....	43
Figure 37. The time variation of the HAST sample A at 120°C. ....	44
Figure 38. IV-curve for H2-A4 at 0, 72 and 144 hours.....	44

Figure 39. H2-A sample $P_{mpp}$ average over test time.....	45
Figure 40. The different test types, DH and HAST, compared in transmittance development. .....	46
Figure 41. The measured values and the trend lines corrected of the top value after regeneration with base of 100 % for DH and HAST. ....	47
Figure 42. $R_{ser}$ of DH and HAST. ....	47
Figure 43. DH-B3 and H2-B3, completely cracked after lamination. ....	48
Figure 44. The back sheet foil slipped on the DH-B4.....	49
Figure 45. The back side bus bars of the DH-B3 at 500 hours, showing the typical discolouring of the B samples. The smudge in the left corner is left over from the lamination is what caused the cell to crack. ....	50
Figure 46. B sample corroded only at the skew cell DH-B4.....	50
Figure 47. A small corrosion start to show on the back side of DH-B3, 1500 hours. ....	50
Figure 48. The typical B sample corrosion after 2000 hours, DH-B2. ....	50
Figure 49. DH-B transmittance development over test time.....	51
Figure 50. The transmittance average, regarding only degradation and not the initial improvement, shown over the DH test time.....	51
Figure 51. Average $P_{mpp}$ for DH-B samples.....	52
Figure 52. H3 sample showing corrosion after 48 hours .....	52
Figure 53. Clear front side of the leads but corrosion on the back side of the H2 leads after 72 hours HAST.....	52
Figure 54. A light corrosion appear on the front of the connector lead at 72 hours at 130°C and the back looking worse, H3-B2. ....	52
Figure 55. Light backside corrosion on the H1 samples after 72 hours.....	52
Figure 56. The Transmittance measured values and the trend for H2-B samples over time. ..	53
Figure 57. DH-B transmittance development over test time.....	53
Figure 58. Average $P_{mpp}$ for H2-B samples.....	54
Figure 59. Transmittance over time in both DH and HAST for the B samples. ....	54
Figure 60. DH and HAST 120°C in relation to each other over test time. Trend line calculated from top value after regeneration. ....	55
Figure 61. $R_{ser}$ development in the DH respective HAST.....	55
Figure 62. The broken cells and a cell with large cracks, H1-C5 .....	57
Figure 63. A typical view of the yellow spots on the C samples. ....	58
Figure 64. Back side bus bar of the C samples heavily corroded after 1500 hours. ....	58
Figure 65. The DH-C at 1000 hours, it shows a growing de-lamination on front side close to the bus bars.....	59
Figure 66. The complete back side of the module have de-laminated. c) The DH-C at 1000 hours, with severe de-lamination behind the cells. ....	59
Figure 67. The C samples now de-laminate at the front side as well and not only at the bus bar.....	59
Figure 68. The heavy de-laminated and corroded back side of the 2000 hours C sample.....	60
Figure 69. The thermoplastic falling out of the C samples. ....	60
Figure 70. Transmittance average over DH testing time .....	61
Figure 71. Average transmittance degradation in DH over testing time with initial improvement removed and only considering degradation. ....	61
Figure 72. DH-C average power over DH test time.....	62
Figure 73. Yellow spot on the H1 samples after 24 hours. ....	62
Figure 74. H2-C Yellow spot and de-lamination of the H2 at 48 hours .....	63
Figure 75. Browning and bubbles of H2-C samples at 48 hours. ....	63
Figure 76. Front side de-lamination begins at 12 hours in the 130°C HAST.....	64

Figure 77. The back side of each H-C sample at 12 hours of HAST, H1, H2 and H3, with different stages of bubbles and de-lamination, also the front of the H3-C1 is seen. The already corroded leads shows a brown discolouration outside the modules.....	64
Figure 78. The melted embedding in the C samples after 24 hours at 130°C.....	65
Figure 79. This is from the melted H3 samples after 48 hours. The front side start to de-laminate as well and some of the cells brake and flow out with the embedding material. ....	65
Figure 80. Front side delamination of the H2-C samples at 72 hours together with a back side example. ....	65
Figure 81. H2-C5 at 72 hours, the de-laminated area is clear to see as a darkened area on the cell from the EL photo. ....	66
Figure 82. Increasing front side de-lamination after 96 hours. H2-C sample, back side is completely de-laminated as the back sheet foil can be removed without any resistance from the glue. ....	66
Figure 83. HAST transmittance for H2-C samples at 0, 12, 14, 48, 72 hours of testing. ....	66
Figure 84. Transmittance degradation for H2-C samples. ....	67
Figure 85. Average $P_{mpp}$ for H2-C samples.....	67
Figure 86. $P_{mpp}$ for DH and HAST with measured values and corrected trend lines.....	68
Figure 87. HAST and DH series resistance development over time.....	68
Figure 88. The DH-C2 at 0 hours of testing at the top left, at 1000 hours during EL testing top right; dark clouds at the cell edge implies higher series resistance. The bright area at the bus bar low left is probably due to a bridge over the cell edge causing a short circuit. Bottom left; the same DH-C2 at 1500 hours. The de-lamination influence is becoming clear to see due to the darkened areas. Bottom right; finally at 2000 hours. ....	69
Figure 89. Left H2-C2 at 0 hours, right at 96 hours, shows that this also apply for the C modules, similar to DH. ....	69
Figure 90. Corrosion after 500, 1000, 1500 and 2000 hours of DH, DH-D5. ....	70
Figure 91. Discoloured back side and corrosion on the back side bus bar, DH-D5. ....	70
Figure 92. The broken off corner and front side similar to an untested cell, from the DH-D5 after 500 hours.....	71
Figure 93. DH-D4 sample show signs of corroded copper after 2000 hours DH (the small strip above the bus bar). ....	71
Figure 94. DH-D1 has a black discolouration on the front after 2000 hours DH. ....	71
Figure 95. Average $P_{mpp}$ for DH-D samples. ....	72
Figure 96. The broken H2-D1 after it was dropped. Cracked of part of H1-D4.....	72
Figure 97. The grey discolouring appears on the backside in HAST to, after 12 hours. ....	72
Figure 98. The corrosion development over 12, 24, 48, 72 and 96 hours in HAST .....	73
Figure 99. Development of average $P_{mpp}$ for H2-D samples.....	73
Figure 100. DH and H2 $P_{mpp}$ over testing time. The initial measurements removed and starting the degradation of the HAST samples at the top power measured. Measured values plotted.	74
Figure 101. Series resistance development showed for the H2 and DH over testing time. ....	74
Figure 102. Top left, DH-D3 at 0 hours. Top right; DH-D3 show increased dark areas at the top, after 1000 hours. Some small cracks are also to be seen but they are at the same level as at the beginning of the test. Bottom left; at 1500 hours the development continues. Bottom right; DH-D after 2000 hours .....	75
Figure 103. Left; H2-D3 at 0 hours. Right; after 96 hours HAST, at the top some growing darkened areas can be seen.....	76
Figure 104. Transmittance for all three samples over time. Trend lines corrected to 100 %..	77
Figure 105. DH and HAST average transmittance degradation for A sample.....	78
Figure 106. HAST and DH Average $P_{mpp}$ values in W for sample A.....	78
Figure 107. HAST and DH Average $P_{mpp}$ values in W for sample B. ....	79
Figure 108. HAST and DH Average $P_{mpp}$ values in W for sample C. ....	79

Figure 109. HAST sample D cells, with and without the broken cells .....	80
Figure 110. HAST sample D cells, with and without the broken cells .....	80
Figure 111. A comparison of DH average $R_{ser}$ for each sample. ....	81
Figure 112. Comparison of all H2 sample averages and their $R_{ser}$ . ....	81

# Usage of Highly Accelerated Stress Test (HAST) in Solar Module Aging Procedures

1	Introduction .....	16
2	Theoretical Foundations .....	17
2.1	Accelerated Aging Models & Tests .....	17
2.1.1	Arrhenius Model .....	17
2.1.2	Peck Model .....	18
2.1.3	Physical Aging Appearances .....	19
2.1.4	Damp Heat (DH).....	21
2.1.5	Highly Accelerated Stress Test (HAST).....	22
2.2	The Solar Cell, Solar Module & Characterisation .....	25
2.2.1	IV-Characteristics .....	25
2.2.2	Degradation/Regeneration .....	28
2.2.3	Electroluminescence .....	29
2.2.4	Transmittance .....	31
3	Tests & Measurements .....	32
3.1	Design .....	33
3.1.1	Materials .....	33
3.1.2	Sample Design .....	34
3.2	Sample A.....	35
3.2.1	Damp Heat .....	35
3.2.2	HAST .....	39
3.2.3	Comparison.....	46
3.3	Sample B .....	48
3.3.1	Damp Heat .....	49
3.3.2	HAST .....	52
3.3.3	Comparison.....	54
3.4	Sample C .....	56
3.4.1	Damp Heat .....	58
3.4.2	HAST .....	62
3.4.3	Comparison.....	67
3.5	Sample D.....	70
3.5.1	Damp Heat .....	70
3.5.2	HAST .....	72
3.5.3	Comparison.....	73
3.6	Sample Comparison .....	77
3.6.1	Correlation .....	81
4	Results & Conclusions .....	83
4.1	Further Work .....	83
	References .....	84



DH:	Damp Heat, 85°C / 85 % RH
RH:	Relative Humidity
TC:	Thermal Cycling
HAST:	Highly Accelerated Stress Test
THB:	Temperature Humidity Bias
STC:	Standard Test Conditions
$U_{oc}$ :	Open Circuit Voltage
$I_{sc}$ :	Short Circuit Current
$P_{mpp}$ :	Maximum Power Point Power
FF:	Fill Factor
$R_{sh}$ :	Shunt Resistance
$R_{ser}$ :	Series Resistance
$I_{ph}$ :	Photon current
$I_{diff}$ :	Diffusion current
$I_{rec}$ :	Recombination current
E:	Irradiation
RH:	Relative Humidity
LID:	Light Induced Degradation
OE:	Outdoor Exposure
IEC:	International Electrotechnical Commission
DIN:	Deutsches Institut für Normung
EL:	Electroluminescence
EVA:	Ethylene and Vinyl Acetate

# 1 Introduction

The purpose with this thesis work is to find a correlation between two types of accelerated aging, Damp Heat (DH) test and the Highly Accelerated Stress Test (HAST). Aging is a time consuming process which is involved in product testing to secure their quality before they are released for the market. Therefore a great interest lies within accelerating these testing times, hence shortening the total development and production times of the companies. Yet another advantage is that the range of products that will be available for production can be tested more rapidly and if needed rejected at an early stage saving costly testing time.

An outdoor exposure is a complex mixture of factors such as wind, rain, snow, moisture, heat and light. Therefore it is hard to create indoor testing environments that can simulate the natural aging. Various tests are used in order to simulate these factors, in an artificial aging process real life conditions and factors will not be able to forecast and reproduce all factors of the reality.

For the slow climate degradation with moisture penetrating the product the DH test is used. It takes place in an environmental chamber where the substrates are to be kept for over 1000 hours at a temperature of 85°C and a relative humidity of 85%. The HAST have been used over 40 years by microelectronic companies in order to speed up the aging process where a corresponding test time of 48 – 96 hours, to the DH 1000 hours, appears.

As foundation for this work, the Arrhenius model has been chosen. Since it does not imply humidity the extended Peck model expands the theory. From former realized tests a correlation of the Damp Heat to 20 years in Miami climate can be established as shown by Wohlgemuth in his article *Long Term Reliability of PV Modules* (2005) [2]. The damages to the samples will also shortly be compared with outdoor exposed modules, from long term testing at the Technische Universität Berlin [9]. In order to achieve the correlation between this two test types, equal test samples will be tested in both DH and HAST and then the measurements will be compared to give the time span needed in a HAST chamber to simulate the supposed 20 year life time. From other studies it is possible to get an estimation of the HAST time, ranging from 24 hours to over 200 hours depending on the test temperature[7], [8], [10], [11], [14],.

Simple micro modules will be constructed and hand assembled. There will be three embedding materials, an EVA and two thermoplastic samples that will lead to different outcomes. All three have the same type of glass back sheet foil and connectors. The fourth is naked cells going through the same test steps. The tests are carried out parallel in Damp Heat and HAST with an aim of over 2000 hours in DH and about 200 hours of HAST test. The HAST test is divided into three severity levels, 110°C, 120°C and 130°C since the test duration decreases with increasing temperature.

## 2 Theoretical Foundations

Accelerated aging simulate long period of time in an outdoor climate. The simulation is of a too complex nature, due to the dynamic factors working in real life aging, in order to perform accelerated aging with a satisfying accuracy. However the accelerated aging test offers a possibility to find materials where the failure probabilities are small. Previous data exists only in very few cases which make it difficult to create a good correlation between outdoor exposure and accelerated aging, but it helps minimizing the risk. The ambition is to make sure that the products will survive a certain period, according to the company warranty agreements, of more than 20 years. This chapter will shortly describe the basics of artificial aging and some models behind it.

### 2.1 Accelerated Aging Models & Tests

The foundation of the accelerated aging processes is based on a couple of models describing the dependence of the aging to temperatures and humidity. This chapter describes a couple of these models and presents some known result of outdoor aged modules and the aging signs they show.

Damp Heat and HAST are to be correlated towards each other. In order to compare both of them it is necessary to explain how the tests work and what parameters influence the test. What also needs to be considered, is that by comparing results from the aging methods such as DH with natural aging, it has been shown that the test can only partially reproduce the effects [1].

#### 2.1.1 Arrhenius Model

The Arrhenius model is a common used method regarding forecasting lifetime of products depending on the surrounding temperature. Simplified a 10°C temperature increase leads to half the degradation time, that is, with 10°C warmer surroundings a test can be performed in half of the actual life time. As result, for example the Damp Heat (DH) test at 85°C and 85 % Relative Humidity (RH), test can be used. Due to the temperature increase a 20 year lifetime can be accelerated to 1000 hours of test time[2], [3]. The theory behind Arrhenius model is of a kinetic nature, i.e. a collision theory. A higher temperature causes the molecules to move with a higher velocity. Hence the collisions between them increase and create an accelerated degradation process[4].

$$v \approx Ae^{\left(\frac{-B}{T}\right)}, B \geq 0 \quad (1)$$

From (1) the relationship between the damage caused by temperature in relation to the temperature is shown, where  $A$  and  $B$  are specific model coefficients and  $T$  is the absolute temperature in K.

$$t_1 - t_0 = Ae^{\left(\frac{+B}{T}\right)} \quad (2)$$

$$AF = \frac{t_{use}^l - t_0}{t_{test}^l - t_0} = e^{+B \left( \frac{1}{T_{test}} - \frac{1}{T_{use}} \right)} \quad (3)$$

(2) Establishes the relation of the lifetime  $t_l - t_0$  at a certain temperature and shows that it is inversely proportional to the speed of degradation. Here the Acceleration Factor (AF) is added and thus the relation (3) can be set, with  $t_{test}^l - t_0$  as the time to failure for a certain testing temperature,  $t_{use}^l - t_0$  time to failure for a temperature in service use and  $T_{test}, T_{use}$  temperature in test and service use [3].

A disadvantage of the Arrhenius model is that it does not consider humidity, thus a more advanced model is required.

### 2.1.2 Peck Model

The Peck model is an evolution from the Eyring model, described in the Engineering Statistic Handbook [5] which in contrary to the Arrhenius model is a statistical thermodynamic model, and considers both temperature and humidity. The relationship of 1 % humidity responds to 1°C temperature gives a correlation of how the humidity affect the degradation according to the expected degradation increase with higher temperatures.

$$v = H^n e^{\left( \frac{-B}{T} \right)} \quad (4)$$

Similar to Arrhenius a relationship of the temperature damage is established in (4).  $B$  is a constant according to the failure mode,  $T$  is absolute temperature,  $H$  represents the level of humidity and  $n$  is a material constant.

$$t_l - t_0 = H^{-n} e^{\left( \frac{+B}{T} \right)} \quad (5)$$

$$AF = \frac{t_{use}^l - t_0}{t_{test}^l - t_0} = \left( \frac{H_{test}}{H_{use}} \right)^{-n} e^{+B \left( \frac{1}{T_{test}} - \frac{1}{T_{use}} \right)} \quad (6)$$

Further the  $AF$  is calculated in a fashion similar as the Arrhenius model; of course with the difference that humidity accelerates the damage. The lifetime  $t_l - t_0$  at temperature  $T$  and humidity  $H$  is given by (5) and the  $AF$  by (6).  $t_{test}^l - t_0$  describe the failure time for the test,  $t_{use}^l - t_0$  the failure time for a temperature in service use,  $T_{test}, H_{test}$  and  $T_{use}, H_{use}$  are the temperature and humidity in test respectively service use [3]. In this work the humidity will be constant, thus it will not change the various degradation times as it will be held at a constant humidity of 85 % RH.

### 2.1.3 Physical Aging Appearances

Due to the stress conditions in both the environmental chamber and in the Highly Accelerated Stress Test (HAST) (Section 2.1.5), chamber it is expected to see some accelerated aging phenomena. These expected aging symptoms are tied to each other; normally when one does occur it will increase the probability of the others also occurring. In the test environment used in this work a couple of the failures will most likely not occur. Comparing with outdoor exposure (OE) [6], it is not expected that cracks and bleaching due to illumination of the cells appears, since the environmental tests are performed without physical stress and in the dark. However a short description of the most frequently occurring damages in the aging procedure will be made. The methods to decide the aging will be closer discussed in the measurement description.

The aging phenomena strongly depend on the various materials used as embedding materials, the glue, how well the materials interact with each other and with the surrounding climate. As discussed in Section 3.1, the choice of materials is made on the knowledge of which materials are known to have good relations and to be stable. In the case of DH the aging symptoms are not expected to be seen clearly before the test time approaches some 2000 hours. In the HAST test they should appear after some 50-150 hours [7], [8].

Absorption of moisture is to be expected since the embedding materials are sensitive to water. Even though the construction with glass and back sheet foil, Figure 1, have been developed to withstand the water penetration, the aging of the protective materials are supposed to cause a loss of their good features and let more and more damp through. Glass is considered to be a stable material thus the degradation times are very long, it is not expected to see the transparency decrease within the glass. However the glass might dim, especially in the contact area to the embedding materials, thus causing a lower transmittance.

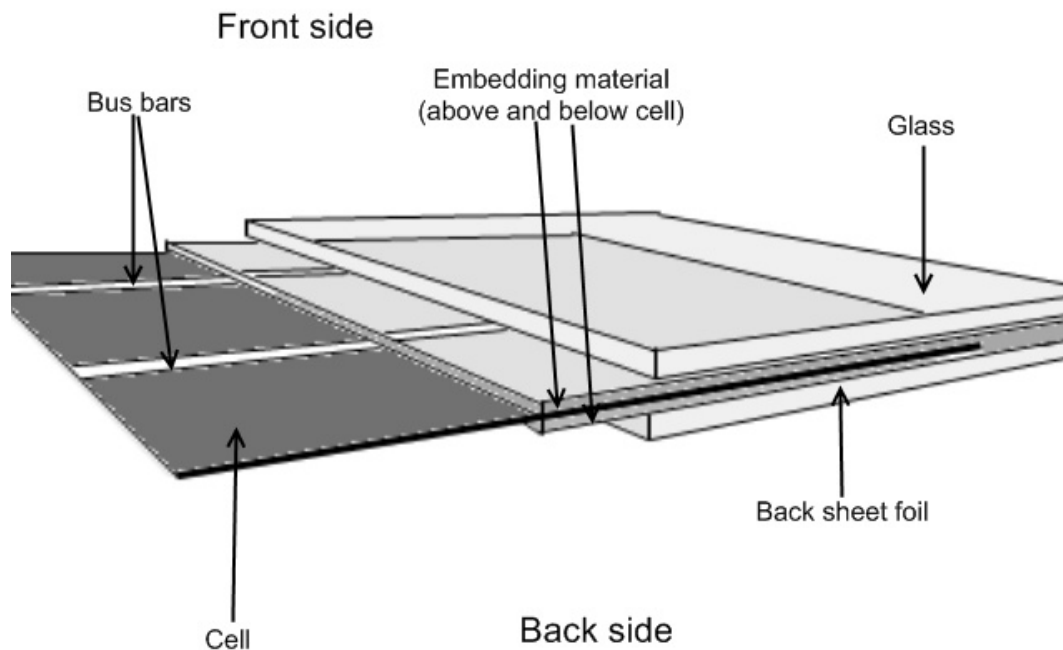


Figure 1. A standard module composition

With aging, the embedding materials tend to get a browning that leads to lower short circuit current ( $I_{sc}$ ) and the fill factor (FF) (Section 2.2.1) decreases. Reasons for this are explained in

the following text. Browning is the process in which the embedding materials get discoloured with a yellow or a brown tone. The result of this discolouration is a lower transmittance mainly in the blue spectral region of the visual light. When blue light is absorbed by the material it results in a lower light transmission through the material and a yellow or brown tone can be seen. This results in lower panel efficiency since the yellow light spectrum contains large amounts of photons, and in return a lower efficiency is dependent of the short circuit current,  $I_{sc}$ . The browning might also cause further failures such as bleached cells, bubbles and degradation of the embedding materials and partial cell corrosion might occur. Due to heat absorption in the materials (through light and environment) and a higher temperature the browning tend to increase [1], [9]. The accelerated process might also cause thermal damages to the embedding materials like bubbles or de-lamination. The glue materials between the different materials, glass – silicon – foils, will loose the grip force and air bubbles occur. In bad cases the de-lamination causes large areas to loose grip with the glass, foil or cell.

Corrosion occurs in the presence of moisture and ionic contaminants such as flux or other alien substances; either left over from the lamination process or penetrated with moisture. The metal bus bars and grid fingers corrode due to heat and moisture exposure. Depending on the moisture resistance qualities of the embedding materials, more or less damp will penetrate the layers, and this will cause an increase in series resistance as an effect of reduced conductivity in the bars, larger series resistance and influence the efficiency of the cells negatively. Results of the corrosion are larger inner resistance, shading (Hot Spots) and bubbles. The discolouration of the leads also results in a discolouration of the embedding materials and influences the transmittance characteristics of the modules. Regarding the IV-measurements, the connectivity needs to be improved by cleaning the corroded leads where the clips are attached.

The shading leading to Hot Spots appears for instance when the corrosion is spread out in the embedding material or between embedding and glass. The light can not pass through the discoloured area and therefore causes a shading effect, bringing current to transform into heat causing the Hot Spot. Furthermore this area can cause a reaction within the material that will provoke bubbles or blisters to appear in the material, this can start the de-lamination process [1], [9].

Cell corrosion occurs as effects of browning, broken glass or/and degradation of the synthetic materials that increase moisture absorption of the panels. It will lead to growing losses in the transmission as well as defective changes in the embedding materials; furthermore strong cell corrosion will lead to a larger amount of bubbles.

The backside of the cells is covered with a paste that improves the adhesive property of the backside electrode and restrains an aluminium electrode layer from exfoliating. This paste could after some time start to dissolve. How long this process can be delayed depends on the features of the paste.

A loss of performance tied to the degradation of the synthetic materials will appear, which under normal operating conditions would be far less than the losses due to browning and corrosion in field testing. At least some optical losses are expected, since they depend on the browning, corrosion, bleach and the bubbles [1], [9].

A common way to measure water absorption is to weigh the sample and see how much the weight has increased. If water is absorbed, it will lead to a heavier sample, depending on the amount of water in the sample. Water absorption is expressed as increase in weight percent.

### 2.1.4 Damp Heat (DH)

The Damp Heat (DH) test in environmental chambers is a well known aging test for electronic components. It has been used since the 1970's on solar modules and is a part of the certification procedure for the modules. Jet Propulsion Laboratory performed some of the first DH tests. With a method of testing at different temperatures and humidities, they could determine that a 10°C temperature rise would lead to a double reaction, i.e. a reduction of the degradation test time to half. Also a relationship of 1 % humidity responds to 1°C temperature change could be established. From this the 1000 hours DH at 85°C/85 % RH corresponded to 20 years of outdoor exposure, according to IEC 61215 [6], in Miami, Florida [2]. The DH test is based on the theories of Arrhenius (temperature) and Peck (temperature and humidity). The relation between aging and temperature is described in Chapter 2.

The DH is the part of the IEC 61215 [6] test that takes the longest time and there can be a lot of savings in the test phase with shortening this step. However 1000 hours of DH does not make a large difference regarding power loss in normal modules today. Therefore much longer testing times are needed in order to establish when the module would fall out of warranty. As most modules need at least 2000 hours to fall under the failure criteria of 5% power loss it would respond to 40 years exposure of Miami's climate, Figure 2.

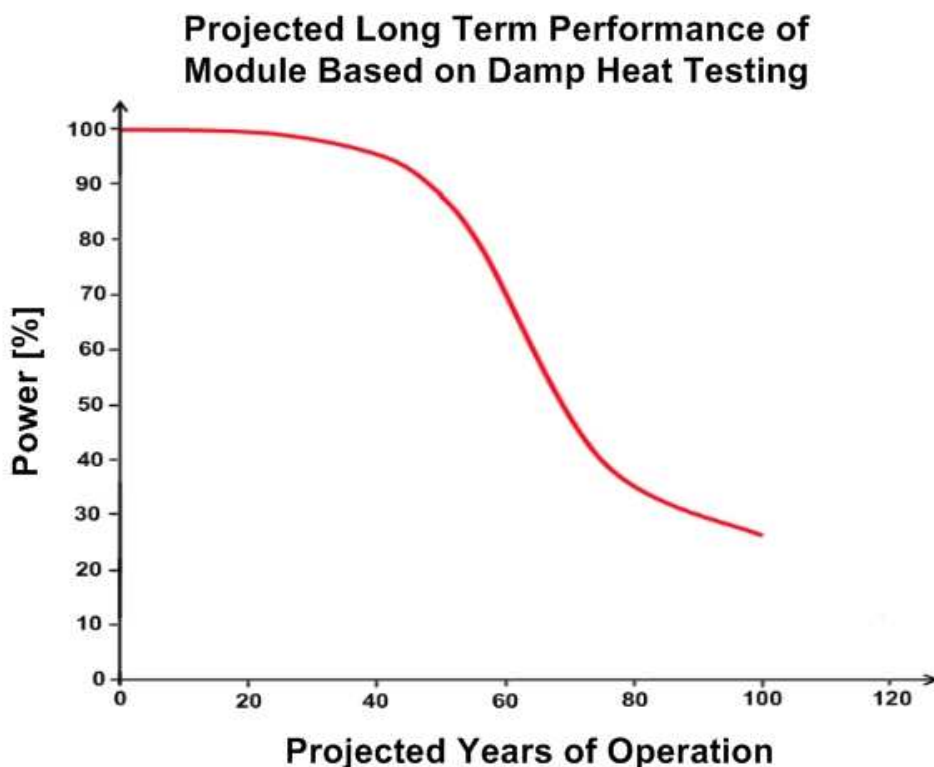


Figure 2. Projected Long Term Performance of Module Based on Damp Heat Testing

A problem with the DH test is that the temperature causes an adhesion loss for some embedding materials that would not appear in normal surrounding temperatures. This does of course not correspond to normal aging and need to be of consideration when testing modules.

As will be shown, it is an even larger issue when applying the even higher temperatures in HAST [2].

The samples are placed in the environmental chamber, all four types together since there is space enough. When the test starts there is a ramp up period according to IEC 61215 standards before the 85/85 testing begins. The samples will there be exposed to 500 hours (some ten years outdoor exposure) before the chamber will ramp down and the samples are shortly removed to be measured. Then the test cycle iterates until 2500 to 3000 hours of testing are achieved. This corresponds to approximately 130 days considering time for measurements. The work took place in the period of October 2008 to February 2009, when the final results were evaluated. A better correlation is achieved with longer test time compared to the standards, this will also improve the eventual correlation to the HAST test.

### **2.1.5 Highly Accelerated Stress Test (HAST)**

Because the 1000 hours of DH testing is a very long period of time for industrial testing, the Highly Accelerated Stress Test (HAST) has been developed. It raises temperature and humidity in order to shorten the aging time. Being used in the quality testing of Integrated Circuits (IC) and their packaging the HAST has become a common aging test and now it is also starting to get more and more usage in other industries. Many companies in other electronic fields, have even given up on the old THB or DH tests in favour of the HAST. However it is not used for solar module testing in the same extent. By increasing the temperature and humidity, the moisture penetration in the material is accelerated; it is done with a pressure regulation in order to prevent the water to reach its boiling point.

The equipment is built up like a pressure cooker with precisely controllable heat and moisture. The ramp up and most importantly the ramp down phases are also controlled. This ramp is done in order to avoid condensation to appear on the samples and affect the result of the test. The acceleration factor (AF) varies of course with different samples and temperatures, but normally a reduction of the test time by a factor of 50 is expected [7].

The water absorption in the HAST is much higher than in the DH, this is due to the higher pressure in order to make it possible to work with temperatures over the boiling point. In Figure 3 the relation between temperature and pressure is showed. The three HAST tests, at 110°C, 120°C and 130°C, are needed to work over the water boiling point and therefore a higher pressure is needed to keep the same vaporization level, 85 % RH, as in the DH at 85°C

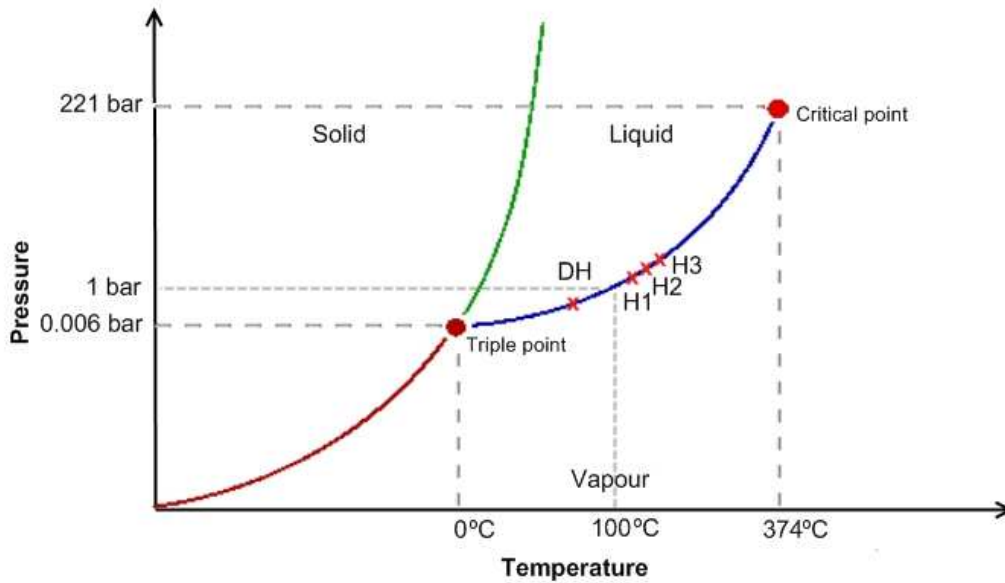


Figure 3. Phase diagram over water states according to pressure and temperature.

The HAST test is known to have a higher rate of moisture absorption compared to Temperature Humidity Bias (THB) test, basically the DH with an added bias, the relationship between THB and HAST is seen in Figure 4 [10]. Corrosion, bubbles, degradation of embedding materials and cracks can increase the amount of water absorption. However, this was outside the focus of this work..

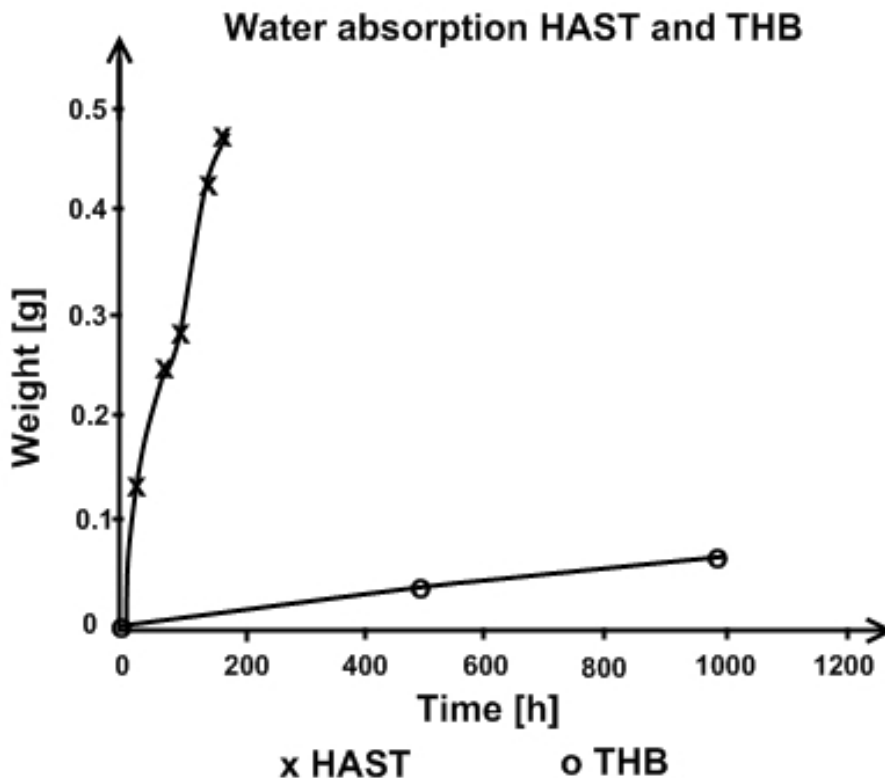


Figure 4. The HAST relative THB water absorption over time.

Comparing with the 1000 hour THB test, which relates to the DH (as THB without bias), the expected times are HAST tests of 96-100 hours at 130°C and 85 % humidity. According to SiliconFarEast.com the HAST test can be recommended “for the qualification of any change that can potentially affect the corrosion resistance of the product” and “for changes in the die

glassivation, metallization or thin film resistors, as well as changes in the molding compound. It is also used for the reliability assessment of lots suspected to be prone to corrosion due to ionic contamination” [8].

The degradation time in the HAST chamber according to the DIN EN 60068-2-66 is depending on the severity level as in the following Table 1 [11]:

Exposure Temperature [°C] <sup>1)</sup>	Relative Humidity (RH) [%] <sup>2)</sup>	Exposure Time [h] <sup>3)</sup>		
		I	II	III
110	85	96	192	408
120	85	48	96	192
130	85	24	48	96
<sup>1)</sup> ± 2°C in the packing space <sup>2)</sup> ± 5 % <sup>3)</sup> 0, +2 h				

**Table 1. HAST temperature modes.**

The pressures are for each temperature: 110°C – 0.12 MPa, 120°C – 0.17 MPa, 130°C – 0.23 MPa. The temperature is to be held constant for the test time according to the Table 2. A ramp up time of 1.5 hour and maximum 3 hours allows the chamber to get to the test conditions before the timer starts. The ramp down time after the test is conducted is to be in the time span of 1 to 4 hours.

The 130°C mode could be a limit for the materials, especially the embedding material since it approaches the normal lamination temperatures. The values of the times in the second column of the table are close to the calculated values below. This is an indication that the expected times are in a plausible range. This work uses the 1000 hours DH as standard. Calculating an increased degradation, according to the 10°C leads to half the test time; result in the following relationship to HAST:

$$110^{\circ}\text{C} - 85^{\circ}\text{C} = 25^{\circ}\text{C} \rightarrow 1000 \text{ hours} * \left(\frac{1}{2}\right)^2 * \frac{3}{4} = 187.5 \text{ hours}$$

$$120^{\circ}\text{C} - 85^{\circ}\text{C} = 35^{\circ}\text{C} \rightarrow 1000 \text{ hours} * \left(\frac{1}{2}\right)^3 * \frac{3}{4} = 93.75 \text{ hours}$$

$$130^{\circ}\text{C} - 85^{\circ}\text{C} = 45^{\circ}\text{C} \rightarrow 1000 \text{ hours} * \left(\frac{1}{2}\right)^4 * \frac{3}{4} = 46.875 \text{ hours}$$

Humidity is to be, like the temperature, held at a constant level, in this test at 85% RH (Relative Humidity). After the ramp up time the RH is constant ±5%. The level of the humidity is controlled through pressure in the chamber. In the HAST, the humidity will be held at a constant 85% RH at all three temperatures [11].

The HAST test will be arranged so that the set of samples will go in pairs in order to shorten the total time needed for the test. There will be 20 samples that need to go through the test at all temperature stages. With the possibility of placing up to 15 samples at the time in the HAST chamber two cycles will be enough, compared to five when testing the set of samples one by one. Two cycles for each temperature will result in six test runs to start with, each of them doing 48 hours in the chamber before switching to the next set. This gives a time span of two weeks to put all the samples through the chamber. The samples go in pairs A – B and C – D for each HAST mode respectively. The HAST will run until the samples falls apart, the time limit, mid February 2009, for the work ends or a no relation to the DH test can be established.

## 2.2 The Solar Cell, Solar Module & Characterisation

To establish the pre-aging characteristics of the samples each of them will go through the test steps before having spent any time in the test chambers, therefore the following pre-test measurements were applied:

The samples for the DH test were produced first and therefore also are the first ones measured. An EL measurement was performed before and after the laminations of the cells, this in order to make sure that the cells have no serious cracks and if some injuries occurred during the lamination process. Then the IV curves were measured after the modules have been constructed, as well as the transmittance of the glass-embedding-back sheet foil compound.

The HAST samples did not have the same pressed schedule as the DH ones and therefore it was able to make a pre-lamination IV-measurement as well, this in order to establish the average of the naked cells compared to the naked DH cells and also to see how much the lamination would decrease the power of the cells.

### 2.2.1 IV-Characteristics

Changes in the relationship between produced current and voltage of the cell (I-V characteristics) are shown as performance losses when the cell is being flashed. In order to estimate the aging, the power changes are decisive. The major part of the power losses can be derived to optical degradation of the glass, degradation of cells and/or embedding materials. They occur in combination with each other and it can be difficult to estimate exactly which loss is caused by what degradation process.

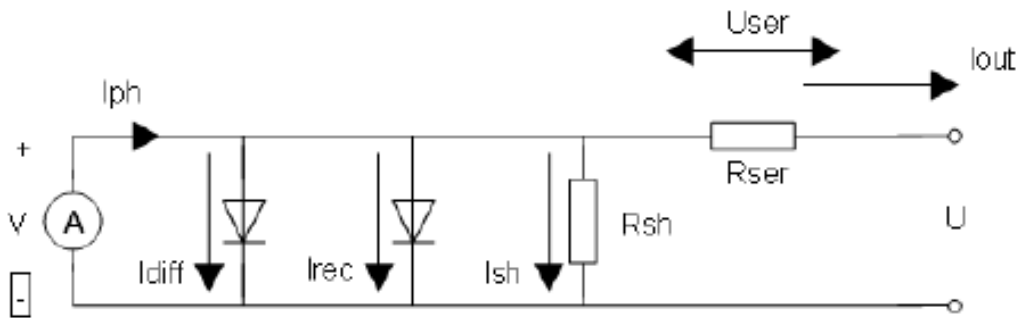


Figure 5. The 2-diode model describes the inner characteristics of a solar cell.

$$I = I_{ph}(E) - I_{diff}(T, V, I) - I_{rec}(T, V, I) - I_{sh}(V, I) \quad (7)$$

$$I = I_{ph} - I_{0,diff} \left[ e^{\frac{q}{kT}(V + IR_{ser})} - 1 \right] - I_{0,rec} \left[ e^{\frac{q}{2kT}(V + IR_{ser})} - 1 \right] - \frac{V + IR_{ser}}{R_{sh}} \quad (8)$$

The 2-diode model seen in Figure 5 is used to describe the losses from recombination and diffusion in the silicon as well as losses due to connective material such as grid fingers and bus bars. The relationships are described in (7). It can be seen that the output current ( $I$ ) is equal to the photon current ( $I_{ph}$ ), directly depending on the luminous flux on the cell, subtracted with the diode losses ( $I_{rec}$ ,  $I_{diff}$ ) and the shunt current  $I_{sh}$ . In (8) the same relationship is stated but here also considering the diode characteristics, shown by the exponential expressions, depending on the Boltzmann constant  $k$ , temperature  $T$  and the losses over the series resistance,  $R_{ser}$ . The IV-characteristics are measured from output current and voltage which are corrected regarding the flux according to the formulas. The measurements are carried out at standard test conditions (STC), that is  $E = 1000 \text{ W/m}^2$ ,  $T = 25^\circ\text{C}$  and air mass (AM) 1.5 [6], [9].

The shunt resistance ( $R_{sh}$ ) should be possibly large in order to decrease the current losses over the pn-junction. A smaller  $R_{sh}$  reduces the efficiency especially under low light conditions. The  $R_{sh}$  is extracted from the dark IV-Characteristics. It is the slope of the IV-Curve in a bias range from a 0.08 V backward to 0.08 V in forward bias.

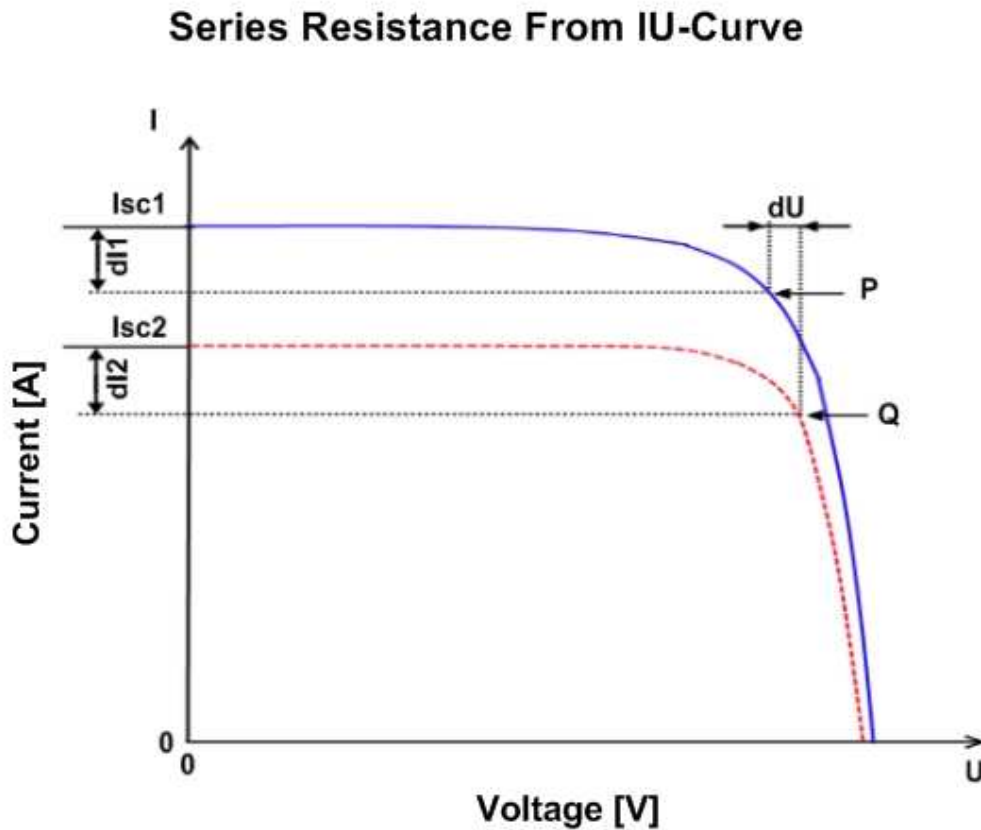


Figure 6. The series resistance decided from measurements at 1000 W/m<sup>2</sup> and 500 W/m<sup>2</sup>.

$$R_{ser} = \frac{U}{I_{sc1} - I_{sc2}} \quad (9)$$

To calculate the series resistance  $R_{ser}$  two measurements, as seen in Figure 6 [12], are used. In this work the irradiance lays at 1000 W/m<sup>2</sup> and 500 W/m<sup>2</sup>, wherefrom the  $R_{ser}$  can be calculated using (9). The two measurements result in a more accurate result. The  $R_{ser}$  influences the power according to the formula (10):

$$P_{loss} = RI^2 \quad (10)$$

The series resistance  $R_{ser}$ , is a combination of different resistances (connector, bars, grid fingers and emitter) and inner diodes. It has not a constant value, but is a function of the current  $I$ . The changes on power from the  $R_{ser}$  can be difficult to measure since a doubled resistance gives about 5 % losses in the power. However to minimize the losses, the resistance should be as low as possible to avoid large voltage losses. The lead corrosion is expected to increase the  $R_{ser}$  [9], [13], [14], [15].

The fill then describes how good the IV curve of the cell or module correlates to an ideal IV relation. Ideally the FF is the top right corner of the rectangle drawn from  $I_{sc}$  and  $U_{oc}$ , which would correspond to a 100 % FF. In reality there is always a knee, where the  $P_{mpp}$  occurs as shown with the black curve, and the FF gives a value of how close to the ideal value it comes. The FF is strongly depending on the  $R_{ser}$  and  $R_{sh}$  [14].

In Figure 7 the red/dotted curve is an example of what happens when  $R_{ser}$  and  $R_{sh}$  are altered. The resistances deform the FF resulting in a lower  $P_{mpp}$ . A decreased shunt resistance lowers the  $I_{sc}$  and an increased series resistance lower the  $U_{oc}$ . The arrows showing the  $R_{ser}$  and  $R_{sh}$  decrease are exaggerated examples just to show the principals. The current  $I$  and voltage  $U$  are affected and not the  $I_{sc}$  and  $U_{oc}$ .

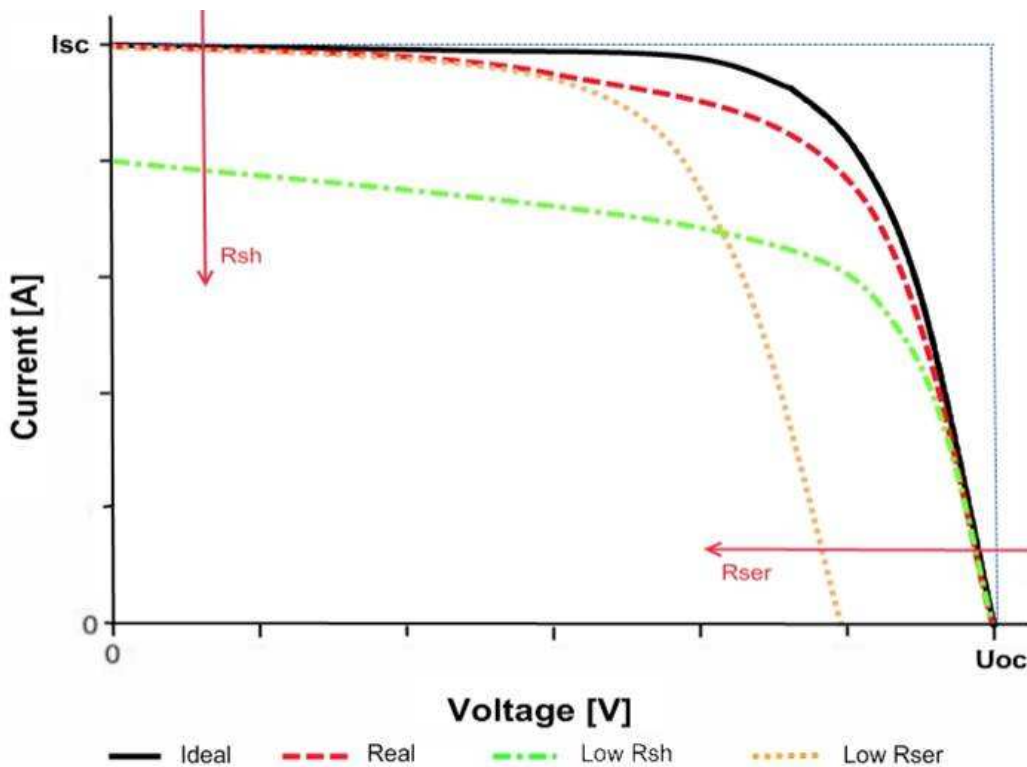


Figure 7. An exaggerated relation between the FF,  $R_{sh}$  and  $R_{ser}$  to  $I_{sc}$  and  $U_{oc}$ .

The cells are illuminated and the current and voltage is measured, hence the I-V characteristics can be resolved:  $I_{sc}$ ,  $U_{oc}$ , series- and shunt resistance and maximum power point (MPP). The test is performed at standard test conditions (1000 W/m<sup>2</sup>, T 25°C) [6]. The power losses are compared to the pre test measurements made. The dark curve gives the shunt resistance, since it will give the best result of the shunt resistance. A double flash at 500 W/m<sup>2</sup> and at 1000 W/m<sup>2</sup> is performed to calculate the series resistance.

The test is performed through a flasher, which reproduces the double flash. Before each measurement the double flash is stabilized and the flash is calibrated with a calibration cell, of the same type as the mono-crystalline cells used in the samples, to give the correct irradiance. By measuring the dark IV characteristics it is possible to calculate a decent estimation of the shunt resistance. First the dark curve characteristics are measured and then a flash of a high transmitting lamp illuminates the cell for around 30 to 40 ms. During the flashes the current,  $I_{sc}$ , and voltage,  $U_{oc}$ , produced by the cell are measured and then a I-V curve is extracted and plotted into a graph. The measured values are saved in .prn ASCII files and .mdb database files, which can reproduce the graphs [4].

### **2.2.2 Degradation/Regeneration**

The degradation of solar modules can be divided into two types: Light Induced Degradation (LID) and Continuous degradation. In a field test or when solar modules are operating, also known as outdoor exposure (OE), both of these degradations work together, causing aging and reducing the power of the module. However in this artificial aging only the latter happens, of course the cells have been exposed to light prior to the tests and therefore some LID has taken place.

Continuous degradation is the aging of the materials due to exposure of light, heat, moisture, wind, physical stress (snow, hail) and so on. There are various tests according to the IEC 61215 standard, where a lot of them are focusing on physical stress, Thermal Cycling (TC) which means the module is exposure to a cycle where the temperature varies between -40 and 85°C according to a set time interval. The focus in this work lays with the Damp Heat (DH), the long time degradation test at 85°C and 85 % Relative Humidity (RH) [6] [16].

In this work the LID and regeneration is not considered giving a major influence over the results which are searched. The description is however needed in order to explain the initial increase in power during the first test rounds. The LID follows from the physical properties of the silicon. When a silicon cell becomes illuminated with long wavelength light, the response of the cell decreases and gives lower open circuit voltage ( $U_{oc}$ ) and short circuit current ( $I_{sc}$ ), see Section 2.2.1, together with lower cell efficiency. Therefore the effect of the cell decreases, the percentage depends on the content of boron and oxygen within the silicon, and this is related to the manufacturing methods and environments. With a temperature treatment of the cell at approximately 175°C, the LID process is reversible; the cell is regenerated.

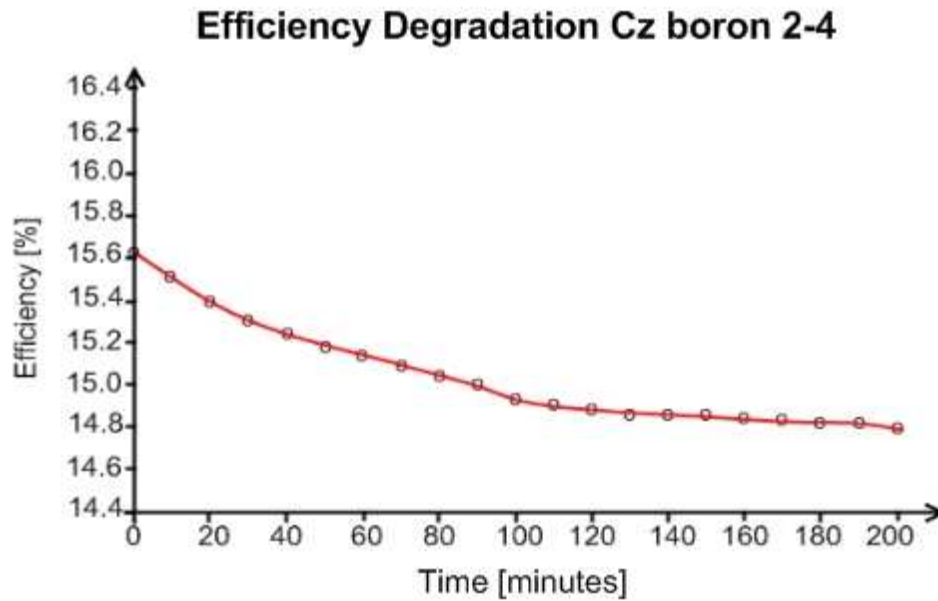


**Figure 8. Efficiency degradation of Cz boron cells.**

It has been shown that the LID can cause a 0.5 % loss in absolute efficiency. From the Figure 8 it is seen that the LID could lead to a power loss of 4-5 % for Cz-mono-crystalline cells [17].By following the steps of OE according to IEC standards the photon degradation is reconstructed.

### 2.2.3 Electroluminescence

In order to make the electroluminescence photos a current need to flow through the cells. Due to the current that is flowing through the cell, charge carriers are made available, causing some of the holes and electrons to recombine and emit an electroluminescent radiation at a wavelength approximately 1100 nm.

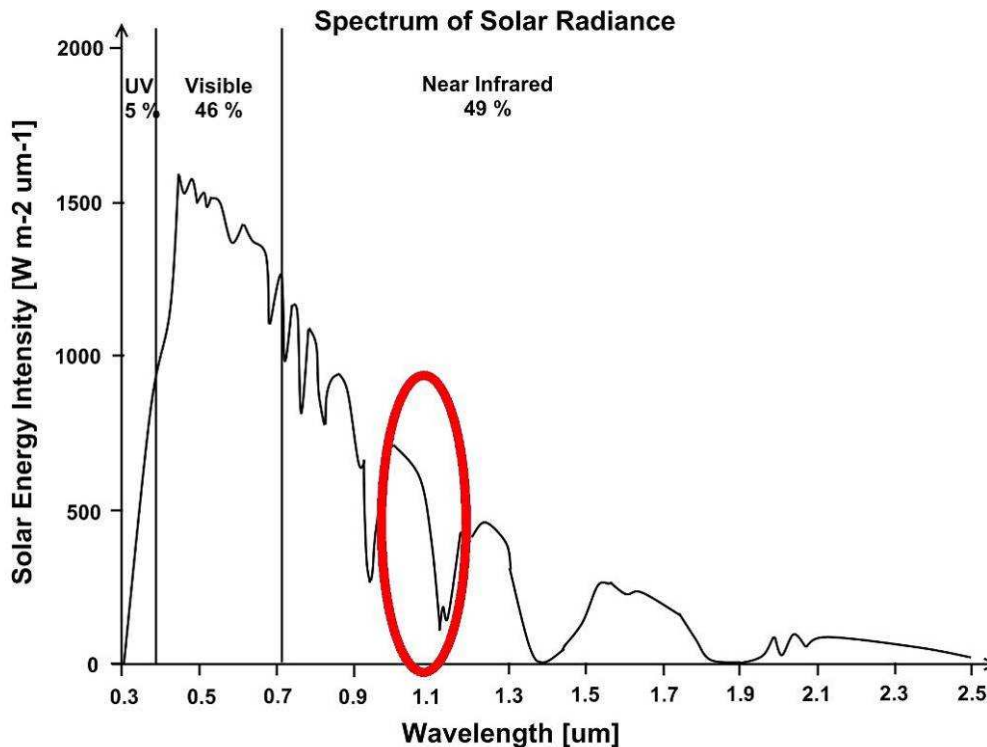


Figure 9. The spectral region concerned for the EL pictures.

The cell or module is connected to a power supply in order to get a suitable current flowing through the cell in forward bias at small voltages. The correct direction of the current can be seen due to the much larger voltage that would be needed to get a current flow in the reverse direction.

A camera according to the listings in Chapter 3.3 with a sensitive object and a filter to reduce the visual light is used. Cameras have their largest sensibility in the visual spectral region but for the EL a picture around 1100 nm, as seen in Figure 9, is needed; at the far end of the camera sensor abilities. Therefore a long shutter time is required in order to get a good photo.

With the EL picture it is possible to see some of what is going on inside the cells, cracks or if the cells are broken will be easy to see. Brighter areas indicate a good condition of the cell. There is also a possibility to see darker areas, that implies shunts (low  $R_{sh}$ ), high  $R_{ser}$ , bad material quality, cracks, broken parts and some manufacturing traces (from machines). In these dark areas the current does not flow as easily. Cracks can be seen as black lines that diagonally crosses the cell. Micro cracks as small, black stripes, often seen close to the bus bars [10].

For the cell type chosen for these tests the current is approximately adjusted to the  $I_{sc}$ , therefore 7.0 A is used, which requires a voltage of 1-2 V, the cell voltage is about 0.7 V and the higher voltage needed is caused from the larger series resistance caused from cables, leads and bus bars. Corrosion does also increase the voltage due to a worse connection between clamp and lead. The samples are placed on a table with the camera hanging directly above them. The current is connected and the photo is taken. The shutter time is chosen to 10 seconds to give a clear picture of the cells.

## 2.2.4 Transmittance

In order to measure the degradation in the glass, encapsulation and back sheet materials further a transmittance test is performed.

Light is passing through, first with only air between the lamp and the sensor, and then with the sample breaking the light and entering an integrating sphere where the measurements with and without sample are compared. Then the results are plotted as transmittance rate over wavelength. The test equipment used is connected to a computer via USB. The spectrometer is working in the spectral range from approximately 400 nm to 1100 nm. The measurements are performed in a darkened room, at room temperature 25°C.

At first the measurement software needs to be calibrated, that is, cut of the surrounding light sources and stabilize the transmittance from the test lamp. A dark spectrum is measured, then a reference spectrum and when the sample is placed between the lamp and the measure sphere the difference in transmittance are measured.

### 3 Tests & Measurements

Type	Examples		
	Weak	Medium	Heavy
Corrosion			
De-lamination			
Discolouring			

**Table 2. Expected visual ageing appearances of the modules.**

The samples were constructed using the same type of materials to create as equal results as possible. Due to different test temperature and pressure, when comparing the DH and HAST, the different samples A – C respond differently, because of variations in temperature and material characteristics. All the measurements have been conducted as equally as possible for the samples, following STC standards or in dark rooms at room temperature, 25°C, for transmittance and EL. Calibrations have been conducted using the same calibration cell.

Due to the long testing time for 110°C HAST and the too high temperature in 130°C, that caused the C sample embedding material to melt, the standard for comparing have been chosen to 120°C HAST test. Partly the other will be discussed in order to show likenesses or differences supporting the theories, since the pressure inside the HAST chamber creates a different environment compared to the normal pressure environment in the DH.

The test time maximal extent was to the middle of February, hence limiting the DH to 2000 hours and the HAST 120°C to some 144 hours. From measuring every 12 hours a change to 24 hours and then 48 hours for the 120°C and 130°C samples and 48 hours for the 110°C tests was made in order to speed up the results of the aging process. The Damp Heat at 85°C and 85 % RH samples have been measured every 500 hours in order to achieve a continuous development of the samples in the environmental chamber. In order to compare the two tests it is needed to find some distinguishing characters of each time region. A physical difference to exist between the two test chambers; in DH the samples lie on a horizontal layer while in HAST they stand vertically. In this thesis any possible differences regarding the position in the test have been ignored, while the pressure in the HAST is assumed to create an equal moisture in the chamber without concern to the position.

Notable is that between 1500 and 2000 hours an error occurred with the DH chamber, causing the moisture level to sink to 75 %. The test is continued anyway, taking in regard that the aging process might have slowed down.

### **3.1 Design**

The design of the samples and test equipment are crucial for the result of this work. Therefore a description of materials, processes and test equipment will be shown. Since the interest lies within the establishing of a correspondence between the DH and HAST tests and not to test new materials. However some advantages with other materials have made them better suited than normally used materials. The base of what is relevant for the manufacturing of today and some what will be used in a near future make the foundation of the material selection. The normal construction of a mini solar module was shown in Figure 1.

#### **3.1.1 Materials**

The basic part of a solar module is the cell; chosen are mono-crystalline cells since they are stable. All samples have the same cell type in order to make comparable results for the different substrates/samples. However the mono-crystalline cells are reacting to heat exposure and a regenerating process within the silicon takes place, resulting in a power increase of up to 5 % [17].

The only differences in the composition of the substrates there are various embedding materials that were used. Three types were used for the modules, one EVA and two thermoplastics. One of the embedding is chosen because of known bad results (fast degradation time) with aging tests in order to provoke some early results. The two other are well known stable materials.

The back sheet foil is a material that protects the sensitive embedding materials from moisture and UV-light. A transparent back sheet foil is used because it will allow inspections of the backside of the cells and also measurements of the transmittance, without having to leave a clear spot of glass. These advantages make this type of foil preferable with rather than the normally used non-transparent foil.

The glass size is chosen to be large enough to minimize leakage due to small areas between the cell and the edge of the glass. Another crucial point is also that the samples must fit into the HAST chamber used. Thus the maximum size of a module is 200 mm across, allowing up to 10 samples to run parallel in the HAST chamber. Therefore the 200 x 200 mm glasses are chosen and for a correct relationship with DH, the 200 x 200 mm glasses are used for these samples as well. A crystal clear glass is to prefer before a structured one while it allows a good view of what happens inside the module and allow the measurements to be performed with a low influence of the glass surface.

The cells were pre-stringed from the production with an automated stringer and only the cross leads providing the connection to the cells without damaging the materials of the module are soldered by hand. As a comparison naked cells (soldered) will go through the same tests.

### 3.1.2 Sample Design

Five cells for each sample are built, giving a total of 15 modules and five naked cells for each test type. The five cells should give a sufficient statistical result. Also each HAST test can be shortened to two runs per HAST temperature as 10 cells fit into the chamber. The DH chamber is large enough for all samples at once. The transparent materials for embedding and back sheet foil, together with the clear glass offers a good environment for visual inspection and for transmittance test. It also enables the possibility to see what happens on the back of the cells, what would be impossible with a coloured back sheet foil. The same glass and foil type are used for all samples. The leads out of the module are hand soldered to the already pre-stringed cells. The leads both come out on one side of the module to allow easy measurements. Since all samples, including the naked cells, are built up on the same structure, the lead resistance should be similar in all cases and provide comparable results. The sample structure is shown in Table 1 and the prototype is shown in Figure 10. The typical module design for all samples.

Sample	Glass	Cell	Embedding	Back sheet foil
A	Crystal	Mono-crystalline	EVA	Transparent
B	Crystal	Mono-crystalline	Thermoplastic	Transparent
C	Crystal	Mono-crystalline	TPU	Transparent
D	-	Mono-crystalline	-	-

Table 3. Modules and test sample structure.



Figure 10. The typical module design for all samples.

## 3.2 Sample A

All samples of the A type managed the lamination process well. There were no broken cells or cracks to be seen in the EL photos afterward, except from some micro cracks that are not known to influence the cell performance in a greater sense. The micro cracks are seen on 5 of the totally 20 A sample cells. Visually they all have a clear transparent combination of glass-embedding material-back sheet foil.

Unfortunately it was not possible to measure the IV-curves for the DH samples due to the long test time and the DH needed to begin as soon as possible, therefore only the HAST samples were measured. Comparing the result of the HAST measurements before and after lamination there was a maximal voltage loss in  $U_{oc}$  of 1.3 mV (H2-A2),  $I_{sc}$  of 0.15 A (H1-A3) and  $P_{mpp}$  of 0.08 W (H1-A1). Generally the modules have a 1.2 % lower  $P_{mpp}$ , 1.5 % lower  $I_{sc}$  and 0.1 % lower  $U_{oc}$ , taken as a percent difference, comparing pre-laminate and laminated samples, of the averages of all modules and cells.

### 3.2.1 Damp Heat

At the first measurement of the Damp Heat there were some interesting changes to the samples. The previously completely transparent modules had developed a white haze inside the material making it difficult to see through the materials. The area over the cell was not showing any large change to the bare eye comparing how clear the cell was seen underneath the glass, possibly giving the explanation that the haze lies in the embedding material – back sheet foil combination rather than glass – embedding material. This theory was also supported by the IV measurements since no large loss in power occurred the first 500 hours of DH.

Visually the A sample starts to show changes already at 500 hours of testing, where a white haze appears seen in Figure 11. In the figure it is also seen that over the cell itself there appears no white discoloration, what implies that the change lies with the back sheet foil or the combination embedding material – back sheet foil. When the samples are held against a light yellow/brown tone is seen through the materials, compared to the white light passing outside the module. At 1000 hours this would also prove itself as the embedding composition has gotten a clearly brown tone, Figure 12. The discolouring of the module continues slowly to worsen until 2000 hours.



**Figure 11. The sample A shows a white haze after 500 hours, appearing after being all transparent at the beginning.**



**Figure 12. At 1000 hours the white haze has a brown tone.**

The corrosion began at 500 hours, mostly on the part of the connector leads, that are outside of the protective closure, but also at the backside of the bars inside the embedding, Figure 13. After 1000 hours it is also possible to see some corrosion appearing around the edges of the leads, coming over to the front side, Figure 14. At 2000 hours there were signs of severe corrosion as the bus bars on the back side of the cell starting to show a blue-green colour, meaning that the corrosion now has reached the inner copper core of the leads, Figure 16. At the connection leads, a brown discolouration growing out from the corroded metal leads into the embedding. This would with further aging worsen and possibly cause de-lamination.



**Figure 13. The fronts of the DH-A3 lead after 500 hours DH and the clearly corroded back side of the same lead.**



**Figure 14. DH-A2 show beginning corrosion on the front side leads as well.**



**Figure 15. At 1500 hours DH-A show corrosion on the bus bars on the back of the cell.**

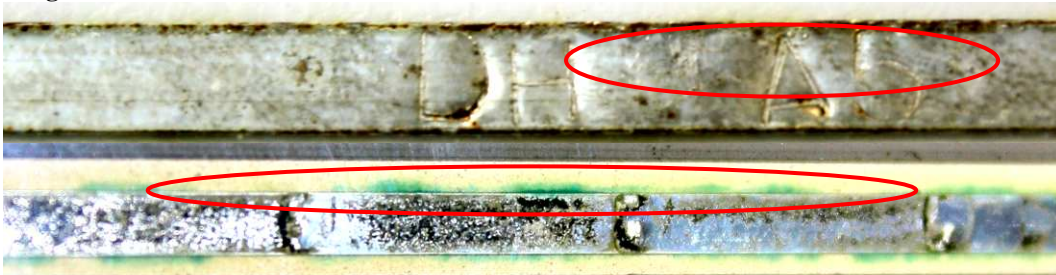


**Figure 16. DH-A5 at 2000h front side corrosion and at the back side bus bar also green copper corrosion is to be seen.**

There are de-lamination signs showing on the A sample in the edge region of the glass. They appear after 1000 hours of testing and look like the back sheet foil is being drawn towards the middle of the module. This leaves a strip of de-laminated back sheet foil at the corners where the embedding no longer grips to the foil. After 2000 hours it has expanded, now covering all the edges of the module with an up to 8 mm loose area, Figure 17 - Figure 19.

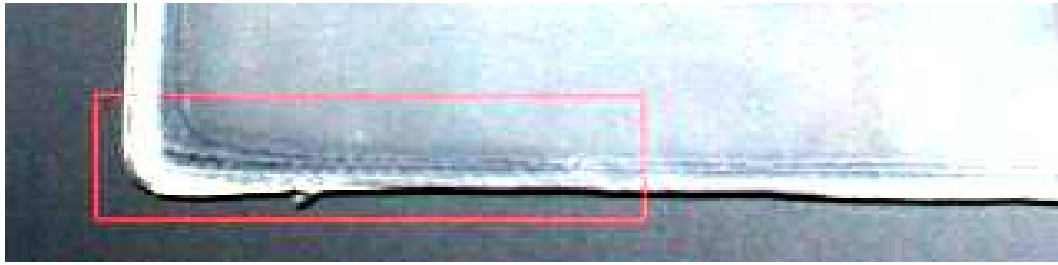


**Figure 17.** The sample A show a proceeding de-lamination at the corners at 1000h, it is seen that the back sheet foil no longer grips the glass.



**Figure 18.** At 1500 hours it is slowly getting worse, now covering the entire edge of the cell.



**Figure 19.** At the 2000 hours stage the sample A de-lamination at the edges is clear.

Due to the haze, the transmittance features had naturally changed. It was a clear reduction of the transmittance features of the non aged modules; Figure 20 show an integrated average of the transmittance development over the time together with a trend line. The value decreased from 0.88 at 0 hours to 0.80 at 500 hours, which is with almost 10 %. Figure 21 show the transmittance spectra at the different measurement points. The transmittance degradation continues over the test time until 2000 hours when an improvement is seen, where the transmittance suddenly increases from 0.61 to 0.69, with 13 %. From the figure a 5 % loss of transmittance appears after 500 hours, that gives a 1% loss every 100 hours. Considering the DH test time of 1000 hours to correspond to 20 years it can be interpreted as 1 % loss every 2 years or 0.5 % per year or 50 hours. A base of the degradation can therefore be set at 0.5 % per year. The average trend line is placed higher than the measurement points, this because the transmittance improves itself at 2000 hours, and the line is calculated on the average slope.

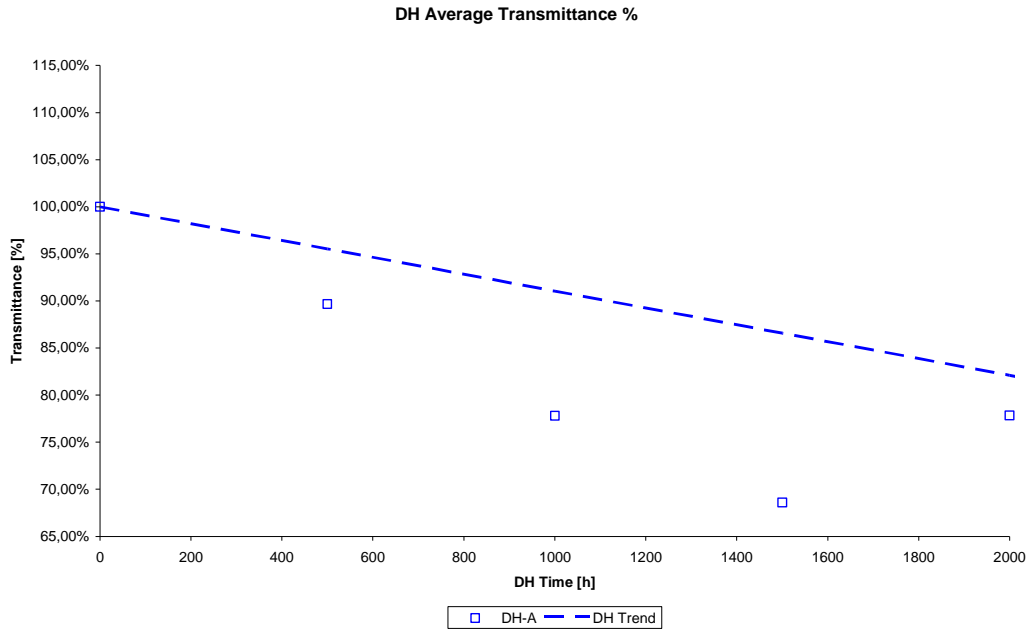


Figure 20. Transmittance average for DH over test time.

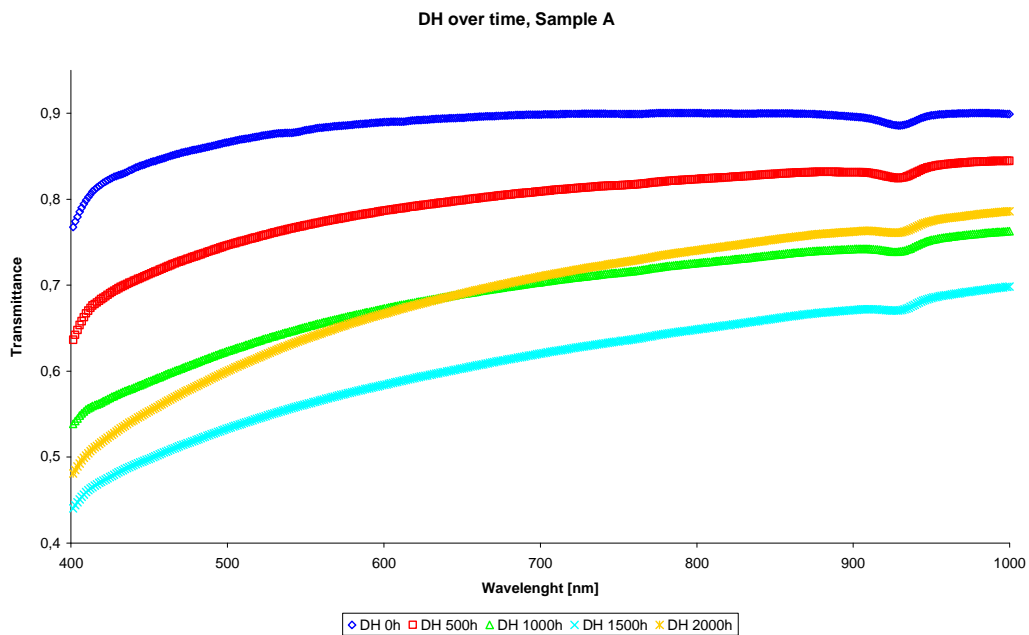


Figure 21. The DH-A samples at 0, 500, 1000, 1500, and 2000 hours.

Since there are no large differences in the IV-curve of a typical DH-A sample seen in Figure 22, taken at the transmittance extreme values at 0, 1500 and 2000 hours. The conclusion is that the change in transmittance rather lies behind the cell in the embedding material or in the transition between embedding material and back sheet foil.

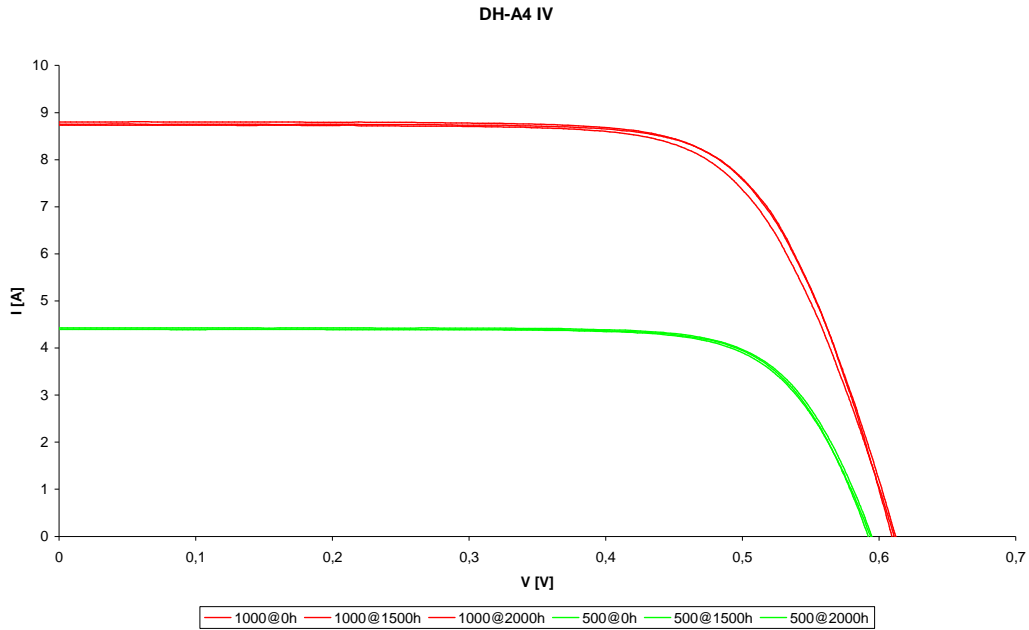


Figure 22. IV-characteristics at 0, 1500 and 2000 hours of DH for DH-A4

The power degradation of the modules are as expected relatively small as seen in Figure 23 showing the  $P_{mpp}$  development. A 1 % decreases every 800 hours leads to 400 hours of testing in order to achieve 0.5 %

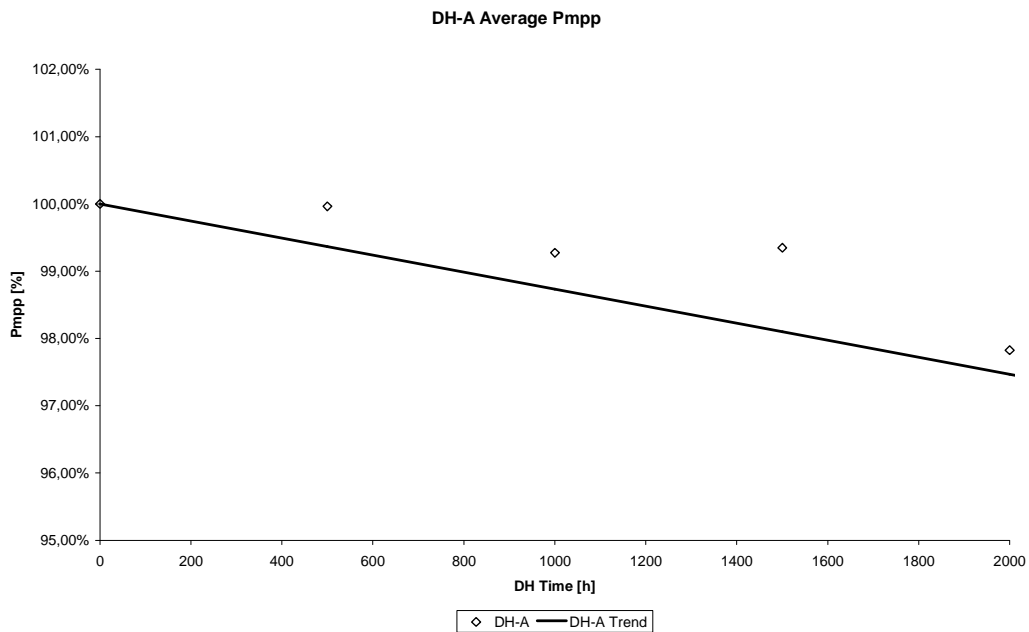
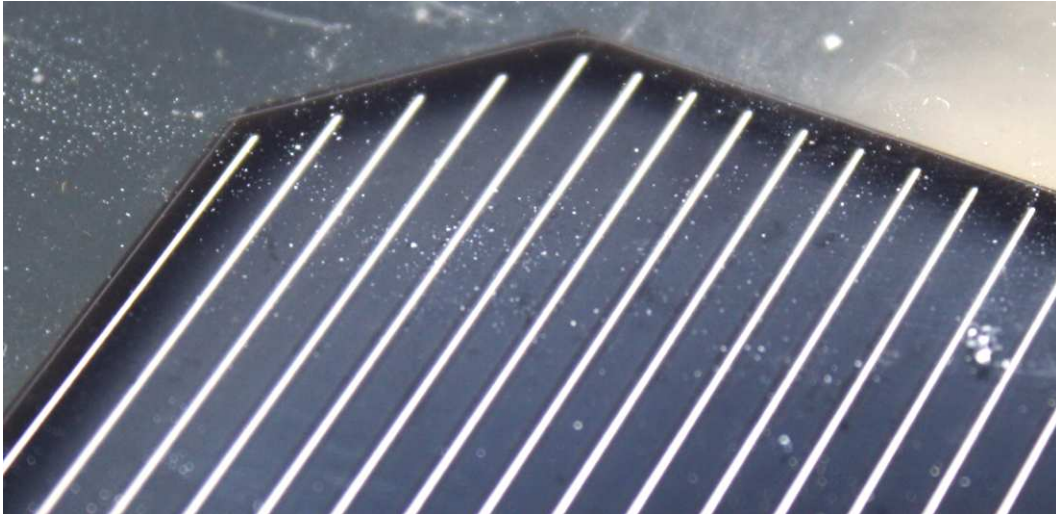


Figure 23.  $P_{mpp}$  degradation over DH test time

### 3.2.2 HAST

In difference to the Damp Heat the HAST does not cause a white haze in the embedding material. A reason is that the higher temperature, close to the laminating temperature about 140°C, suits the sample A materials better than the lower DH temperature. However, in the case of HAST testing, a white haze appear over the cells. At 48 hours a light browning could be seen in the transparent embedding, but not in the same extent as with the DH samples. There was no recognisable change to the bare eye over the test time.



**Figure 24. Pale area on the front side of the H3-A cells at 48 hours.**

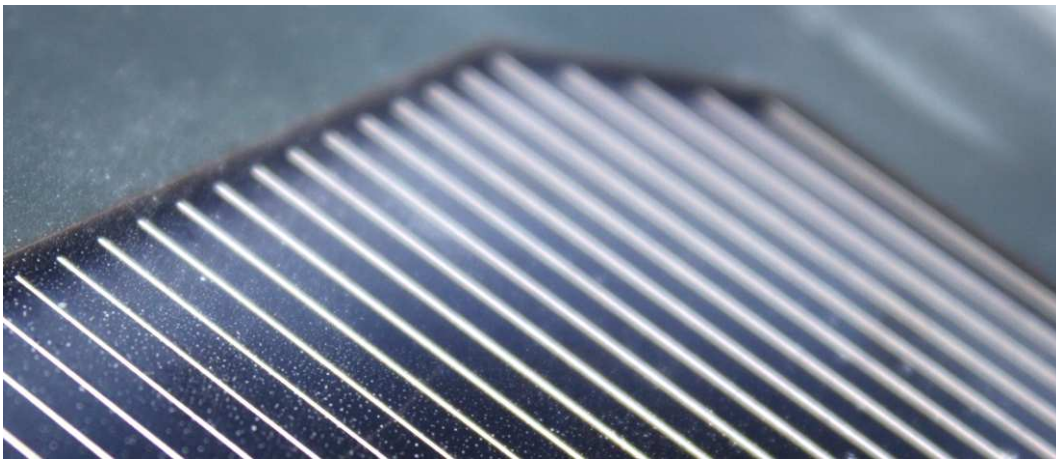


**Figure 25. The H1-A samples also show a clear discolouring above the cell after 72 hours.**

At 12 hours in the HAST a light corrosion on the outer leads appears, however the embedded part are almost unaffected from the test. During the test time the corrosion grows until covering the complete bars at 144 hours.



**Figure 26. No corrosion after 12 hours.**



**Figure 27. Corrosion inside the A sample at 48 hours of HAST on the back of the lead.**



**Figure 28. Here H2-A2 showing front side corroded leads after 72 hours.**



**Figure 29. H3-A3 front side corrosion after 96 hours.**



**Figure 30. Corroded back side bus bar in the H3-A samples at 72 hours, this occurred at 96 hours for the H2 samples.**

Regarding de-lamination at the edges, the back sheet foil was not gripping already after 24 hours. In the A sample a small area could be seen on the H2-A2 sample above the cell; a group of small bubbles between glass and cell Figure 33. These bubbles were however not expanding over the test time, so it does not seem like it is a degradation de-lamination.



**Figure 31. HAST 24 hours: A samples show some de-lamination at the edges similar to DH.**



**Figure 32. The same view of the A module at 48 hours. Now the embedding have a light browning but the bubbles does not seem to expand. The de-lamination at the edge is also seen.**

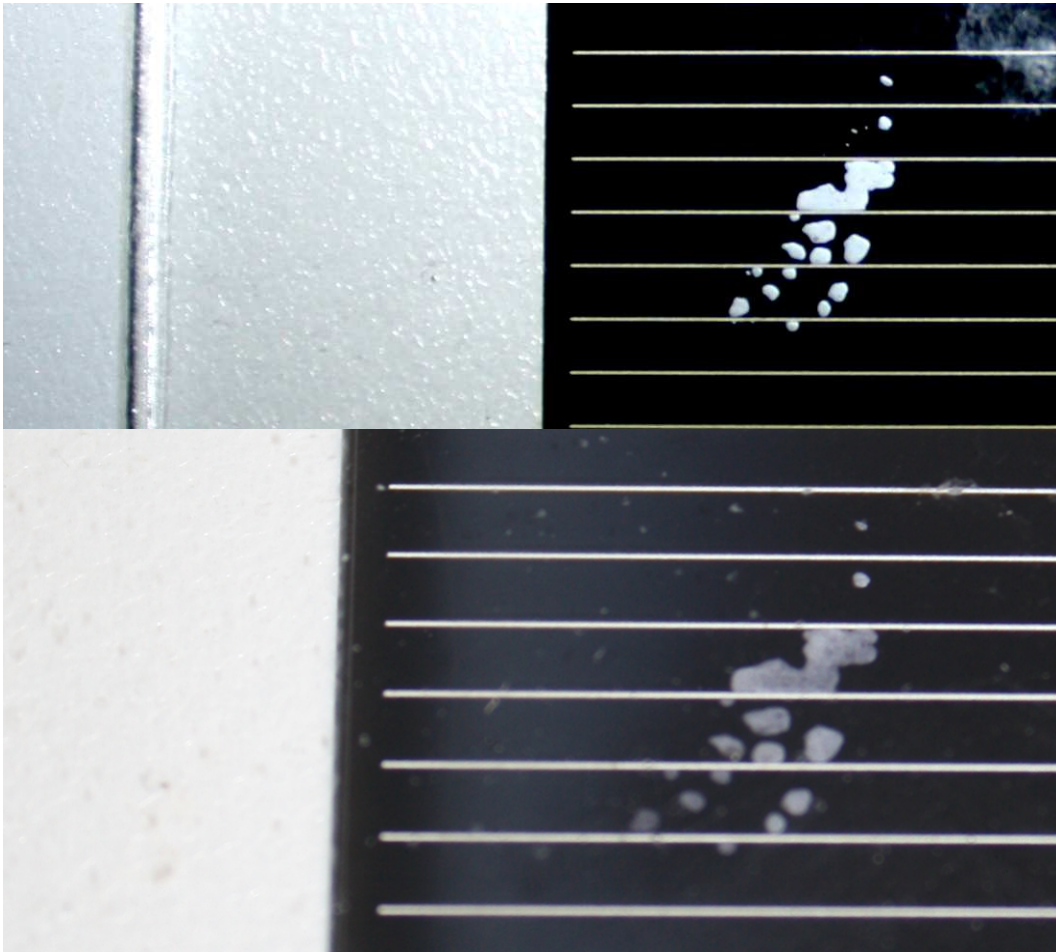


**Figure 33. The A modules are still transparent (left part) in difference to in DH and some bubbles between cell and glass at 24 and 48 hours.**

In the transmittance there is a degradation also in the HAST, but not as fast as expected from the theory. The fastest HAST, at 110°C, arrives the 80 % break first after 250-300 hours following the trend in the Figure 34. The other two; 120°C reaches 80 % after 400 hours and 130°C after 500 hours. This does not relate to the theory, where each 10°C step should reduce the time to the half. That is if the 110°C last 300 hours, 120°C should be 150 hours and 130°C 75 hours. This could however be explained taking in regard that the worst visual degradation took place at 85°C, that is the higher temperature seem to reduce the transparency degradation.

In Figure 34, it is seen that a similar process takes place in the transmittance for the H2-A samples. It reaches the lowest curve at 72 hours and then improves itself up to 144 hours. This could suggest approximate 70 hours of HAST correlation to each 1000 hours of DH. 144 hours would then be around 2000 hours of DH, where an improvement in transmittance was seen.

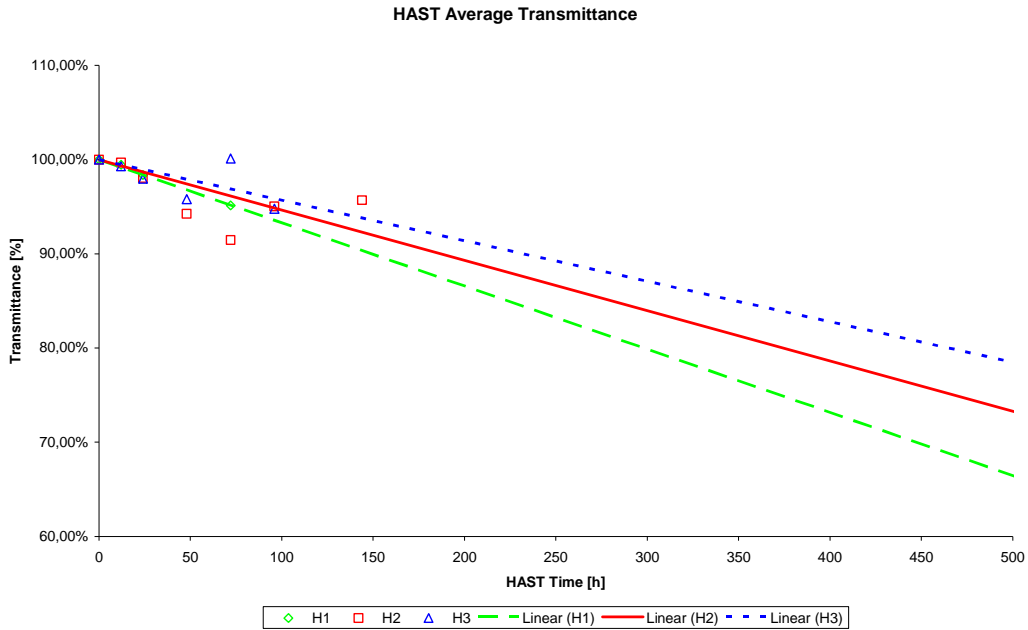


**Figure 34. Transmittance average for HAST (H1: 110°C, H2: 120°C, H3: 130°C) over test time.**

In the Figure 35 the integrated average of the transmittance curves is shown. A 5% reduction can be read out at approximately 130 hours. This gives 1 % every 26 hours and the 0.5 % rate at 13 hours. A lowest measurement is made at 72 hours and then the transmittance recovers according to Figure 36. The IV curves at the extreme values at 0, 72 and 144 hours are basically constant and does imply that the transmittance reduction have not taken place between cell and glass Figure 37.

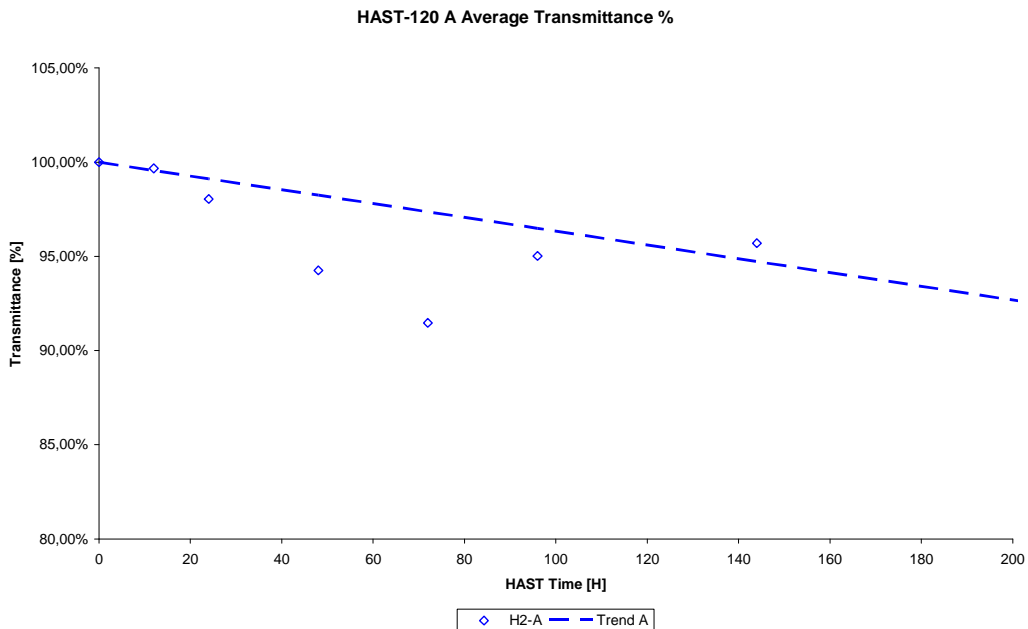


**Figure 35. HAST 120°C A sample transmittance degradation with trend line.**

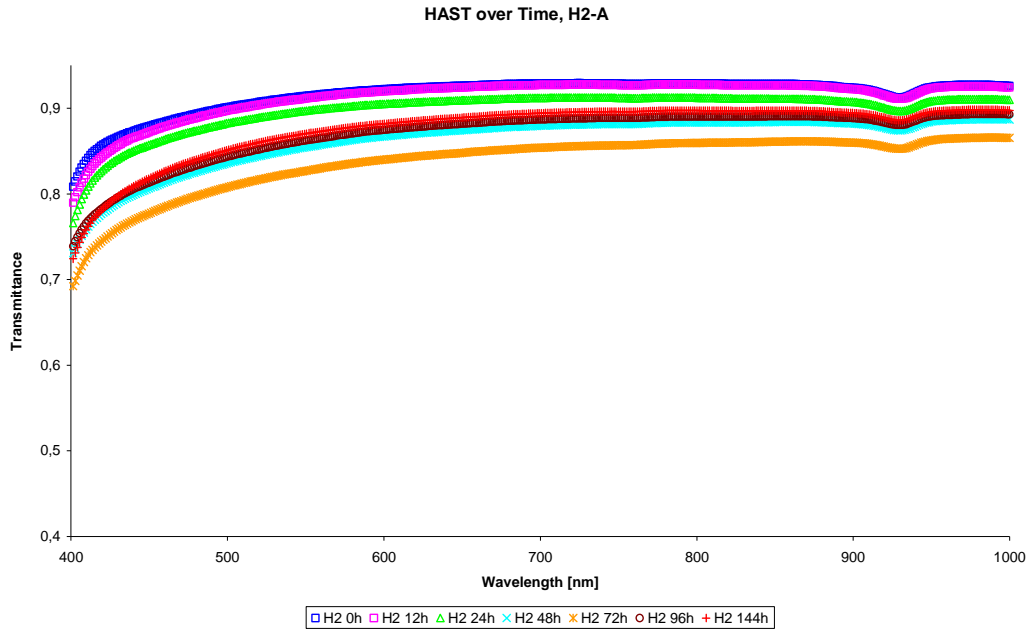


**Figure 36. The time variation of the HAST sample A at 120°C.**

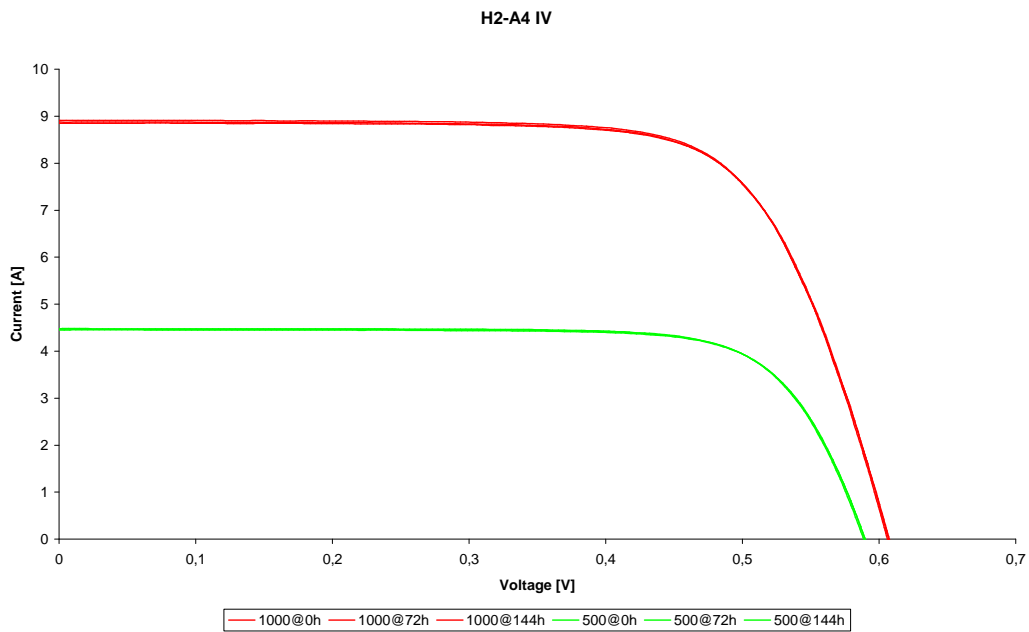


**Figure 37. IV-curve for H2-A4 at 0, 72 and 144 hours.**

Figure 37 show that the same conclusion can be made regarding the IV-curve and transmission as with DH, that is, the changes lies rather with embedding behind than in front of the cell.

The power decrease in the case of HAST 120 °C, seen in Figure 38, show of a 0.25 % decrease in 130 hours, this can be approximated to 0.5 % in 250 hours.

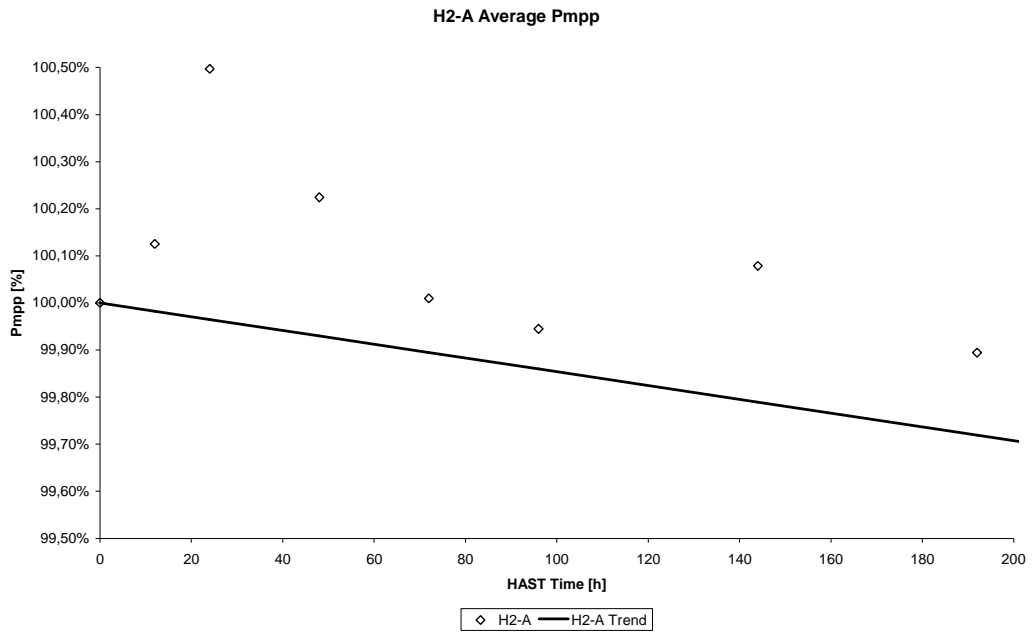


**Figure 38. H2-A sample P<sub>mpp</sub> average over test time.**

### 3.2.3 Comparison

The visual control of the cells gave a couple of similar developments, and some totally different. The variation in colour were most likely to trace back to the temperature ranges the DH and the HAST works in. Corrosion appears faster in HAST, already at 12 hours the first signs were there on the outer leads. However 12 hour would relate to somewhere less than 250 hours in DH and the samples in the DH chamber could not be inspected at that moment.

Figure 39 shows all the integrated average transmittance values for DH and HAST samples. The HAST time scale has been corrected to 500 hours and it shows an almost parallel degradation in 110°C, the other two were close as well. Although not meeting the expectation of reducing the time it shows that there is a connection between the two tests and the materials tested have to be considered regarding the results and the test type.

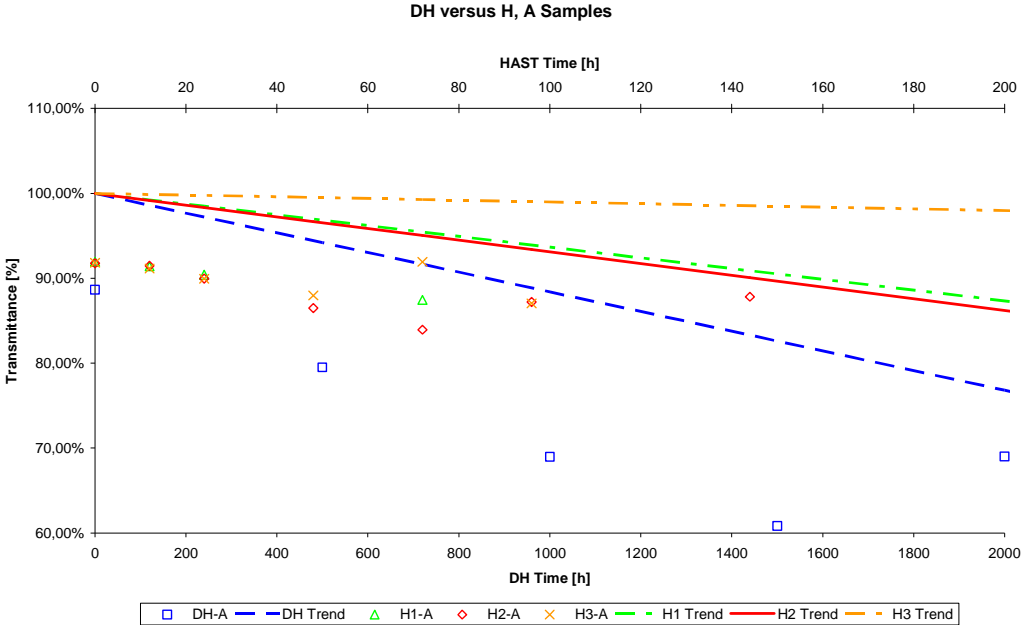
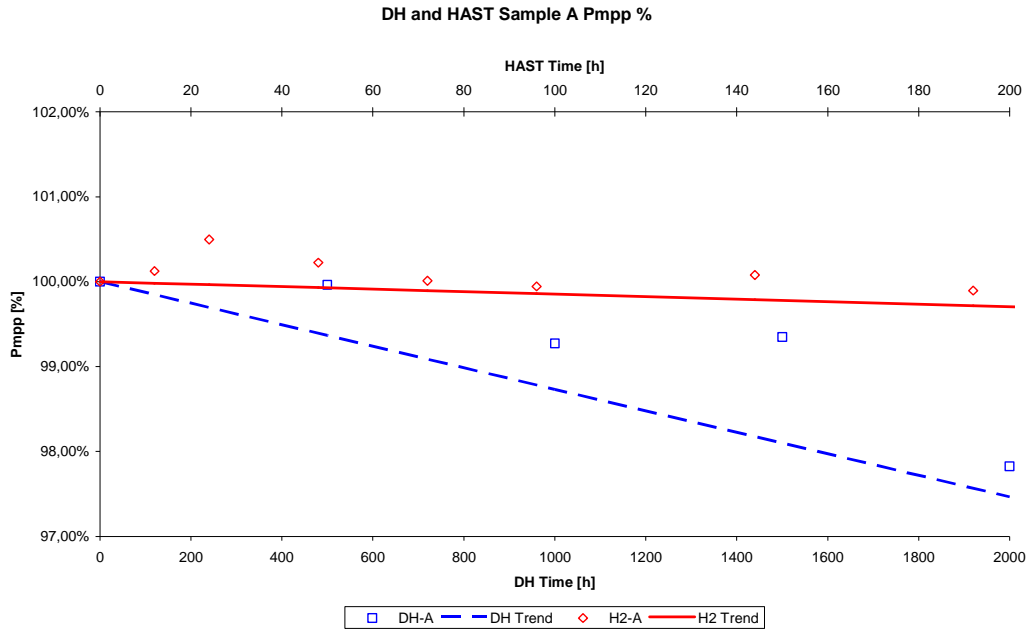


Figure 39. The different test types, DH and HAST, compared in transmittance development.

Considering the results of the 0.5 % degradation from Chapter 3.2.1 and 3.2.2 the following relation appears: in DH the 0.5 % time was 50 hours and in HAST 13 hours. This would result in an acceleration factor of 50/13 that is around 4 times faster testing in HAST.

Due to the initial power increase the trend of the HAST power is also increasing, since the effect of this is much smaller in the DH the trend is not influenced. Figure 40 shows the trend lines in both cases. The figure show that the degradation for the A samples seem to go far slower than with 10 times the speed, giving the AF of 4 from the transmittance more relevance. However it is needed to remember that the power degradation normally work slower in artificial aging compared to real life experience. The heavier degradation in DH have also been supported by the lower temperature HAST being more similar to the 85°C DH. If assumed that the transmittance degradation would be equal in both tests the power trends would also close in on each other.



**Figure 40.** The measured values and the trend lines corrected of the top value after regeneration with base of 100 % for DH and HAST.

The series resistance grow at a rate of about 5 % every 1100 hours in DH and 1 % every 180 hours HAST, Figure 41. The relationship in the  $R_{ser}$  development gives a 110/90 correlation, that is the A samples  $R_{ser}$  increases only 1.2 times faster in HAST.

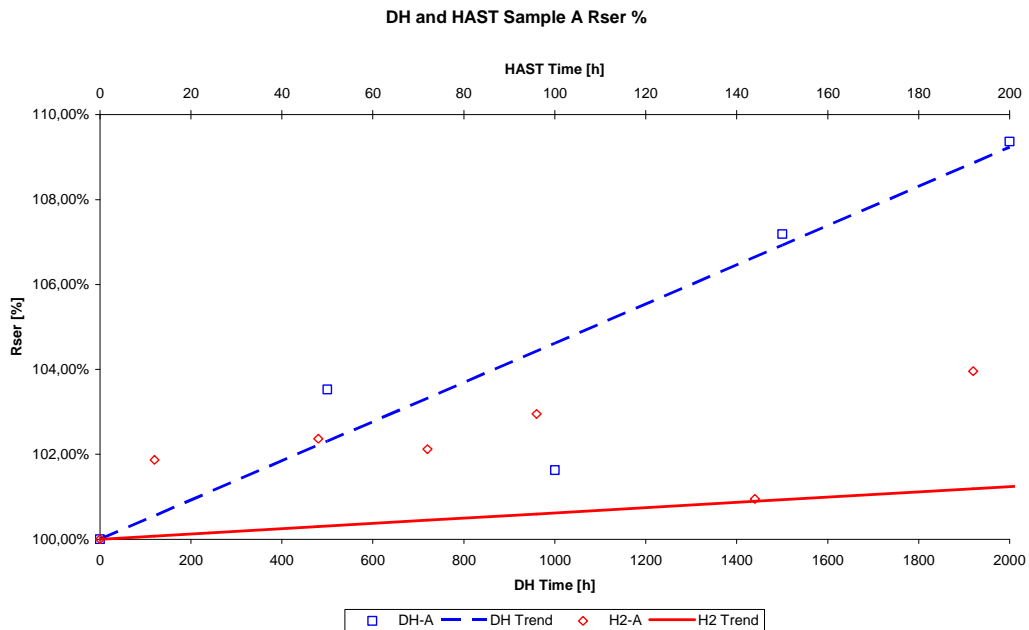


**Figure 41.**  $R_{ser}$  of DH and HAST.

The slow increasing rate of  $R_{ser}$  and the difference in  $P_{mpp}$  averages are of course tied to each other. As known from previous work, the power degradation is slower in the artificial test compared to the outdoor exposure. A possible conclusion is that the higher temperature causes a slower degradation concerning the power and resistance.

### 3.3 Sample B

All cells of the B sample have a thick white haze inside the embedding material, however not covering the cell in the same extent. Two samples had visible cracks after lamination and one skew module was produced. On the module DH-B3 the back sheet foil slipped during the lamination and brought the cell with it. However the cell itself is still covered from protective embedding and only a part of the lead comes out in the open.

The sample B has an amount of cells with cracks and other misfortunes that appeared during the lamination process. Only three of the samples do not have cracks, micro cracks or completely broken cells. However the cracks have occurred during the lamination, and since the module itself is intact and the performance is measured before the test starts it should not affect the degradation.

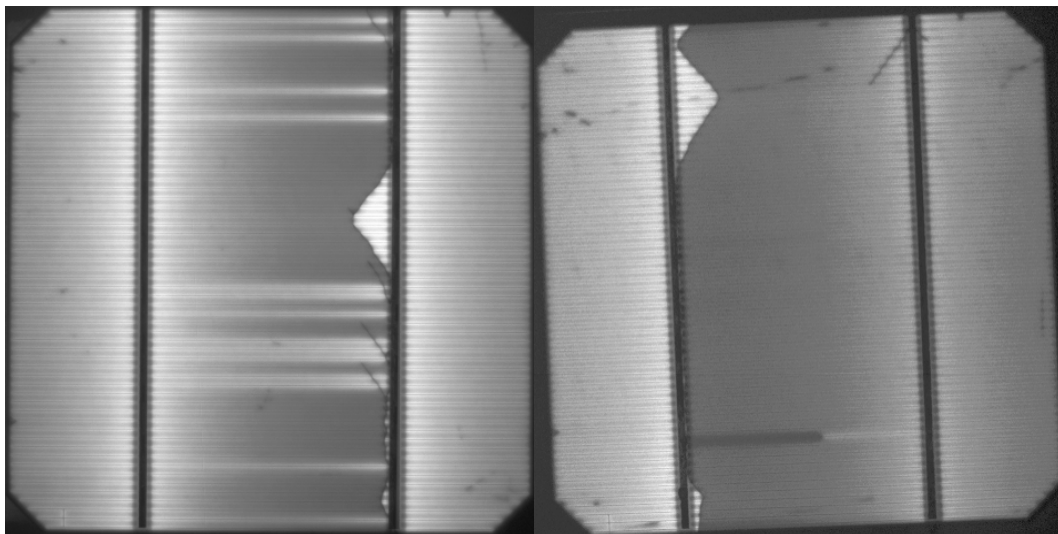
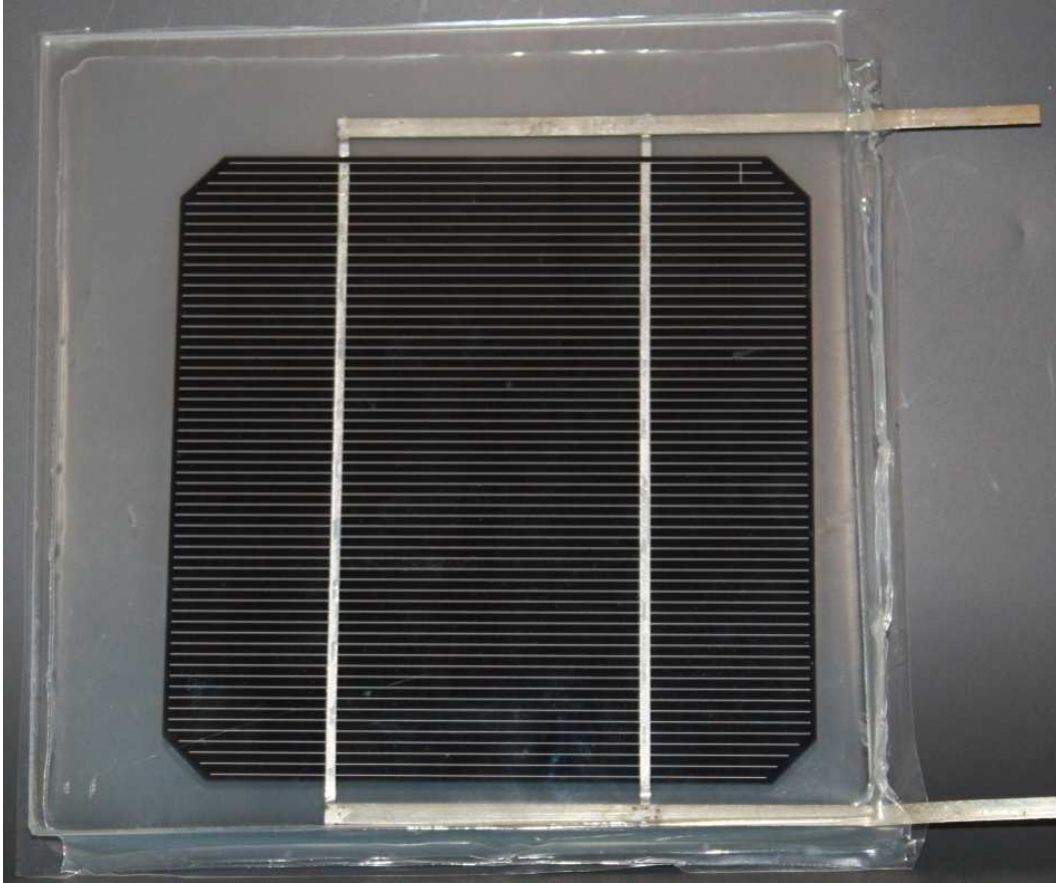


Figure 42. DH-B3 and H2-B3, completely cracked after lamination.



**Figure 43. The back sheet foil slipped on the DH-B4.**

The largest changes in IV-characteristics are of course the broken cells. The H2-B lost 0.27 W or 6,8 % of its power due to the crack when laminated. The average change in current and voltage are of minor effect,  $I_{sc}$  lost 0.7 %,  $U_{oc}$  0.2 %. The average power loss was 1.2 %, which is in average exactly the same  $P_{mpp}$  loss as in the A sample.

### **3.3.1 Damp Heat**

It was not expected after the bad results with the lamination, but the B samples cleared up in transparency and improved. No signs of corrosion or discolouring, not considering the white haze, which was better than after lamination. The B samples are showing the best results in the DH of all the materials. Except from a small discolouring covering the back side as seen in Figure 44, there is no visible degradation. The spots have a yellow colour and are only to be seen close to the bus bar, which are remains from the flux used by soldering. The transmittance even seems to have improved, since the white haze has withdrawn itself compared to just after lamination.

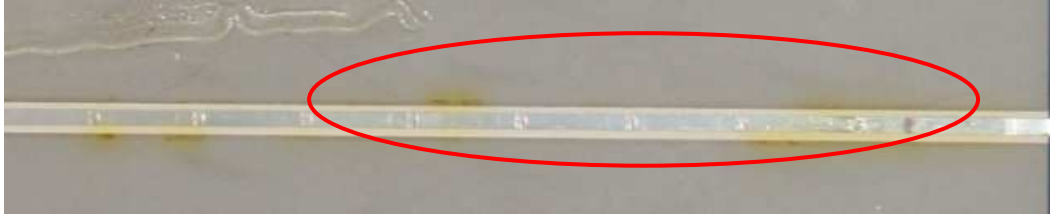


**Figure 44.** The back side bus bars of the DH-B3 at 500 hours, showing the typical discolouring of the B samples. The smudge in the left corner is left over from the lamination is what caused the cell to crack.

No corrosion is to be seen inside the embedding. The DH-B4 is the first sample to show inner corrosion at 1500 hours, this due to the sliding that occurred during the lamination process, which caused one of the bars to be exposed outside of the protective glass.

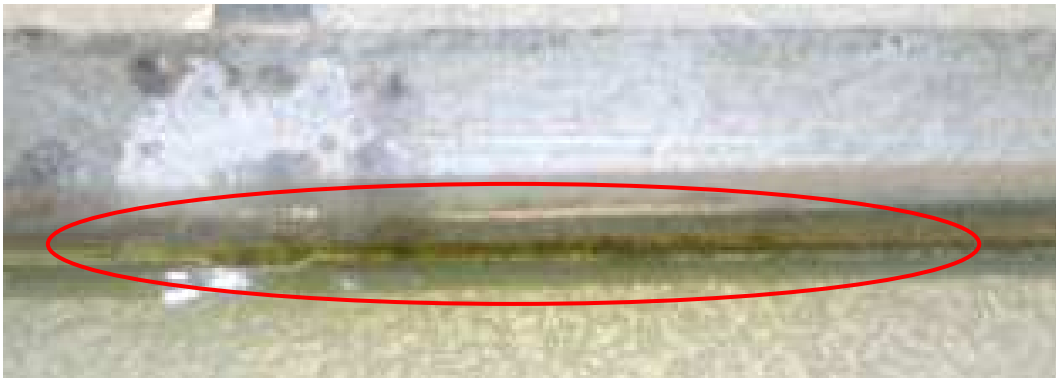


**Figure 45.** B sample corroded only at the skew cell DH-B4

Apart from these two factors more or less nothing seem to happen to the B samples. The bus bars stayed free from corrosion until 1500 hours, when light brown appeared on the back side of the leads. Even after 2000 hours the only example showing corrosion on the front of the leads are the DH-B4.



**Figure 46.** A small corrosion start to show on the back side of DH-B3, 1500 hours.



**Figure 47.** The typical B sample corrosion after 2000 hours, DH-B2.

Not a single one of the samples show a beginning de-lamination after 2000 hours. Disregarding the outer part of the leads and the white haze that do not influence the power as shown in the IV-characteristics, there is nothing changing for the naked eye with the B samples.

The transmittance of the DH-B shows an interesting recovery after some time in the DH chamber. From the poor results at the beginning the results improved with a 12 %

transmittance gain after 500 hours of DH, in Figure 48 it is seen that after 2000 hours it was beneath the initial improvement again. In Figure 49 the degradation is shown, with the initial 12 % improvement, and after 2000 hours the transmittance has reduced with almost 20 % according to the trend line. A 5 % loss can be seen after 500 hours, giving the 0.5 % after 50 hours.

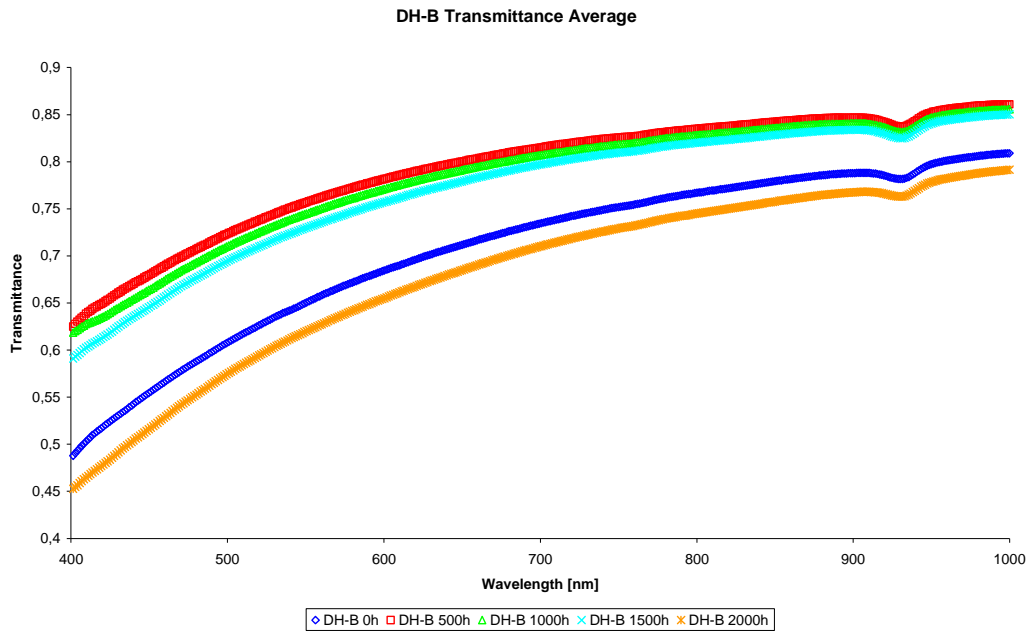


Figure 48. DH-B transmittance development over test time.

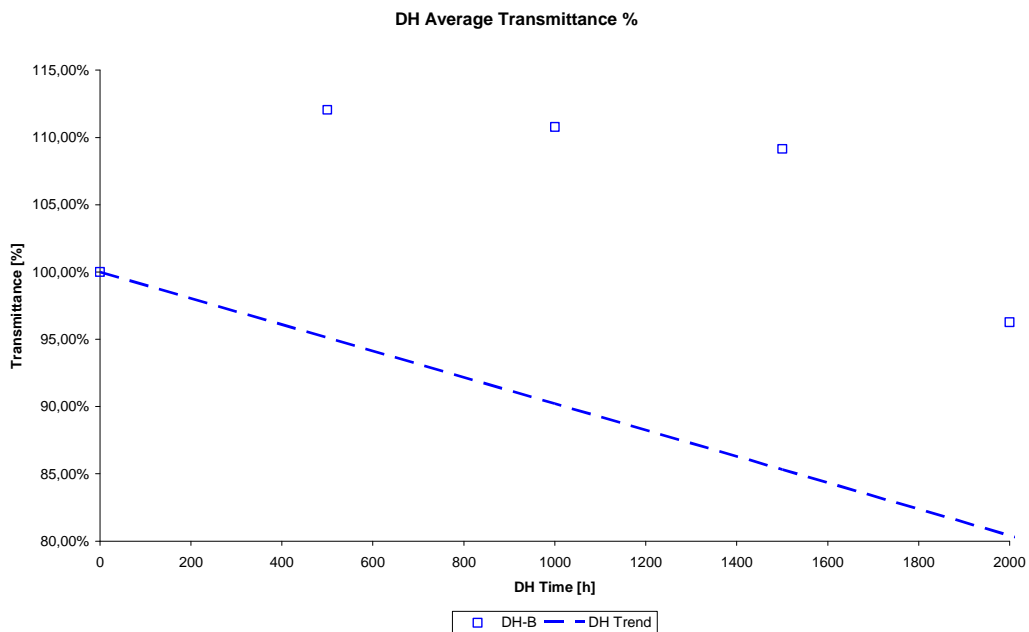


Figure 49. The transmittance average, regarding only degradation and not the initial improvement, shown over the DH test time.

DH-B show as in Figure 50 a 0.5 % reduction in  $P_{mpp}$  every 900 hours.

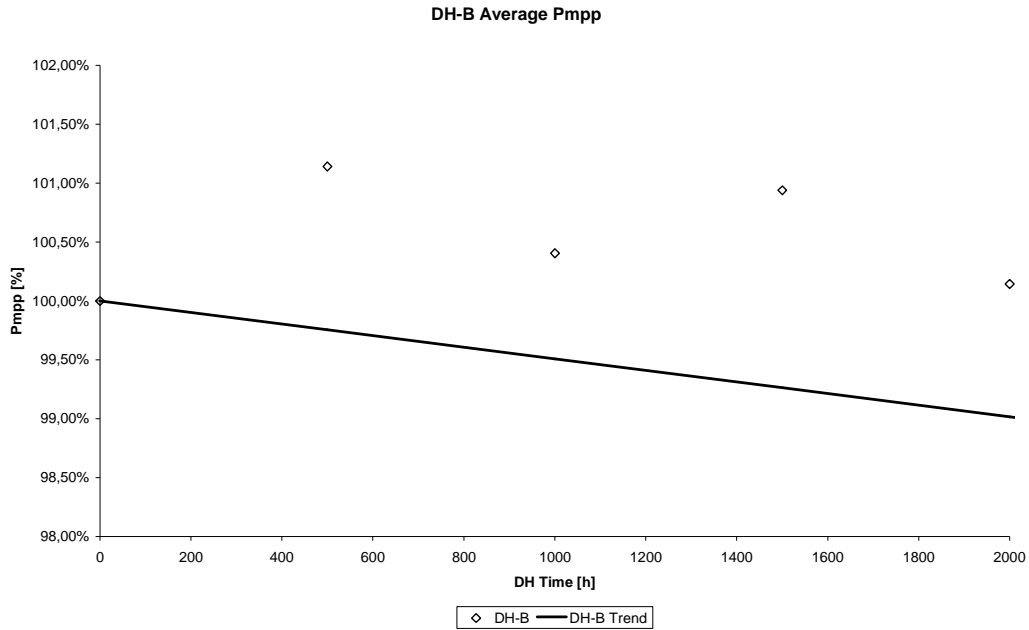


Figure 50. Average P<sub>mpp</sub> for DH-B samples

### 3.3.2 HAST

In the HAST 120°C range nothing passed until after 72 hours when the H2 leads slowly started to corrode on the back, Figure 52. At 72 hours the first front side corrosion also appear in the 130°C test.



Figure 51. H3 sample showing corrosion after 48 hours



Figure 52. Clear front side of the leads but corrosion on the back side of the H2 leads after 72 hours HAST.

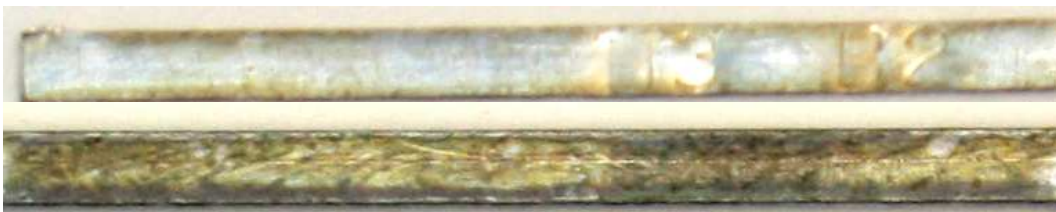


Figure 53. A light corrosion appear on the front of the connector lead at 72 hours at 130°C and the back looking worse, H3-B2.



Figure 54. Light backside corrosion on the H1 samples after 72 hours.

Since it is almost not possible to notice any difference with the bare eye to changes in the white haze of the HAST samples, the development is best described with the transmittance measurements.

In Figure 55 it is clear that the HAST makes the transmittance worse and does not improve it. Once again the embedding materials temperature parameters make the difference. The B sample clear in 85°C thus a better transmittance, and in higher temperature closer to the lamination temperature the white haze thickens, this is seen as a faster degradation. With the integrated values of the transmittance curves the 0.5 % degradation can be related to 5 hours, from 5% lower transmittance after 50 hours.

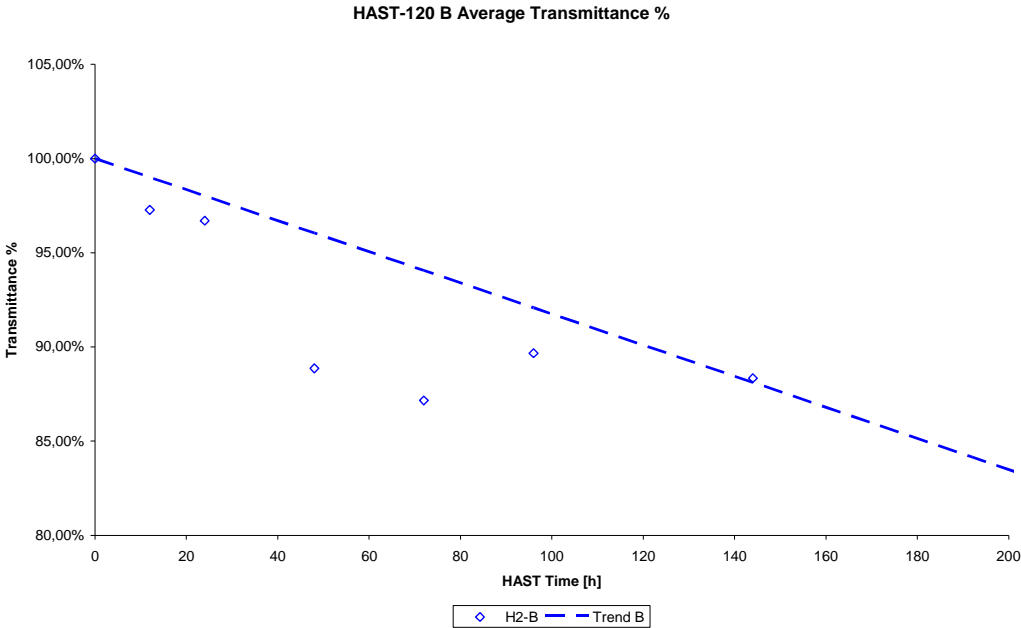


Figure 55. The Transmittance measured values and the trend for H2-B samples over time.

The H2 samples reaches a degradation minimum at 72 hours and then it improves itself a little after 144 hours.

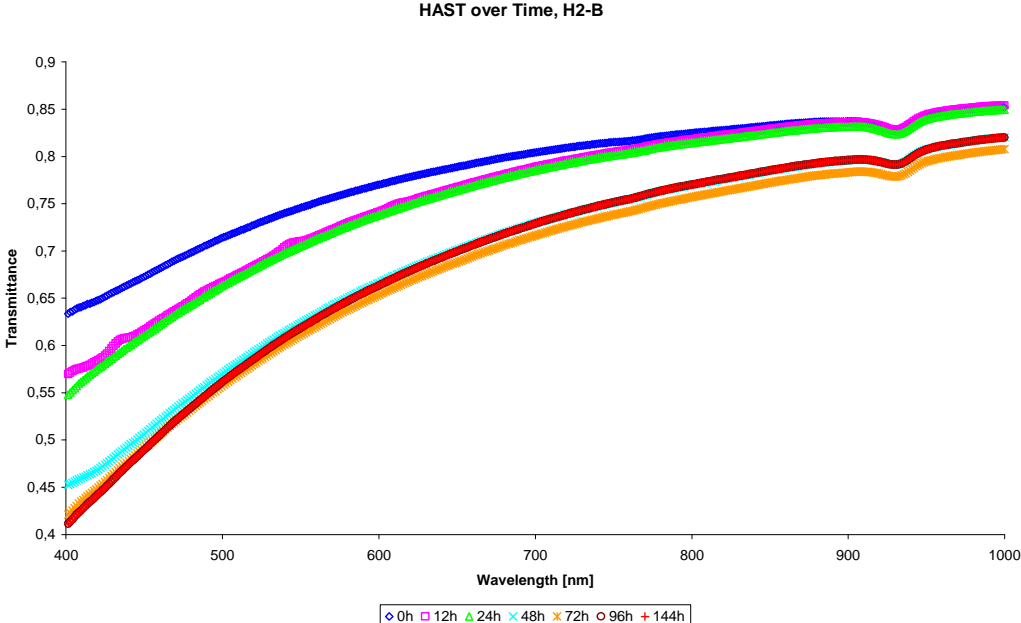


Figure 56. DH-B transmittance development over test time.

The  $P_{mpp}$  show a 0.5 % reduction for every 400 hours in the case of B samples, Figure 57.

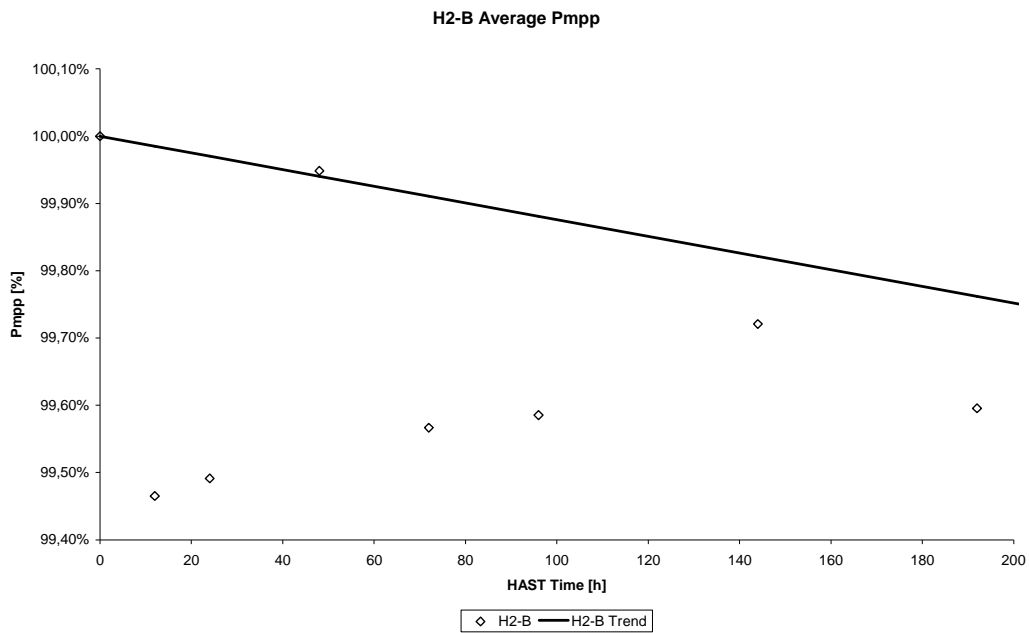


Figure 57. Average  $P_{mpp}$  for H2-B samples

### 3.3.3 Comparison

As shown in Figure 59 the correlation between the two tests in transmittance is not the same according to power.

It is however possible to withdraw a relation between DH and HAST the 0.5 % comparison degradation gives an AF of 10 in this case, that is 100 hours of HAST relates to 1000 in DH.

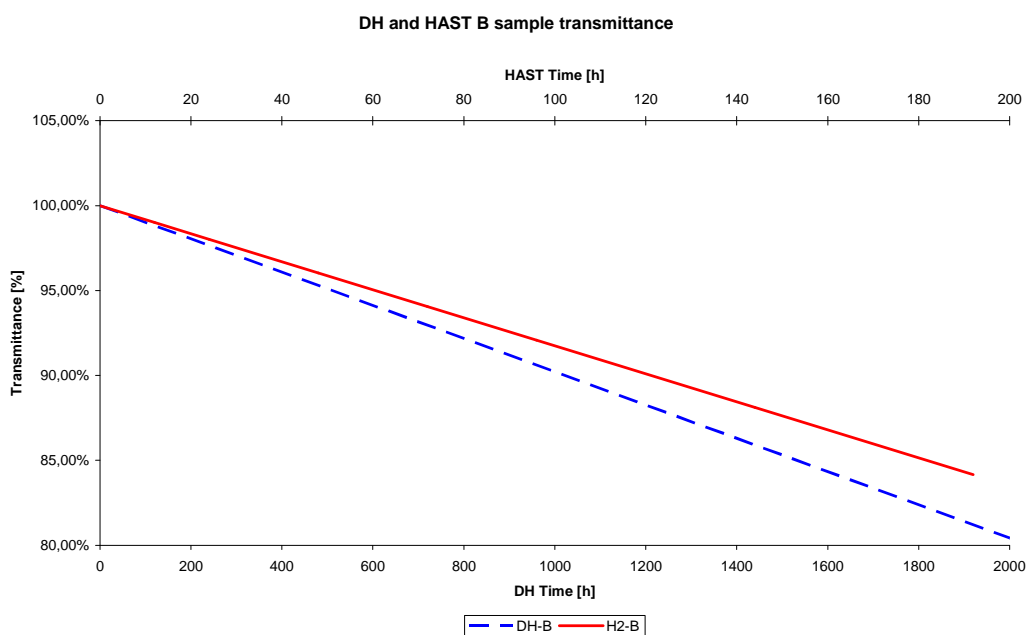


Figure 58. Transmittance over time in both DH and HAST for the B samples.

Regarding IV-characteristics and power the B samples show very good features. As seen below, when the initial power increase is removed the samples show an almost parallel

development to the DH. With basically no power loss over the test time, the B samples hold the best records in this work.

A larger similarity is also seen in the  $P_{mpp}$  in Figure 59, a factor around 2.5 correspond between the both tests. Taking the single line results from previous chapters a relation in transmittance of 10 times, can be seen and the  $P_{mpp}$  degradation comes to 2.25.

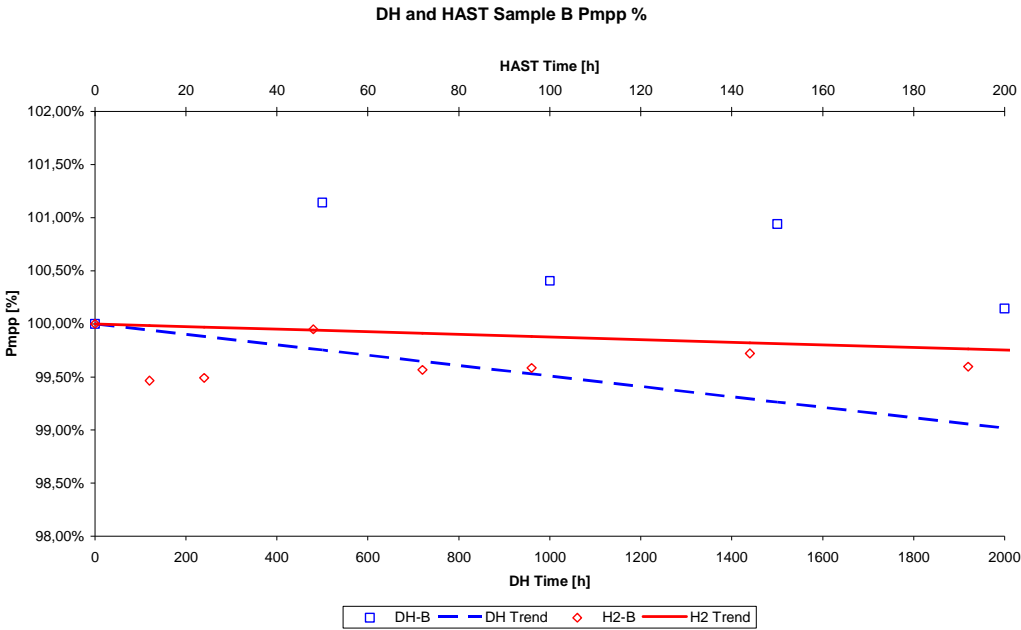


Figure 59. DH and HAST 120°C in relation to each other over test time. Trend line calculated from top value after regeneration.

Looking at the trend lines of the series resistance developments over time the process in the HAST seem to take place with just over 10 times the speed of the DH, Figure 60.

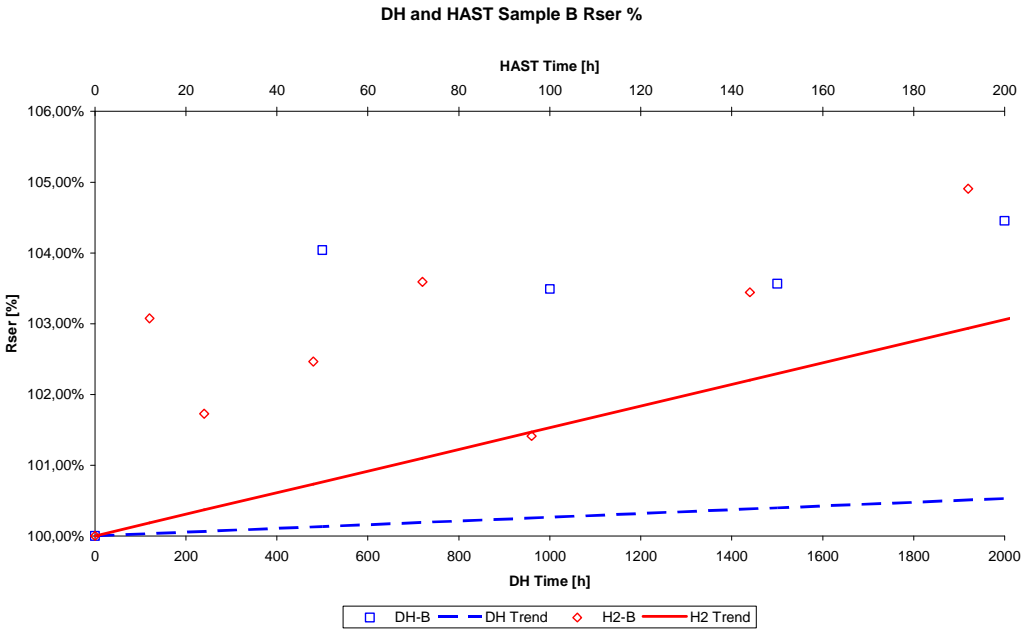
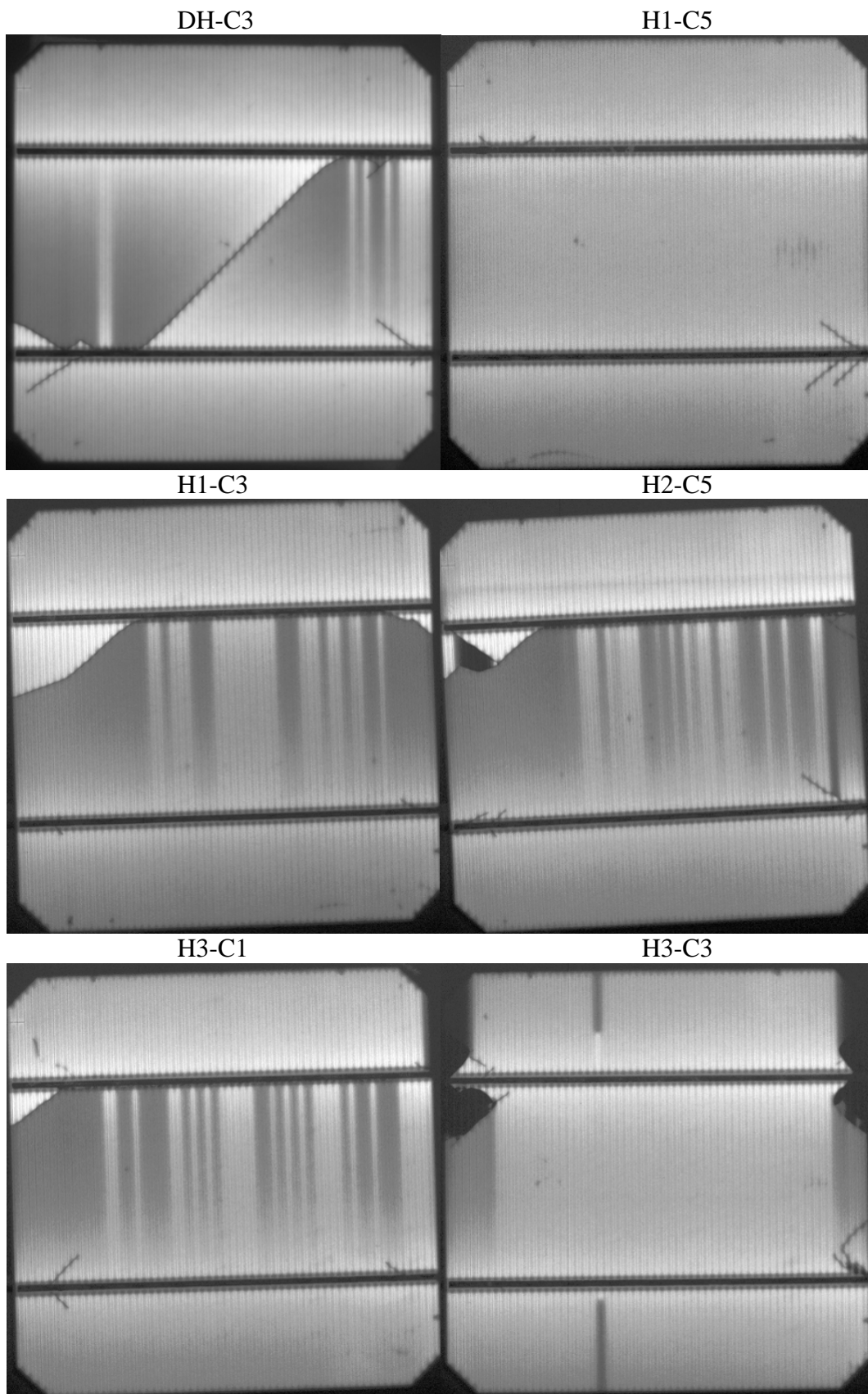


Figure 60.  $R_{ser}$  development in the DH respective HAST.

### **3.4 Sample C**

The C samples were in a large extent difficult to build, four of the cells survived the lamination without any micro cracks. Five of the cells, DH-C3, H1-C3, H2-C5, H3-C1 and H3-C3 have cracks that cover large areas of the cells. In the Figure 61 below the five broken cells and one example of less serious cracks H1-C5 showed as they appear in the EL photos.

Visually there is a white haze in the C samples as well, but a light one that is fairly transparent. The lamination also left some air bubbles in the embedding material, where the vacuum was not able to remove all air. These should not affect the test since they are far away from the edges and a good distance of closed embedding material hold from the glass edges.



**Figure 61. The broken cells and a cell with large cracks, H1-C5**

The influence of the lamination on the power has caused a large change in before and after lamination power, mainly because of the many cracked and broken cells. An average  $P_{\text{mpp}}$  loss of 4.4 %, with the maximal power loss of 0.54 W or 12.2 %. The voltage only show a 0.3 %

reduction and the  $I_{sc}$  a 3.6 % decrease. In the case of the C samples a loss of almost four times the average power compared to the two other, A and B, samples.

### 3.4.1 Damp Heat

The haze that was to be seen in the C embedding materials has after 500 hours of DH almost completely disappeared and the modules look fully transparent. However, more interesting are the yellow spots going into a brown colour at the centre of the spots closest to the metal as seen in Figure 62, where it clearly appears at each soldered corner of the bus bars. The same discolouration also appears on the back of the cell, following the bus bars.

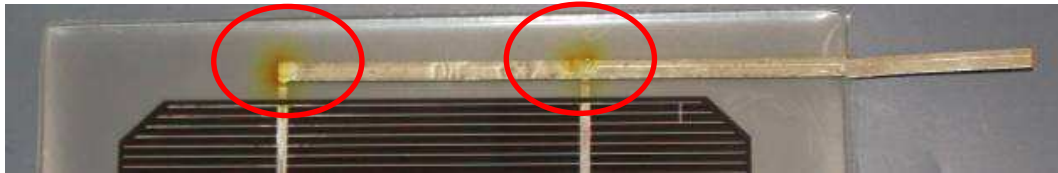


**Figure 62. A typical view of the yellow spots on the C samples.**

Also the brown corrosion is clearly to be seen both out- and inside of the embedding on the leads, it is also seen on the back side bus bars. At 1500 hours a copper corrosion also appears, a blue-green colour follows the back side bus bars as seen in Figure 63.



**Figure 63. Back side bus bar of the C samples heavily corroded after 1500 hours.**

Passing 1000 hours the visuals of the cells show clear signs of aging. The C samples have severely de-laminated and a clear browning has appeared. This process continues over 1500 and 2000 hours, ending with no grip at all between back sheet foil and glass/cell. The cell grips to the glass, but the de-lamination grows on the front side between cell and glass from 1500 hours of DH. Inside the module the embedding material slowly breaks down and starts to fall out of the module, Figure 64 - Figure 68



**Figure 64. The DH-C at 1000 hours, it shows a growing de-lamination on front side close to the bus bars.**



**Figure 65. The complete back side of the module have de-laminated. c) The DH-C at 1000 hours, with severe de-lamination behind the cells.**



**Figure 66. The C samples now de-laminate at the front side as well and not only at the bus bar.**



**Figure 67. The heavy de-laminated and corroded back side of the 2000 hours C sample.**



**Figure 68. The thermoplastic falling out of the C samples.**

The C sample show an initial improvement in transmittance as the white haze disappears after the first 500 hours of DH, see Figure 69, thereafter the degradation increases and if the initial improvement is removed there is a clear loss of transmittance with 15 % over 2000 hours. Figure 69 also confirms the initial improvement and then show a rapid decrease in transmittance and 0.5 % degradation is calculated to 20 hours of DH.

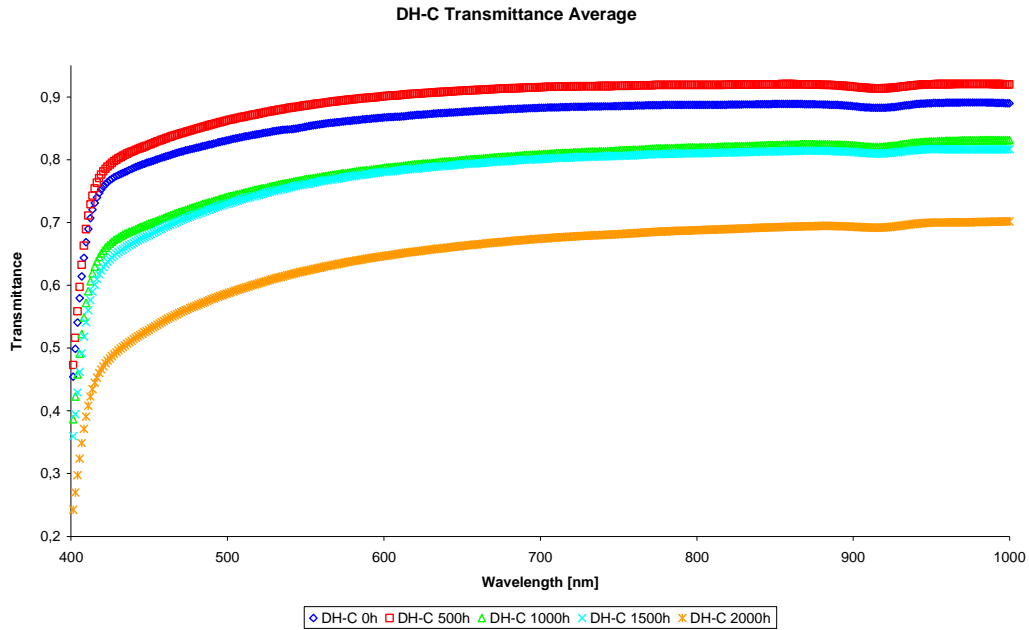


**Figure 69. Transmittance average over DH testing time**

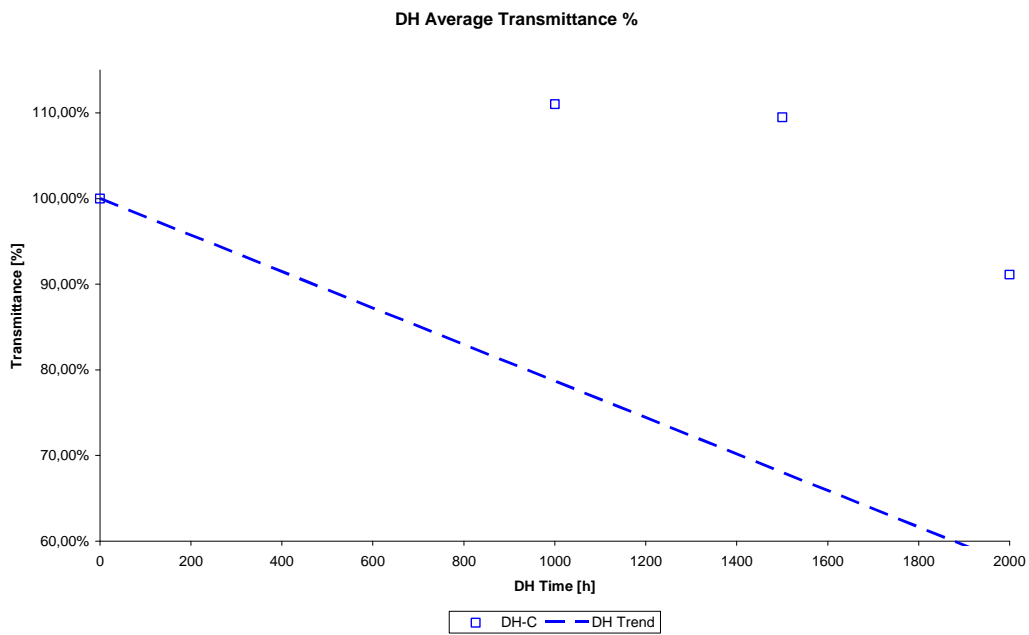


**Figure 70. Average transmittance degradation in DH over testing time with initial improvement removed and only considering degradation.**

Figure 71 gives the degradation to 0.5 % every 40 hours, which is almost the double from the transmittance degradation above.

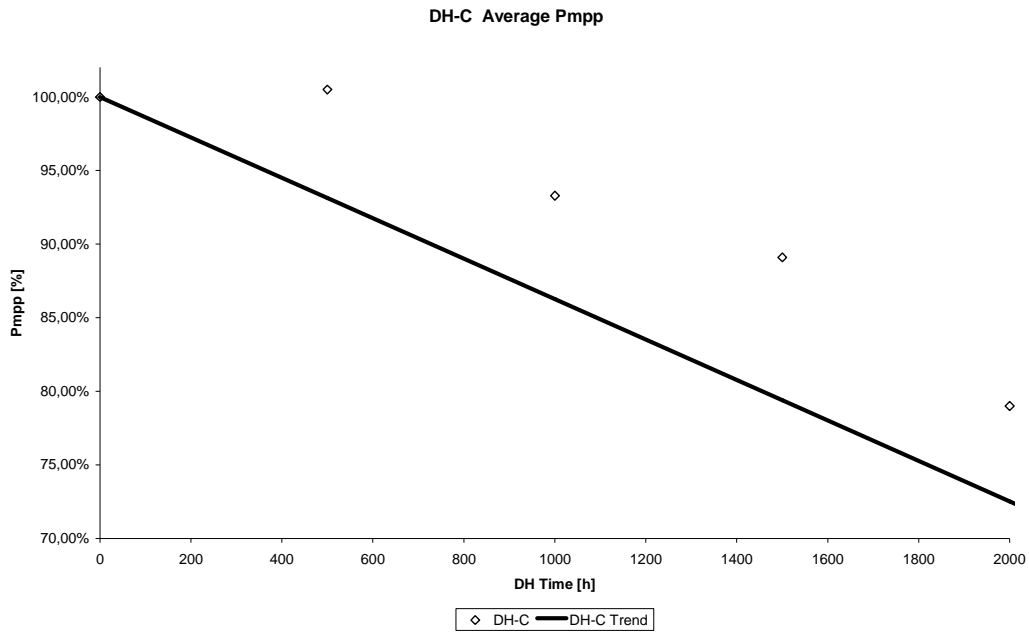


**Figure 71. DH-C average power over DH test time.**

### 3.4.2 HAST

The C samples show large changes already at 12 hours of HAST. Bubbles are seen on the 110°C and 120°C samples on the back of the cell. At 130°C the embedding material appears to have melted, with some of the material floating out of the module. Hence the back side is delaminated in large areas. At 110°C there are beginning spots to be seen on the C samples as in the samples at 500 hours of DH, however not as large, Figure 72. At 48 hours the H2 samples show small yellow areas, Figure 73 at the solder point between bus bar and connector lead. A brown shade is also seen in the embedding material, Figure 74.

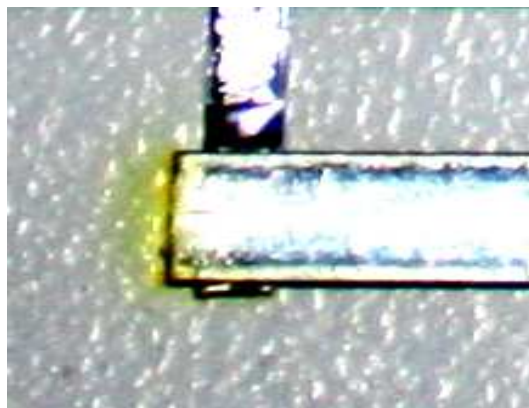


**Figure 72. Yellow spot on the H1 samples after 24 hours.**

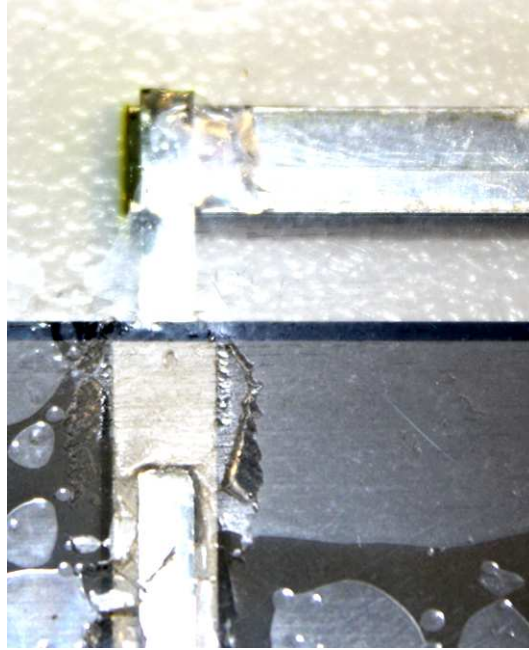


**Figure 73. H2-C Yellow spot and de-lamination of the H2 at 48 hours**



**Figure 74. Browning and bubbles of H2-C samples at 48 hours.**

Considering that the corrosion it is a lot stronger corrosion in the HAST, where the bus bars also show a much more rapid corrosion, like in the case with the bubbles in the C embedding. Not even at 2000 hours of DH does the bars have the almost black corrosion as they achieved after 48 hours of HAST. The H1 mode samples are the most similar to the DH, but also here it is clearly seen that the corrosion appears in a much greater extent.

At 24 hours the 130°C samples had started to de-laminate at the glass edges as well and at 48 hours the complete back sheet foil barely could be held in place by the embedding material.

The lower temperature samples showed growing blisters, the 120°C samples they were now covering the entire backside of the cell. A HAST front side de-lamination can be seen already after 48 hours. It is obvious that the humidity comes from the back side of the cell initially, clearly to be seen on the broken samples, where the humidity was pushing through the cracks and causing a front side de-lamination Figure 75. The cracked cells are also causing an accelerated de-lamination since there is moisture pushing through from the back and an area with loose grip can be seen along the cracks. At most times the de-lamination also follow the bus bars, while there a less compact lamination of the embedding materials appears, Figure 76 - Figure 81.



**Figure 75. Front side de-lamination begins at 12 hours in the 130°C HAST.**

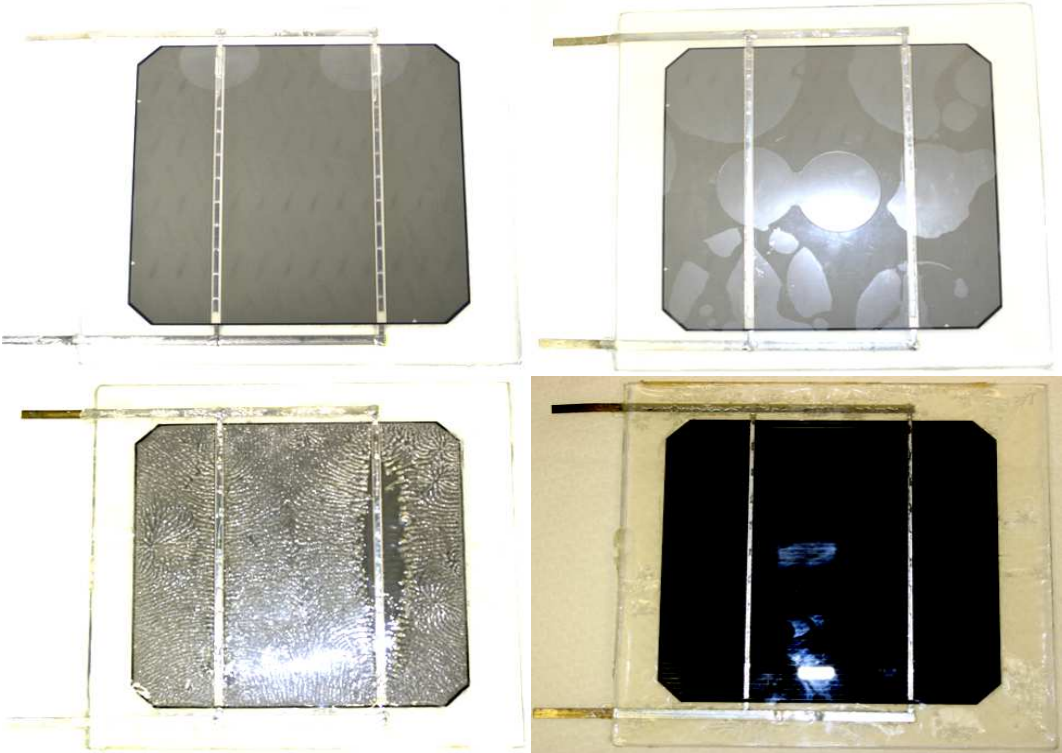


**Figure 76. The back side of each H-C sample at 12 hours of HAST, H1, H2 and H3, with different stages of bubbles and de-lamination, also the front of the H3-C1 is seen. The already corroded leads show a brown discolouration outside the modules.**

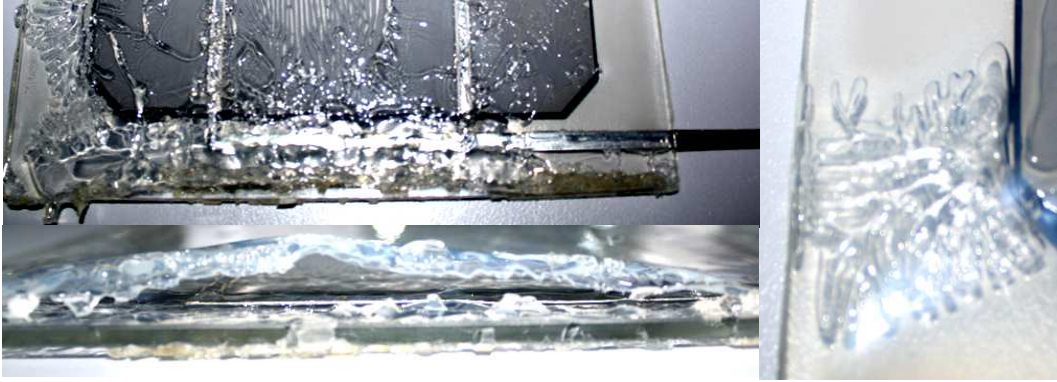


**Figure 77.** The melted embedding in the C samples after 24 hours at 130°C.



**Figure 78.** This is from the melted H3 samples after 48 hours. The front side start to de-laminate as well and some of the cells brake and flow out with the embedding material.

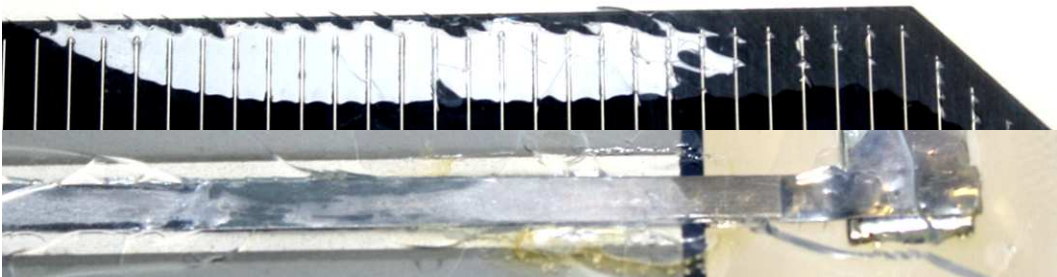


**Figure 79.** Front side de-lamination of the H2-C samples at 72 hours together with a back side example.

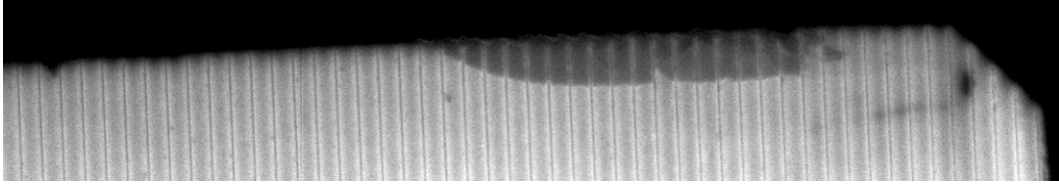


Figure 80. H2-C5 at 72 hours, the de-laminated area is clear to see as a darkened area on the cell from the EL photo.

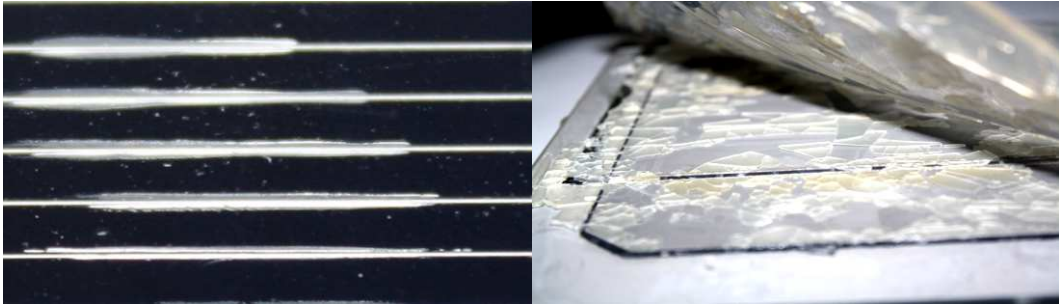


Figure 81. Increasing front side de-lamination after 96 hours. H2-C sample, back side is completely de-laminated as the back sheet foil can be removed without any resistance from the glue.

The transmittance levels get worse with an increasing speed. Comparing Figure 82 with the same of the DH, Figure 69, an approximation of some 70 hours HAST to 1000 hours DH can be set. This would give an AF far over 20; however, looking at the Figure 83 it is seen that the 0.5 % degradation appears every 2 hours and correlated to the DH it gives an AF of 10.

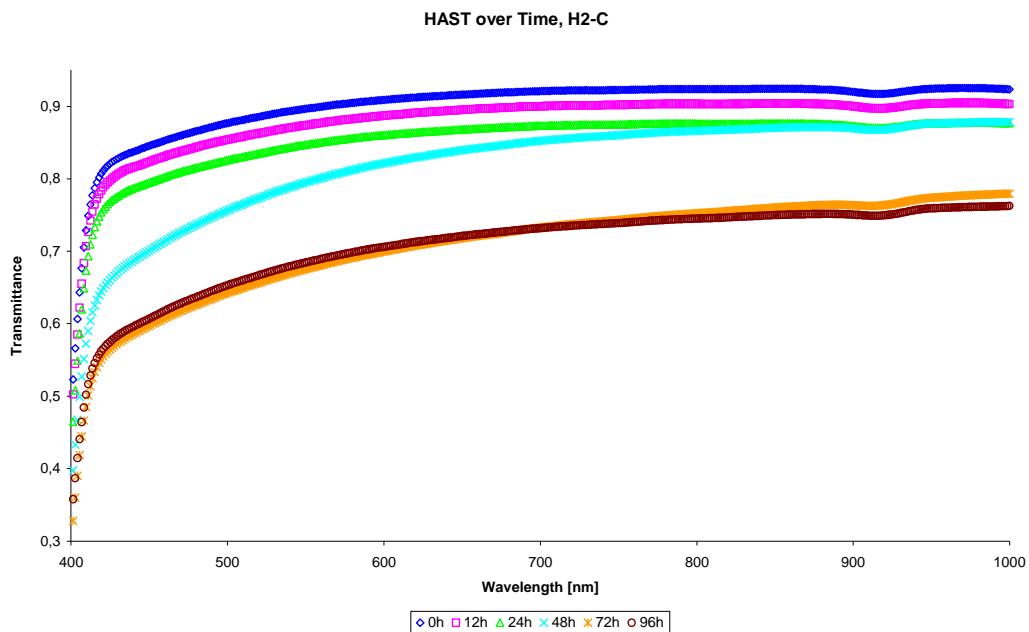


Figure 82. HAST transmittance for H2-C samples at 0, 12, 14, 48, 72 hours of testing.

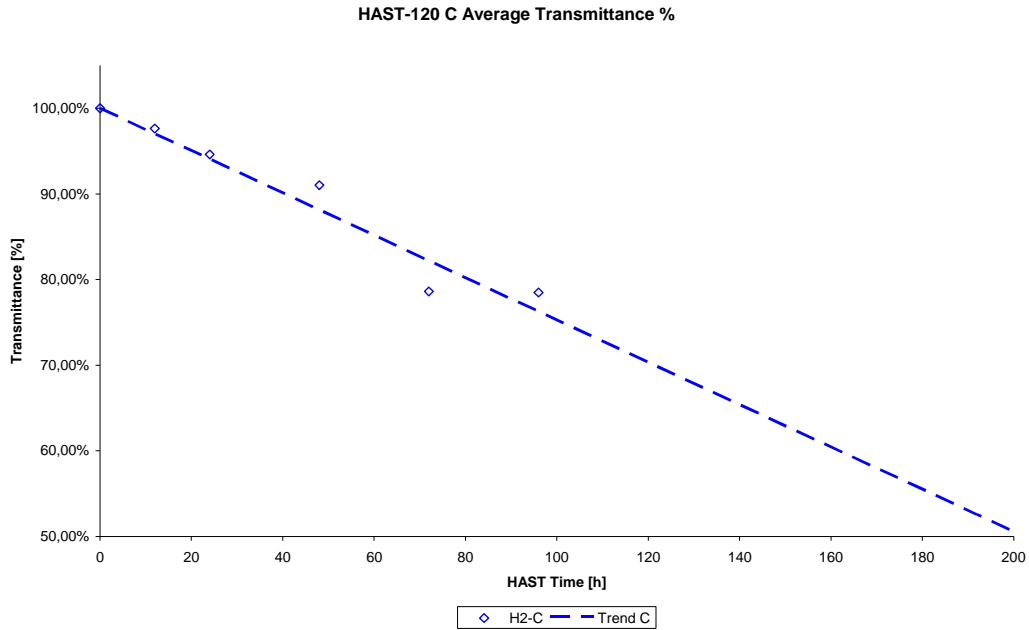


Figure 83. Transmittance degradation for H2-C samples.

The power trend line gives a degradation of 0.5 % every 16 hours

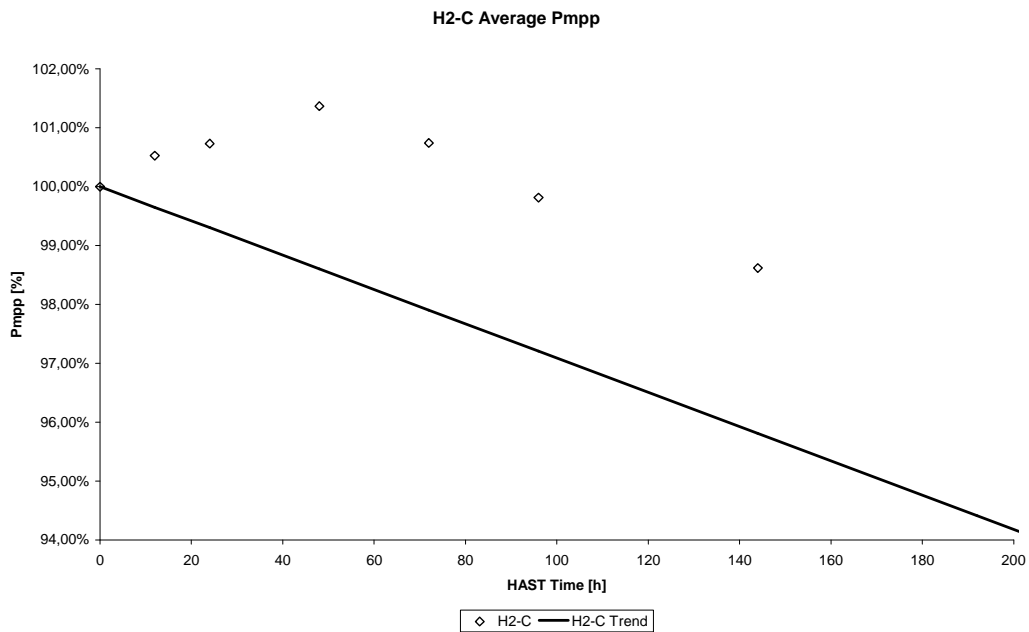


Figure 84. Average P<sub>mp</sub> for H2-C samples

### 3.4.3 Comparison

The IV-characteristics show a third AF, with an almost one to one degradation. A correlation of the two hours HAST and 20 hours DH gives an AF of 10 in this case as well. The P<sub>mp</sub> degradation however suggest a far lower AF with 2.5 times from the relation 16 hours of HAST to 40 hours of DH. From the Figure 85 the following relation is found; HAST degrades with a speed of 2 % every 50 hours, the DH with 10 % every 700 hours. This gives a AF of 2.8.

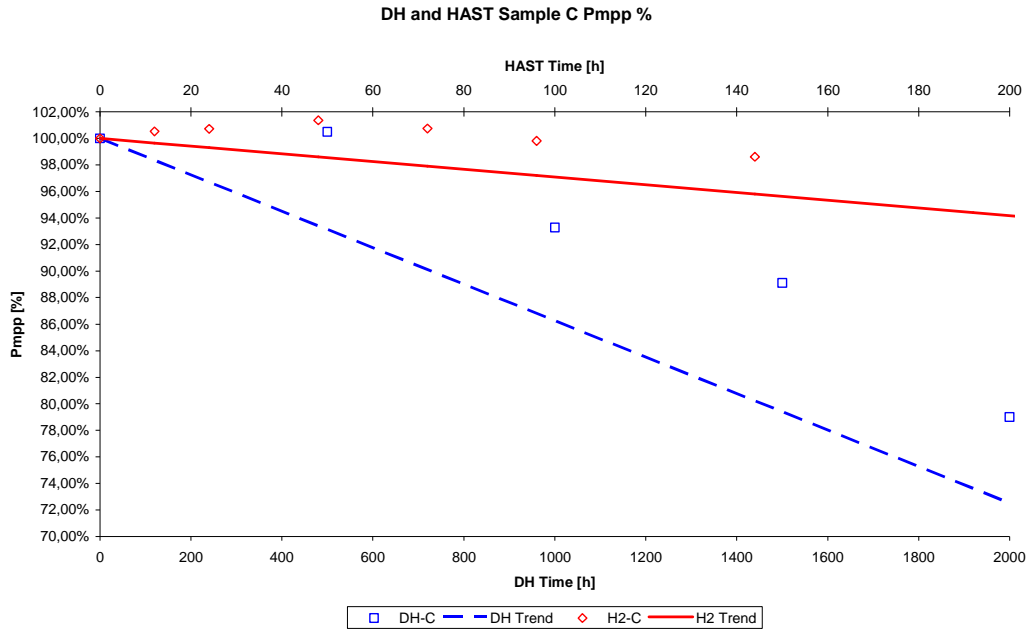


Figure 85.  $P_{mpp}$  for DH and HAST with measured values and corrected trend lines.

The series resistance increase is far more aggressive in the DH, which would also explain the much faster power degradation.

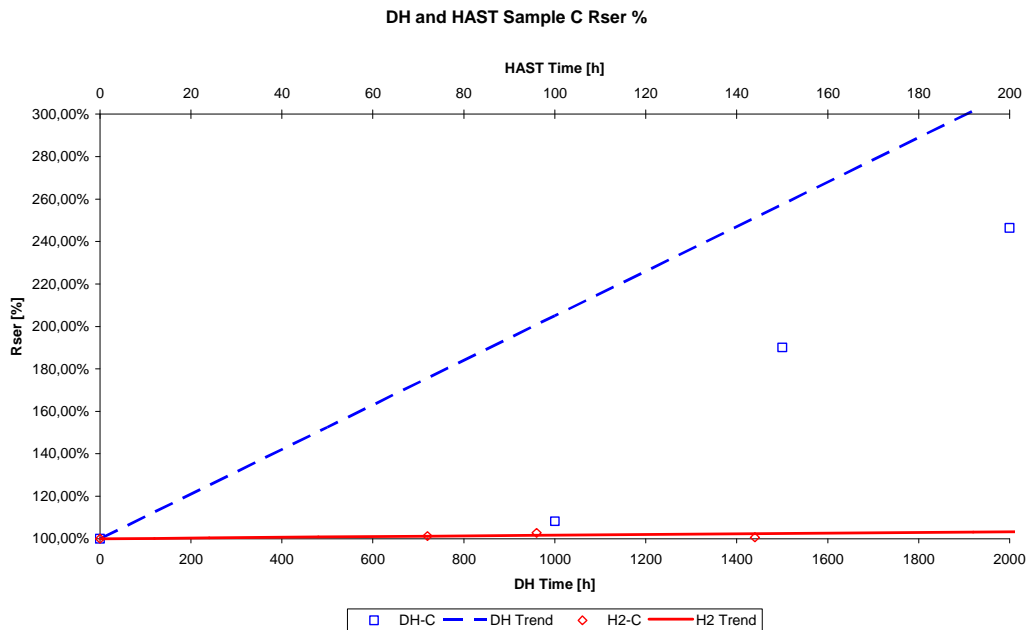
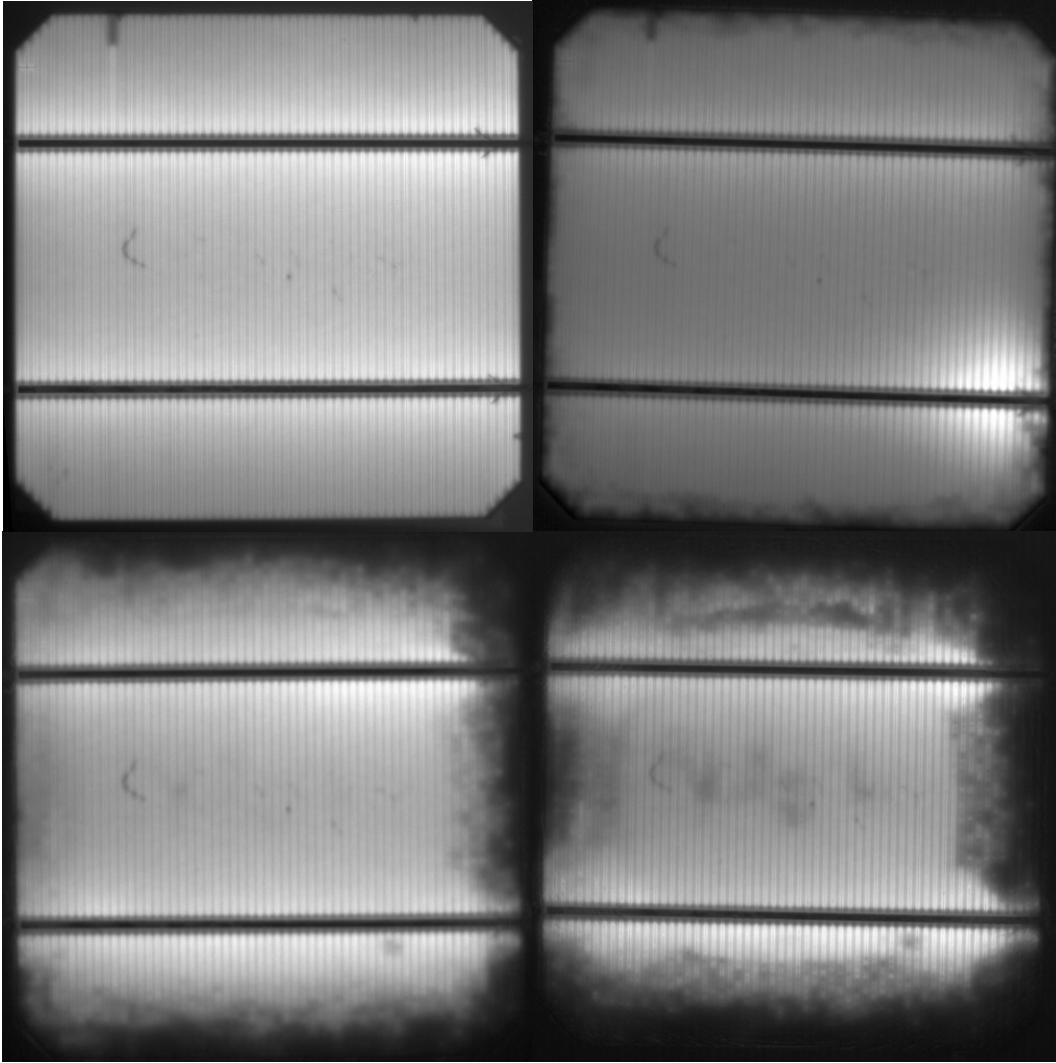
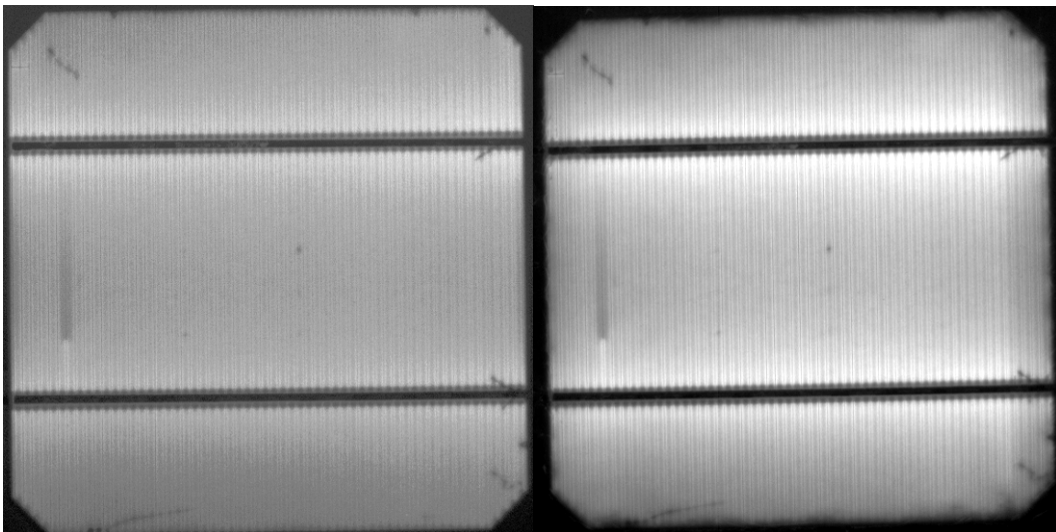


Figure 86. HAST and DH series resistance development over time.

The EL pictures of the de-laminated C samples show a common development with the D samples. Darker areas are seen, where the series resistance have increased and at the C samples there are also micro cracks after laminating have broken off parts of the cells by the de-lamination process. As seen in Figure 87 to Figure 88 below, there is an increased degradation of the de-laminated cells compared to the naked ones.



**Figure 87. The DH-C2 at 0 hours of testing at the top left, at 1000 hours during EL testing top right; dark clouds at the cell edge implies higher series resistance. The bright area at the bus bar low left is probably due to a bridge over the cell edge causing a short circuit. Bottom left; the same DH-C2 at 1500 hours. The de-lamination influence is becoming clear to see due to the darkened areas. Bottom right; finally at 2000 hours.**



**Figure 88. Left H2-C2 at 0 hours, right at 96 hours, shows that this also apply for the C modules, similar to DH.**

### 3.5 Sample D

After soldering the naked cells, 10 out of 20 examples had cracks or micro cracks. However no cells were broken. Since the first step was to solder the cells, no measurements were performed before soldering, except the EL picture in order to make sure that no already cracked cells were soldered or laminated and zero hours IV-measurements. While no lamination took place on the D sample there is also no IV-curve before and after lamination, further the transmittance measurement can not be done since there is no transmittance through the cell or through any embedding, glass or back sheet foil around it.

#### 3.5.1 Damp Heat

The naked cells now show a continuous corrosion, all over the metal bus bars. The front side looks like before but on the back side there is a dark grey colour covering the cell, except closest to the bus bar where the flux is placed by soldering. To notice is also the broken off corner on the D5 cell.

Over the test time there is not much change to be noticed when just visually inspecting the cells. The back side dark grey remains the same ton at 2000 hours. The bus bars show a slow brown discolouration that grows over the time. At 2000 hours it is even possible to see a beginning copper corrosion on some of the cells. At 2000 hours some dark discolouring appears on the front side of the cell, Figure 89 - Figure 93.

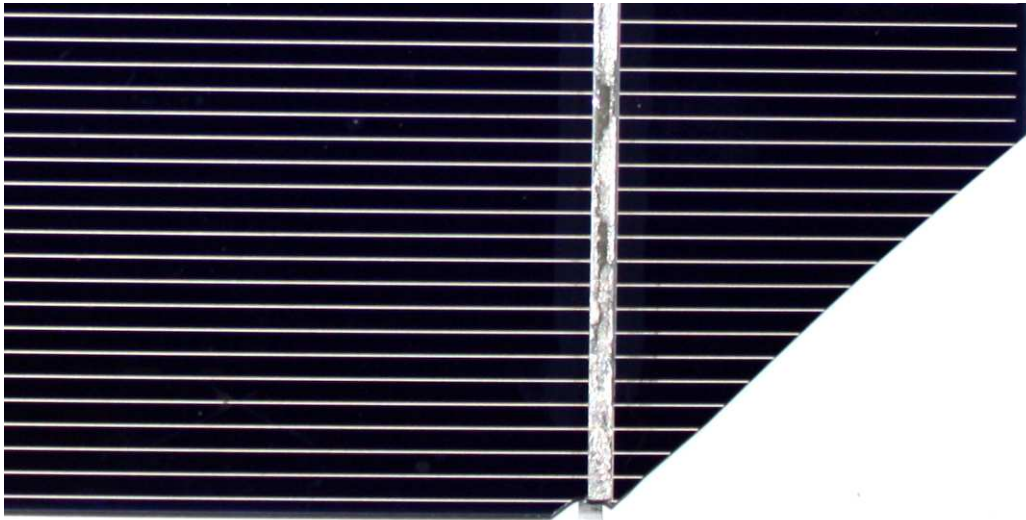
It is possible that it is just the question of dirt and water left on top of the cell rather than cell corrosion.



Figure 89. Corrosion after 500, 1000, 1500 and 2000 hours of DH, DH-D5.



Figure 90. Discoloured back side and corrosion on the back side bus bar, DH-D5.



**Figure 91. The broken off corner and front side similar to an untested cell, from the DH-D5 after 500 hours.**



**Figure 92. DH-D4 sample show signs of corroded copper after 2000 hours DH (the small strip above the bus bar).**

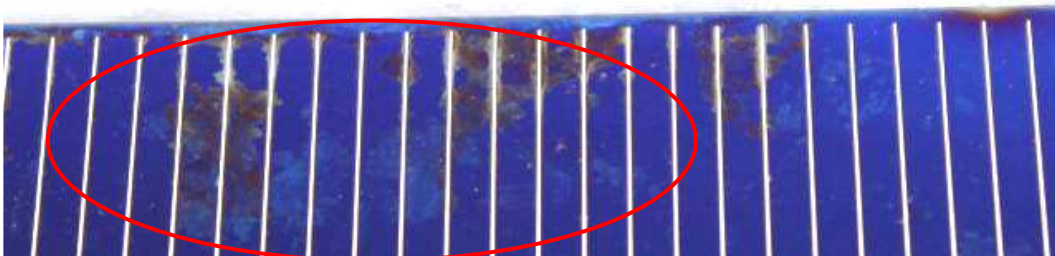


**Figure 93. DH-D1 has a black discoloration on the front after 2000 hours DH.**

The power trend line for DH-D show a degradation of 0.5 % per 175 hours.

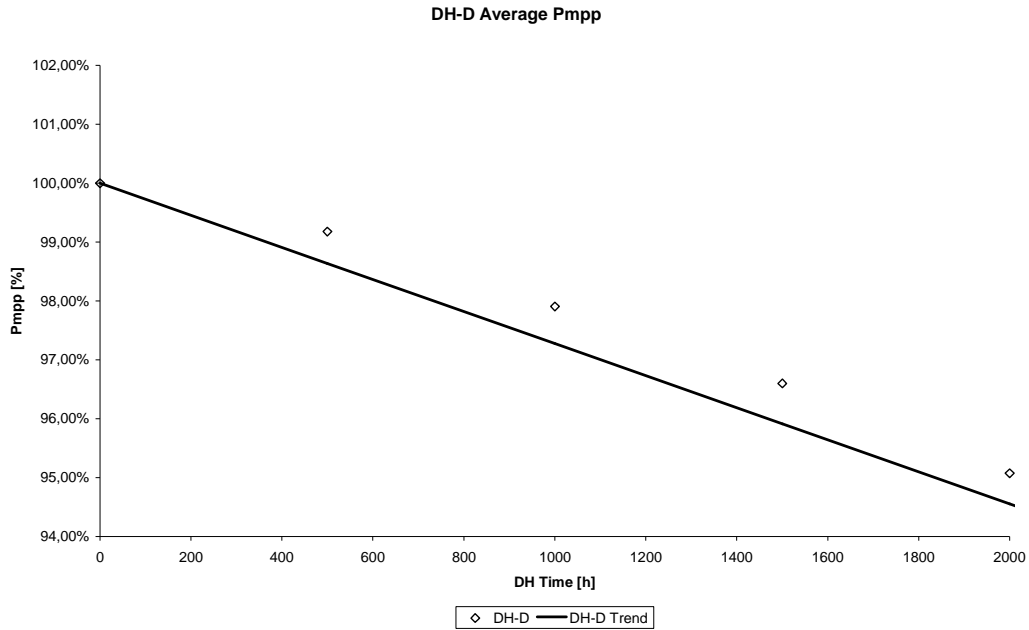


Figure 94. Average  $P_{mp}$  for DH-D samples.

### 3.5.2 HAST

In HAST the H2-D1 and H1-D4 got dropped and therefore cracked, Figure 95. It will however still be tested as long as it gives power as the data could be interesting to compare with the broken cells in the modules.

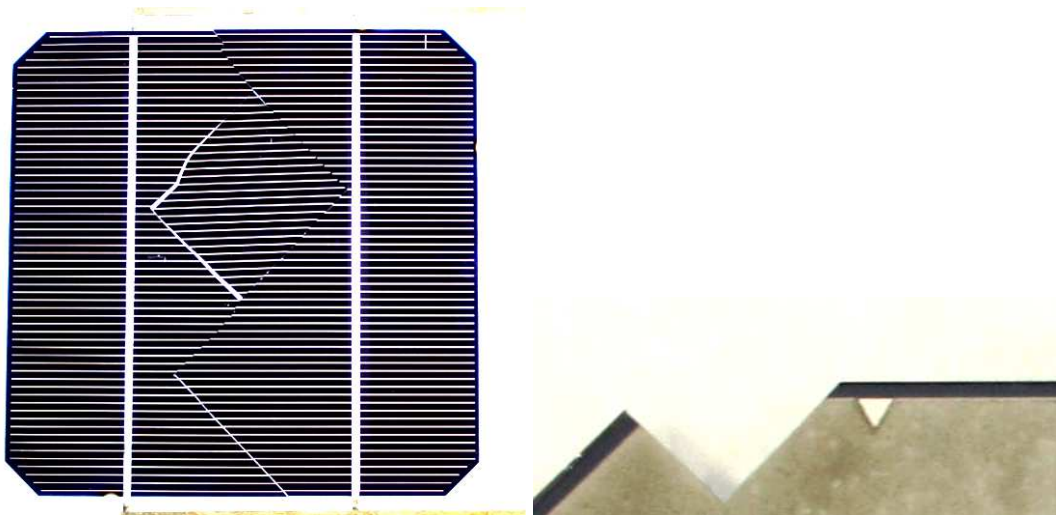


Figure 95. The broken H2-D1 after it was dropped. Cracked of part of H1-D4

A grey discolouring appears on the back of the cell, Figure 96. The bars corrode fast, already at 24 hours the colour is getting brown. The process continues and the colour tends to go in the direction of black at 96 hours, Figure 97.



Figure 96. The grey discolouring appears on the backside in HAST to, after 12 hours.



Figure 97. The corrosion development over 12, 24, 48, 72 and 96 hours in HAST

The degradation calculated for the naked cells in HAST comes to 12.5.

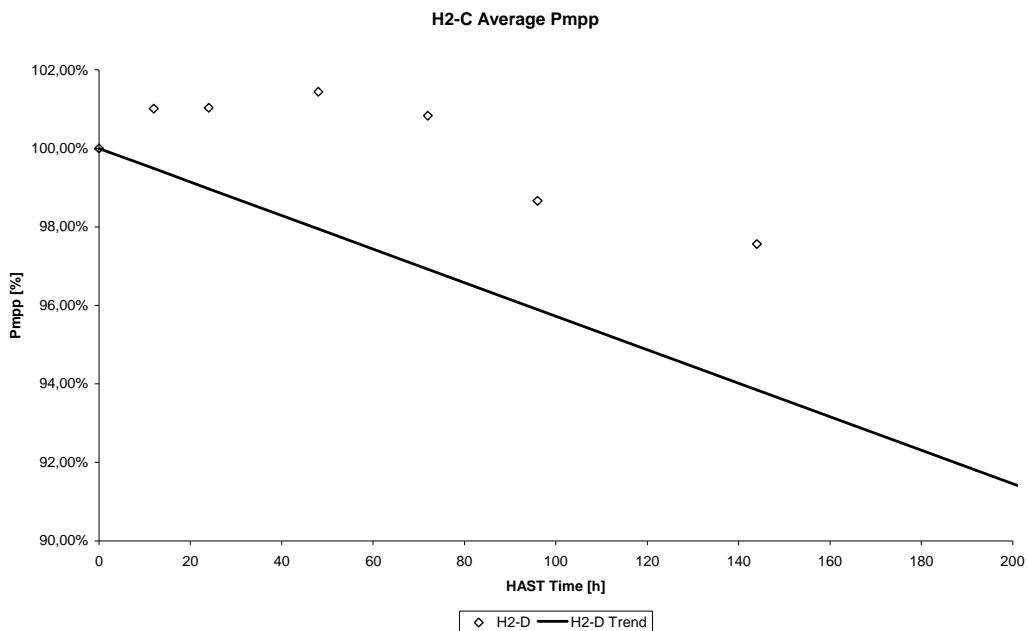
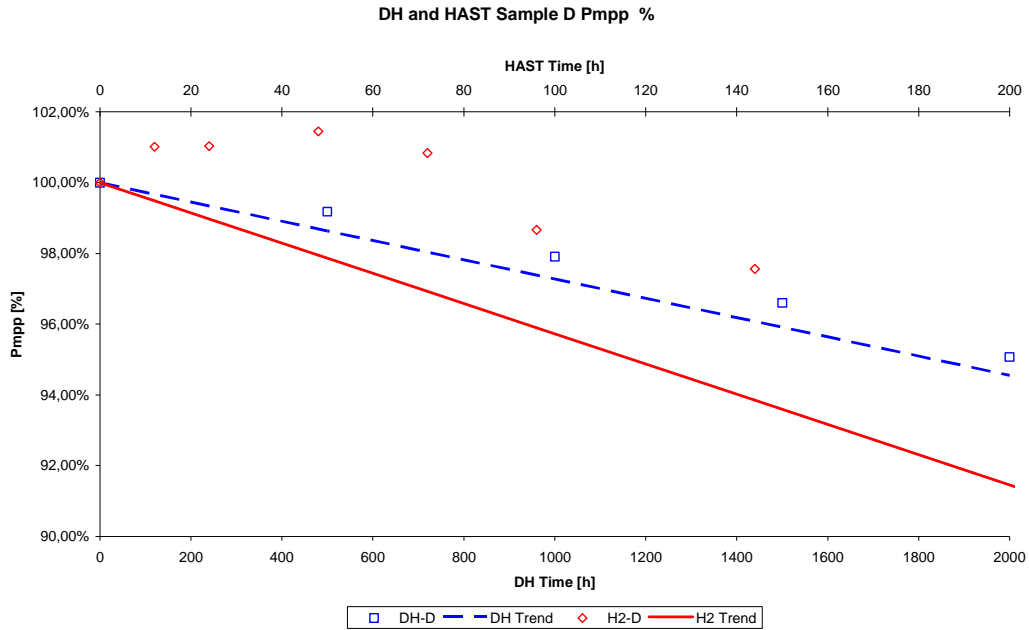


Figure 98. Development of average  $P_{mpp}$  for H2-D samples.

### 3.5.3 Comparison

Starting the IV measurements brought some interesting results. The naked cells, although not in a bad shape noticeable with the bare eye, produced the largest power losses compared to zero hours of testing. That is considering the power increase due to regeneration with the higher temperature in the HAST testing, the power is the same as at zero hours while all other samples improved their power with 1 – 2%,

A comparison of the degradation of the naked cells is interesting, since they show the influence of the tests independent from which embedding materials that are used in the modules and a clear relation between the test types can be made. When the first two measurements are removed, due to the initial regeneration that causes the cell power to rise, an AF around 6 can be determined for the D sample power degradation, Figure 99.



**Figure 99. DH and H2  $P_{mpp}$  over testing time. The initial measurements removed and starting the degradation of the HAST samples at the top power measured. Measured values plotted.**

Sample D shows a large increase in the series resistance of 5.8 %, the overall average increase of 2.6% for all samples. Looking at the resistance changes, it is likely that the dark areas seen in the EL photos are due to increased shunt resistance. The series resistance increase would be due to the corrosion of the leads.

It is seen that the  $R_{ser}$  grow with a faster pace in HAST as in DH, as expected. This is according to the visual check that show a clearly more corroded lead in the HAST case. When starting at the lowest value of the  $R_{ser}$  there is a factor of 7 between HAST and DH.

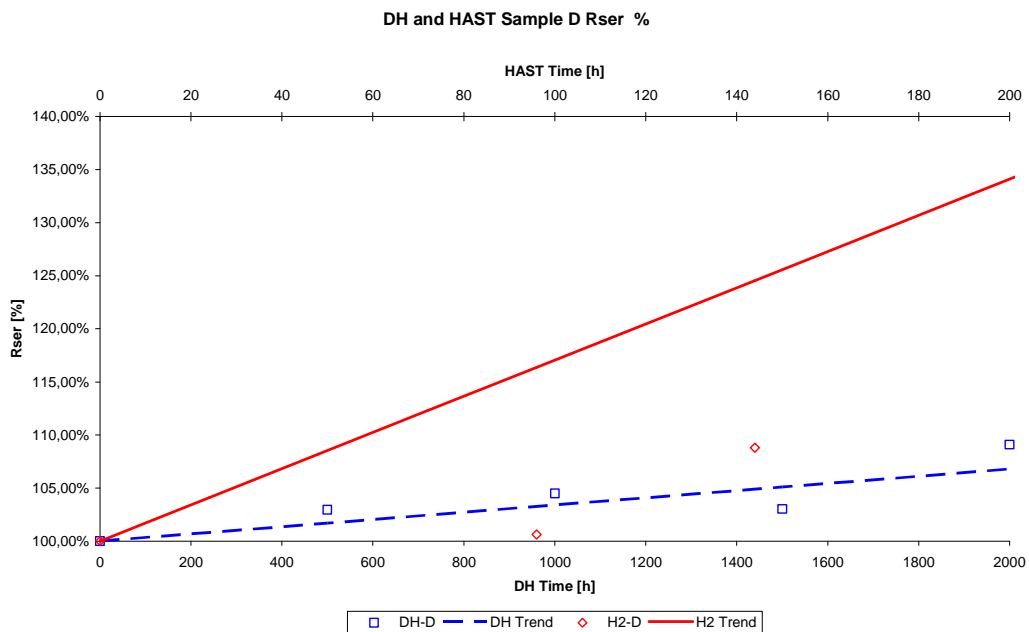


**Figure 100. Series resistance development showed for the H2 and DH over testing time.**

A comparison of the EL pictures also shows some similarities in the development of dark areas, which is with degraded connectivity, shunts or other damages. Looking at the case

study of the cell DH-D3 from 0 to 2000 hours there is clearly seen that the dark areas at the top grows, Figure 101, HAST show it in a slower rate but still possible to see as the H2-D3 show in Figure 102.

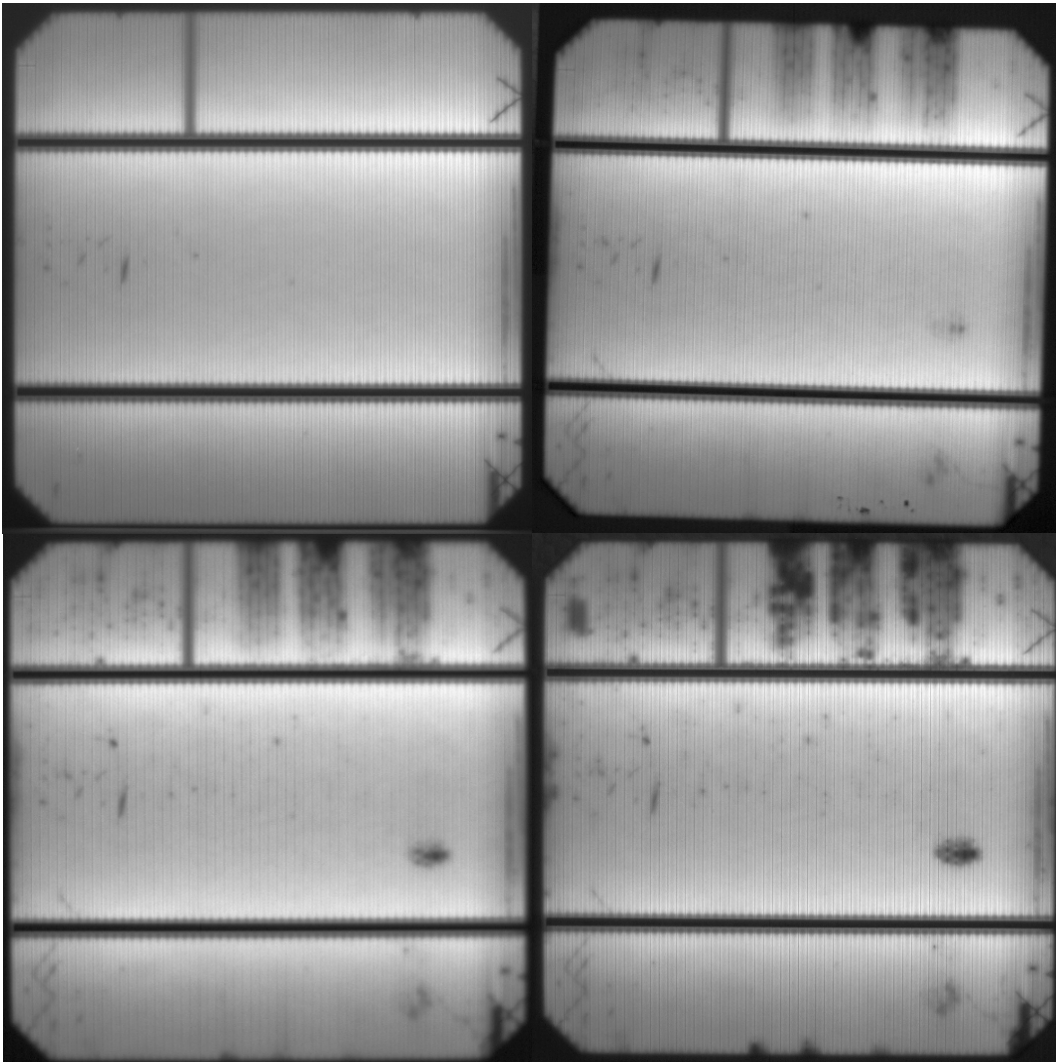


**Figure 101. Top left, DH-D3 at 0 hours. Top right; DH-D3 show increased dark areas at the top, after 1000 hours. Some small cracks are also to be seen but they are at the same level as at the beginning of the test. Bottom left; at 1500 hours the development continues. Bottom right; DH-D after 2000 hours**

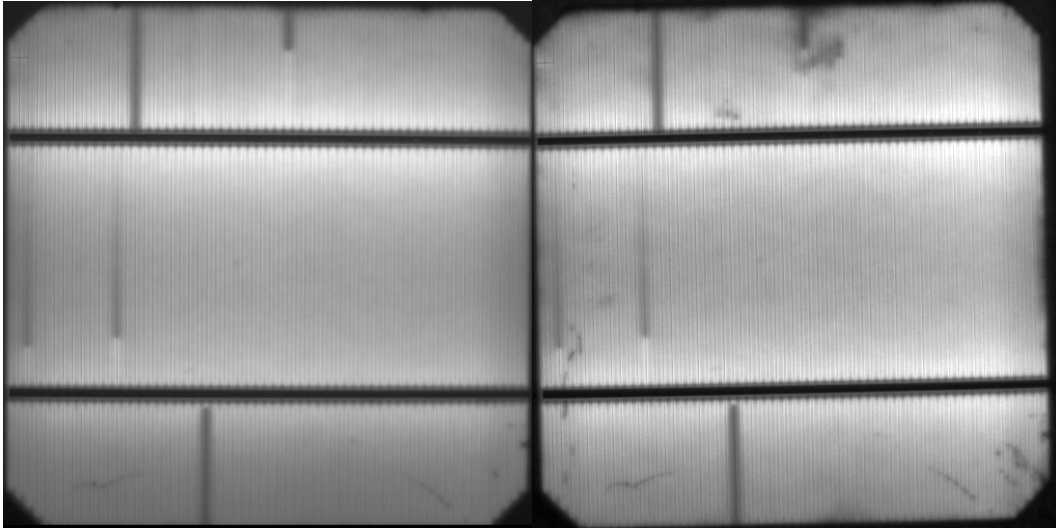


**Figure 102. Left; H2-D3 at 0 hours. Right; after 96 hours HAST, at the top some growing darkened areas can be seen.**

### 3.6 Sample Comparison

Discolouring does not show the same development in Damp Heat and in HAST. The different embedding materials show various responds to the temperatures in which the tests are conducted. The samples in group A improves in HAST but decreases the transparency in DH, with B it is the opposite. The similarities were to see in the C samples, where the yellow discolouring appeared in both test types.

The de-lamination are showing some differences, on a much earlier stage it is possible to see a front side de-lamination on the HAST samples compared to the DH. In DH the front side de-lamination only occurred after a severe damage on the back was already caused, and this was after 1500 hours of testing. The C sample completely de-laminated on the back side of the module in both tests, in DH after 1000 hours and in HAST 120°C after 96 hours, according to what the theory of the degradation increase told.

The corrosion show a much more rapid development in the HAST, the first signs of corrosion appeared already at the first inspection at 12 hours in larger extent than it was to see in the DH. From the test time theory it should have been visible first after some 20 hours at 130°C HAST. This should depend on the higher water vapour penetration in the HAST chamber compared to the DH.

In Figure 103 it is easy to see the large differences in the transmittance for the three different samples during DH. The A and C show an almost parallel decrease, although the C sample completely de-laminated after 100 hours. The explanation is that the transmittances in large amounts no longer were passing through the embedding material, which was non-transparent at 2000 hours, and the measurement was of dirty glass.

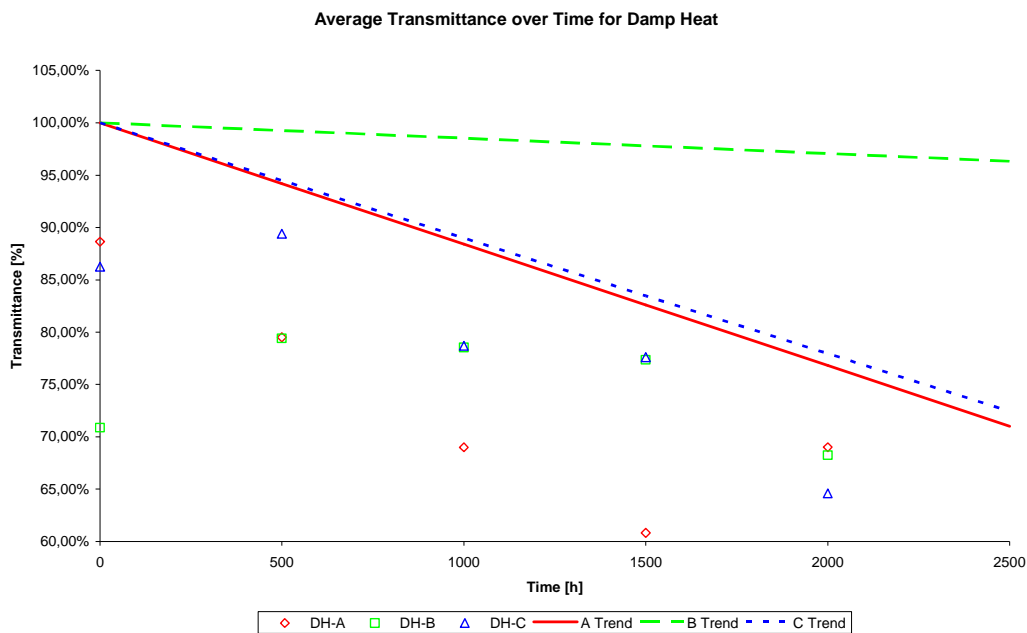


Figure 103. Transmittance for all three samples over time. Trend lines corrected to 100 %.

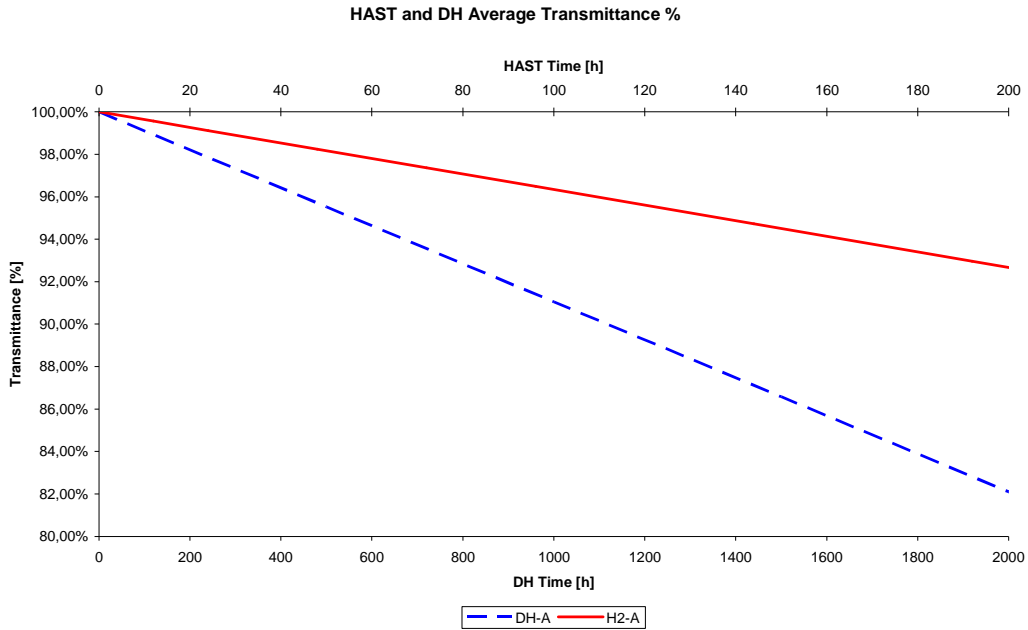


Figure 104. DH and HAST average transmittance degradation for A sample.

Regarding the power degradation, the fact that it is slower than the material degradation in an artificial test, seen in Figure 2, it is expected that a 5 % power decrease normally appears after 40 year of exposure to Miami climate. Therefore first at a later stage it is expected that the  $P_{mpp}$  start to increase with a steeper slope.

The power degradation was in a large extent harder to judge, partly because the regeneration that took place in the HAST did not occur in the DH. The only sample that showed a remarkable increase after 500 hours of DH was the C sample, which was to explain with the embedding material improvements that occurred.

The A sample reaches a top  $P_{mpp}$  value at 24 hours, which is 24 hours earlier than all the other HAST samples. Then a 0.03 W power loss occurs over a 168 hour test time, whereas the DH has lost 0.08W over 2000 hours. It should be remembered that the A sample had the best transmittance results for the HAST Figure 105, and therefore it is logical with a slower  $P_{mpp}$  degradation.

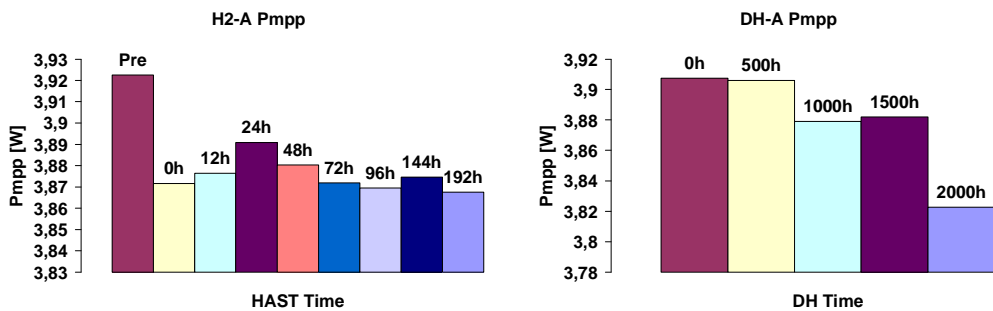


Figure 105. HAST and DH Average  $P_{mpp}$  values in W for sample A.

Similar for HAST and DH in the case of B modules is that the power goes up and down over the test time. There are peaks at 48 hours as expected and then again at 144 hours in the HAST, and in the DH at 500 hours and at 1500 hours. The peak at 144 and 500 hours is explained from the improved transmittance in these samples at these points.

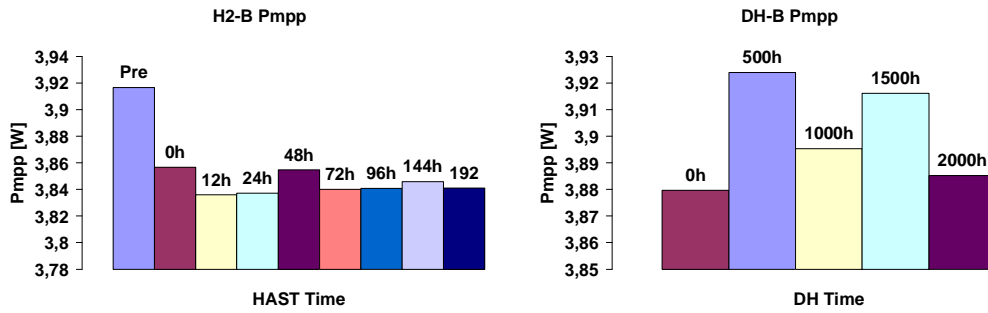


Figure 106. HAST and DH Average  $P_{mp}$  values in W for sample B.

The C samples have a development that does not match with the other samples showed and what was not expected from the theory. At the top values, 48 hours HAST and 500 hours DH, the  $P_{mp}$  of the modules was at the same level, around 3.85 W. Then the DH dropped to 3.58 W at 1000 hours what was not even reached after 144 hours of HAST, the power being at 3.76 W. Although the last big drop occurred between 1500 and 2000 hours of DH, it could be expected that the 144 hours HAST should have reached the level of the 1500 DH. 192 hours would correlate to 2000 hours according to the theory. The 0.11 W power loss over the 96 hours does not come close to the 0.98 W over 1500 hours in DH. The AF in this case would be approximately 1.7, it would take the HAST 900 hours to complete a 0.98 W power decrease with the slope of Figure 107.

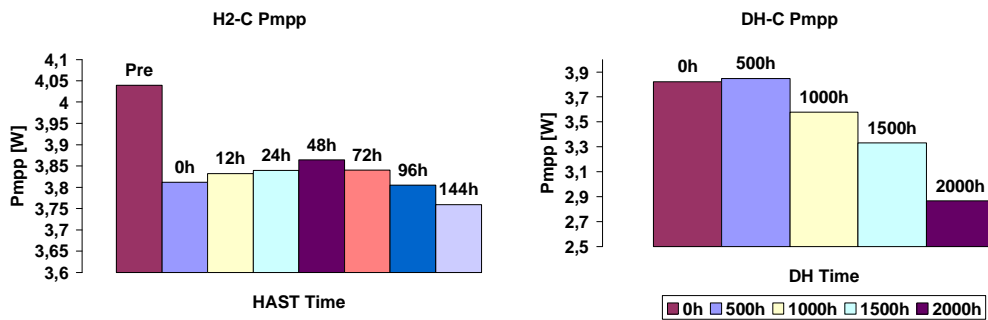


Figure 107. HAST and DH Average  $P_{mp}$  values in W for sample C.

Among the D modules a similar phenomenon occurred, although the DH started to decrease already at 500 hours, and even the difference of the broken cell DH-D5 only made a 0.01 W difference in the average. The HAST samples reached the top value after 48 hours, confirming the regeneration theory that the cells were improving their efficiency until 48 hours of HAST had passed, since there are no transmittance improvements with the naked cells. A factor of uncertainty is however if the peak should have been even higher, considering degradation that occurred during the first 48 hours of HAST.

However the period after the initial 48 hours show a 0.06 W decrease for H2-D until 144 hours, in the DH there was a 0.20 W decrease over the 2000 hours, with the broken cells removed. This gives a hint of the AF actually being in the area of 2000/480 or 4.2. The broken cells do have an influence, but it is seen that the power recovers at 96 hours of HAST. The AF calculated from the average of all cells 0.15 W loss under 132 hours HAST and 0.20 W loss under 2000 h DH, gives 500/44 and the AF 11.4. This however is disregarding the 48 and 72 hours of HAST and assumes that without braking the cell the average would have been continuous like the values of 12, 24, 96 and 144 hours implies.

### H2-D, broken and not broken cells

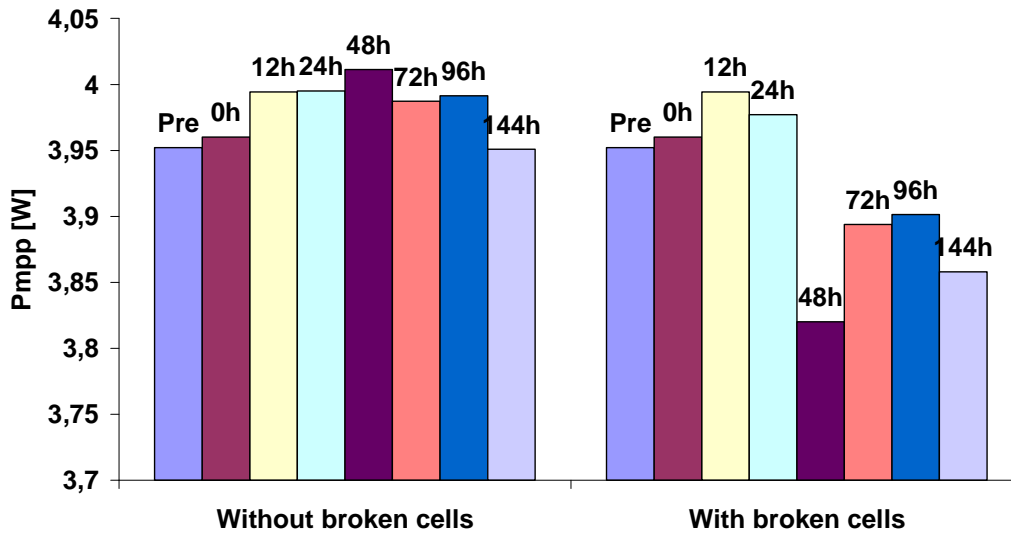


Figure 108. HAST sample D cells, with and without the broken cells

### DH-D, broken and not broken cells

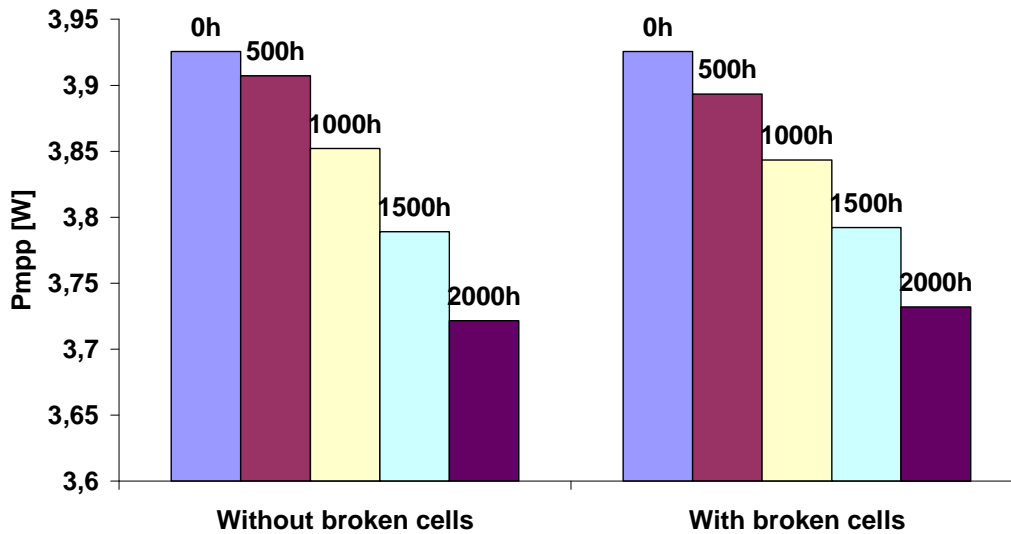


Figure 109. HAST sample D cells, with and without the broken cells

Figure 110 and Figure 111 show some differences in the serial resistance development. In DH the C sample has an extreme slope which of course depends on the de-lamination and the damages caused by moisture that concentrates between back sheet foil and glass. In HAST the  $R_{ser}$  of the naked cells increases, in this case it is explained from the extreme corrosion that occurs on connector leads and bus bars. The lowest  $R_{ser}$  are also the modules that deliver the best power in both tests, DH-B and H2-A. These samples have the best protection against moisture according to the level of corrosion inside the modules, and the differences are mainly due to other temperature coefficients that cause the transmittance to vary between the tests.

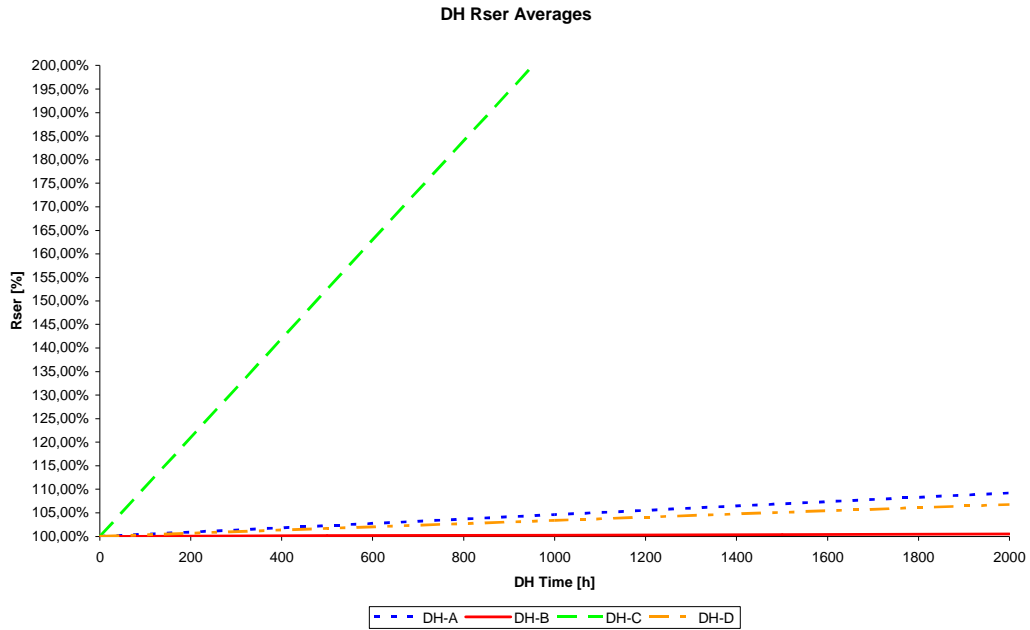


Figure 110. A comparison of DH average  $R_{ser}$  for each sample.

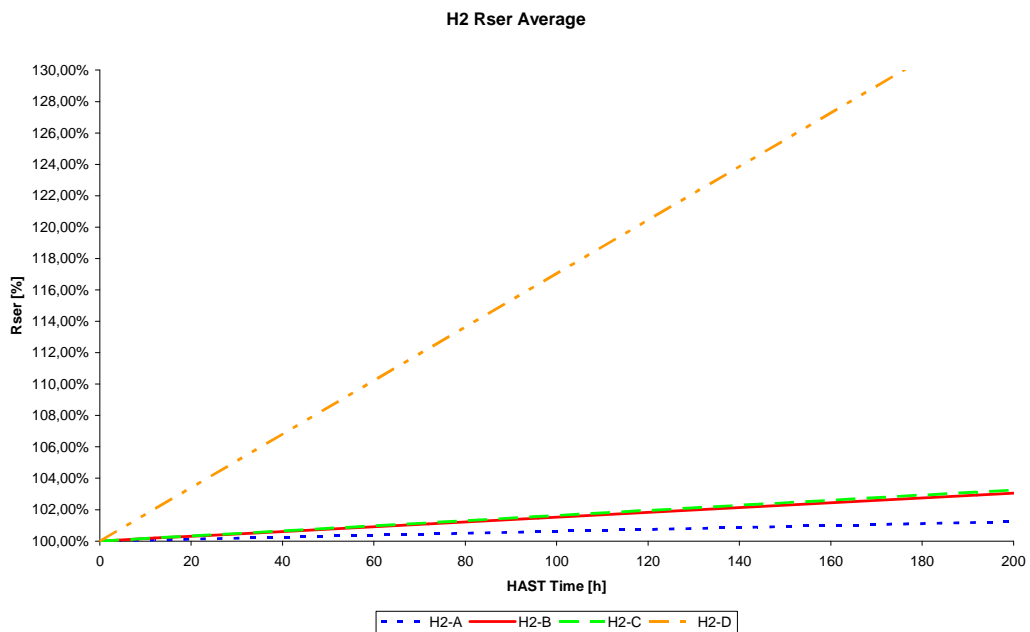


Figure 111. Comparison of all H2 sample averages and their  $R_{ser}$ .

### 3.6.1 Correlation

There is a correlation between the two test types, and in most cases the AF lies around the expected value of 10, as in the theory. However it is needed to reflect on which material types that should go through the HAST test. It have been seen that the high test temperature easily causes temperature sensitive materials to melt or deform in such an extent that it is hard to make a difference between the damaged caused from aging and from melted material.

The AF has been varying from about 2 up to almost 25 depending in the material and test method used. However it gives a mean value close to the theoretical 10 and therefore the correlation can be seen as confirmed. The best value achieved was in the transmittance giving an AF of 8.14, this would give a HAST time of approximately 123 hours for the standard

1000 hours DH. As expected the AF in IV and  $R_{ser}$  are not as good with values of 4.38 and 3.16, time in HAST: 229 and 317 hours, however it is expected that after 200 hours the degradation should increase and correct these AF's.

Sample	Time for a 0.5 % loss to appear.				AF for HAST compared to DH			
	DH		HAST		AF IV	AF	AF	AF
	IV	Trans	IV	Trans		Transmittance	Rser	mean
<b>A</b>	400	50	250	26	1,60	1,92	1,22	1,58
<b>B</b>	900	50	400	5	2,25	10,00	2,25	4,83
<b>C</b>	40	25	16	2	2,50	12,50	-	7,50
<b>D</b>	2000	-	480	-	4,17	-	6,00	5,08
<b>D (broken)</b>	500	-	44	-	11,36	-	-	11,36
<b>Average AF</b>					<b>4,38</b>	<b>8,14</b>	<b>3,16</b>	<b>4,75</b>
<b>HAST Exposure Time</b>					<b>229</b>	<b>123</b>	<b>317</b>	<b>211</b>

Table 4. Calculated AF and the average values reached in this work.

## 4 Results & Conclusions

The expectation and goal of this thesis was to establish a correlation between the two test types, Damp Heat (DH) and Highly Accelerated Stress Test (HAST). The awaited correlation was 1000 hours of DH to 48-96 hours of HAST.

The expectation to establish a correlation between the test types has been made. It has been shown that there are in most cases an acceleration factor (AF) of between 5 and 10, however it is needed to do further measurements in order to confirm the correlation. The test will have to run under a longer time, preferably until the 20 %  $P_{mpp}$  reduction have occurred in both test types. Suggested are also to do the measurements in a ratio 1:10.

To take notice of is that the HAST test appears to be more temperature dependant than the DH regarding the materials. This will need that the material temperature characteristics are taken into the calculation of the test time for the sample to run in HAST.

### 4.1 Further Work

Investigate the position of the samples in the chamber.

See how the temperature coefficients of the materials behave in DH respectively HAST.

Longer test time, until the samples have reached a 20 % power decrease.

To confirm the relationship with the humidity increase, that is, if the 1 % to 1°C correlation stands.

## References

---

- [1] Chianese, D., et al. (2003) Analysis of Weathered c-Si PV Modules: *3<sup>rd</sup> World Conference on Photovoltaic Energy Conversion*. Osaka, IEEE-TISO
- [2] Wohlgemut, J. H., et al. (2005) *Long Term Reliability of PV Modules*, Maryland: BP Solar International
- [3] Tebbi, O., Guerin, F., Dumon, B. (2001) Comparative Study of Accelerated Testing Models, Applications in Mechanics. *IEEE International Conference on Systems, Man, and Cybernetics* Vol. 4, p. 2099 – 2104. Angers, Laboratoire en Sécurité de fonctionnement, Qualité et Organisation Institut des Sciences et Techniques de l'Ingénieur d'Angers.
- [4] Arrhenius Equation (2009) [Online] Available at: [http://en.wikipedia.org/wiki/Arrhenius\\_equation](http://en.wikipedia.org/wiki/Arrhenius_equation) [Accessed: 11 February 2009]
- [5] NIST/SEMATECH e-Handbook of Statistical Methods (2003) [Online] Available at: <http://www.itl.nist.gov/div898/handbook/apr/section1/apr152.htm> [Accessed: 9 February 2009]
- [6] IEC (2005), *IEC 61215 Ed.2: Crystalline silicon terrestrial photovoltaic (PV) modules – Design qualification and type approval*. International Electrotechnical Commission (IEC)
- [7] ESPEC North America (2009) [Online] Available at: [http://www.espec.com/na/chamber\\_faq/answer/question\\_hast/](http://www.espec.com/na/chamber_faq/answer/question_hast/) [Accessed: 4 February 2009].
- [8] [www.SiliconFarEast.com](http://www.SiliconFarEast.com) (2001-2005) [Online] Available at: <http://www.siliconfareast.com/HAST.htm> [Accessed: 4 February 2009]
- [9] Quaschnig, V., Grochowski, A., Hanitsch, R. (1999) *Alterungserscheinungen bei Photovoltaikmodulen: Langzeiterfahrung einer PV-Testanlage and der TU-Berlin*. Berlin: Technische Universität Berlin
- [10] Dominkovics, C., Németh, P. (2004) Reliability Tests of Ultrasonic Bonding Methods Using HAST and THB Technology: *27<sup>th</sup> International Spring Seminar on Electronics Technology*. Budapest, Department of Electronics Technology, Budapest University of Technology and Economics.
- [11] Deutsches Institut für Normung (1995) DIN EN 60068-2-66, Berlin: Deutsches Institut für Normung e.V. (DIN)
- [12] IEC (1994), *IEC 60891: Procedure for Temperature and Irradiance Corrections to Measured I-V Characteristics of Crystalline Silicon Photovoltaic Devices*. International Electrotechnical Commission (IEC)

- 
- [13] Müllejans, H., et al. (2004) Reliability of Routine 2-Diode Model Fitting of PV Modules, Espoo: Endeas OY
- [14] Bowden, S., Rothagi, A. (2006) Rapid and Accurate Determination of Series Resistance and Fill Factor Losses in Industrial Silicon Cells: *17<sup>th</sup> European Photovoltaic Solar Energy Conference and Exhibition*. Atalanta: Georgia Institute of Technology
- [15] King, L., [et al.] (1997) Dark Current-Voltage Measurements on Photovoltaic Modules as a Diagnostic or Manufacturing Tool: *26<sup>th</sup> IEEE Photovoltaic Specialist Conference*. Albuquerque: Sandia National Laboratories.
- [16] Relative Humidity (2009) [Online] Available at: [http://en.wikipedia.org/wiki/Relative\\_humidity](http://en.wikipedia.org/wiki/Relative_humidity) [Accessed: 9 February 2009]
- [17] Rohatgi, A., et al. (2000) Fundamental Understanding and Development of Low-Cost, High-Efficiency Silicon Solar Cells. *Annual Progress Report: Sept. 1998 – Aug. 1999*. p. 67 – 81, Albuquerque, Sandia National Laboratories.